Journal of Energy Technologies and Policy
ISSN 2224-3232 (Paper) ISSN 2225-0573 (Online)
Vol.2, No.1, 2011

Characteristics features, economical aspects and environmental impacts of gen-4 nuclear power for developing countries

Palash Karmokar*[†]
Sirat Hasan[†], Syed Bahauddin Alam[1], Md. Abdul Matin[1], Md. Sekendar Ali[†], Abdul Matin Patwari[†]
Department of EEE, [1]Bangladesh University of Science and Technology (BUET)
[†]University of Asia Pacific (UAP), Dhaka
*palash.eee11@gmail.com

Abstract

The growing demand of energy has delicate the requirement of alternative sources of energies other than fossil fuels. Though renewable energy resources like solar, biomass, hydro and geothermal energy appear as environment friendly, replenishing sources of energy, a comprehensive solution appears far-fetched as far as large scale production and wide-spread dissemination is concerned when long term cost factors are taken into consideration. In this paper, discussions on the advanced fourth generation nuclear power on the basis of environmental contamination, energy security, cost of fossil fuels and electricity generation and have philosophy to the prospects of nuclear power as the ultimate future energy option for the developing countries are done. This study proposes that gen-4 nuclear appears to be a long term environment favorable panacea to the much discoursed problem of energy crisis by maintaining energy security and long term cost concern in developing countries as well as in the whole world.

Keywords: Gen-4 nuclear, reactor, kinetics, neutron, delayed neutron, transient.

1. Introduction

The progress of a country is the degree to which clean, affordable and sustainable energy resources are made available for the mass population. Fossil fuels have remained to be the main source of energy over years, accounting for around 86% of the total primary energy consumption in 2006. As projected by the International Energy Agency (IEA), the prominence of fossil fuels will continue for at least twenty more years. However, the nonrenewable resource based energy trends are obviously unsubstantial from a social, environmental and economic point of view. A balanced energy portfolio, where non-transient energy sources can play an important role alongside fossil fuels, is much called for to meet the future energy requirements economically and substantially. Though renewable energy resources offer the potential of supplying all these forms of energies with the added benefit of environment friendly conditions, efficiency of energy conversion and cost constraints become significant when large scale electricity generation is taken into consideration. To this end, nuclear energy based electricity generation is of utmost importance. In fig.1 Percentage use of nuclear power for electricity generation in different countries is shown.
Nuclear option corresponding to the Italian situation was studied in which suggested the great economic opportunities that nuclear energy can give in accordance with the Kyoto protocol. In nuclear energy has been suggested as a source of electricity, free from CO2 emissions and also an energy source that can play a key role in providing a vital bridge to a sustainable energy path. Emphasis has been put on nuclear waste management in which concludes that if properly handled, the waste from nuclear processes can be very small. The pattern is quite different in terms of new construction. Most of the recent expansion of nuclear power have been centered in Asia and 16 out of the 30 reactors are now being built in developing countries. China currently has four reactors under construction and plans a more than five- fold expansion in its nuclear generating capacity over the next 15 years. India has seven reactors under construction and plans roughly a seven-fold increase in capacity by 2022. Japan, Pakistan and the Republic of Korea also have plans to expand their nuclear power capacity. Countries in the Asia- Pacific region like Vietnam intends to

begin construction of its first nuclear power plant in 2015 where as Indonesia plans to build two 1000 Mega Watt(MW) reactors in central Java. Recently, Thailand announced plans to begin the construction of nuclear power plants by the year 2015. In Malaysia, a comprehensive energy policy study including consideration of nuclear power is to be completed by 2010. Considering the cost of energy generation and electricity production, defilement of environment reliable energy and advanced reactors safety and performance as well as waste transmutation, nuclear power is the best option for future energy reservoir.

2. Gen-4 Reactor Technology (GRT)

2.1 Reactor Kinetics Framework

Consider a core in which the neutron cycle takes' seconds to complete. The change An in the total number of thermal neutrons in one cycle at time t is $(k_{eff} - 1)n(t)$, where n(t) is the number of neutrons at the beginning of the cycle. Thus,

$$\frac{dn(t)}{dt} = \frac{k_{eff} - 1}{l'} n(t) \qquad (1)$$

The solution of this first-order differential equation is

$$n(t) = n(0)\exp\left[\frac{k_{eff} - 1}{l'} n(t)\right] \qquad (2)$$

where n(0) is the neutron population at t = 0. Notice that in this simple model, the neutron population (and hence the reactor power) varies exponentially in time if $k_{eff} \neq 1$. In figure 2, Thermal utilization of gen-4 reactor as a function of time is shown.

2.2 Prompt Neutron Lifetime

The mean time between emission of the prompt neutrons and absorptions in reactors is called Prompt neutron lifetime, l_{fp} . For an infinite thermal reactor time required for neutron to slow down to thermal energies is small compared to the time neutron spends as a thermal neutron before it is finally absorbed. In fig. 3, Decay of neutron lifetime is shown.
Mean diffusion time is td. For an infinite thermal reactor,

$$t_d = \frac{\sqrt{II}}{2_{VT}\left(\sum_a F + \sum_a M\right)} \qquad (3)$$

2.3 Reactor Kinetics for Delayed Neutrons

Considering an infinite homogenous thermal reactor whose thermal flux must be independent of the position. Time dependent diffusion equation for thermal neutron is,

$$T = l_P / (ka - 1)\ s_t - \sum_{a\phi T} = \frac{dn}{dt},$$

where S_T is the source density of neutrons into the thermal energy region, and n is the density of thermal neutrons. In fig. 4, Radioactive decay for heavy particles via kinetics model is shown.
The rate of change of neutron density is,

$$\frac{dn}{dt} = k_\xi (1 - \beta) \sum_{a\phi T} + \sum_{i=1}^{6} \lambda_i C_i \qquad (4)$$

where $n = \sum A e^{\omega T}$, $C = \sum B e^{\omega T}$

The complete solution for n is,

$$n = n_o \frac{\beta}{\beta - \rho} e^{\frac{\lambda \rho t}{\beta - \rho}} - \frac{\rho}{\beta - \rho} e^{\frac{\rho - \beta}{l_p}} \quad (5)$$

Finally it is,

$$T = l_p / (k a - 1)$$

In fig.5, Reactor kinetics for delayed neutrons is shown.

2.4 Characteristic Features of Gen-4 Reactor

In U.S. more than 100 nuclear plants are implemented because of a carbon free alternative to fossil fuels. Nuclear energy is now a great source of electricity generation. In fig.6, Loss of electric load is shown as a transient analysis of reactor.

Gen-4 reactors have a less complicated and more rugged design, making them lighter to maneuver and relatively less vulnerable to operational derangements. These reactors have a standardized design for contracting capital cost and construction time. The climate and energy protection can be exploited by creditworthy planetary atomic energy enlargement. In fig.7, Loss of normal feed water in Log scale is shown as a transient analysis of reactor.

Higher handiness and longer maneuvering life and this reactor tech has contracted possibility of core melt fortuities. This reactor is insubordinate to life-threatening strokes. For trimming of fuel use and amount of waste, higher burn off is occurred. New nuclear power plants integrating Advanced Light Water Reactor (ALWR) technology overpowers a number of regulative, economical, technological and societal disputes prior to licensing, structure, and thriving commence. In fig.8, Boundary case of main steam line break is shown as a transient analysis of reactor.

Efficacious management of low- and intermediate-level waste and radiation exposure modifies nuclear plants to maneuver safely, cost-efficaciously, and with minimum risk to plant personnel, the public, and the environment. Presently advanced nuclear power plants aspect substantial economic, environmental, regulatory and public perceptual experience forces with respect to low and intermediate-level waste (LLW) management and personnel vulnerability to irradiation. In fig.9, Steam generator tube rupture is shown as a Transient analysis of reactor.

Now, nuclear waste is greatly minified by exhausted uranium fuel is recycled and reprocessed into a newfangled quality of TRU fuel that is ingested in advanced burner reactors. It palliates long-term reposition exacts, because the waste is predominately a short-lived fission yield. This sue can protract more energy from the fuel and ensue in less waste necessitating storage in high-level depositaries.

3. Economic Prospects of Gen-4 Nuclear (EPGN)

3.1 Economizer quality and Cost Stability of Nuclear Power for Power Generation

Cost is the most significant factor while implementing a system. Though nuclear power plants have a high initial cost, the electricity production cost per kilowatt hour is significantly less than the others. The most significant factors which establish the urgency of implementing the nuclear energy is that, the cost of this energy production is stable throughout the many years while the generation of electricity by the oil and gas are moving up. Total electricity use is expected to grow by nearly 30% from 2008 to 2035 meaning more electric generating capacity is needed. Nuclear power is more economic than renewable and would help keep future consumer costs down. Many nuclear uprate projects are economic at carbon prices of less than $10 per metric ton,in terms of the cost to society per metric ton of CO2 removed, which is one-fourth to one-eighth the cost of wind generation. California Levelized energy costs for different generation

technologies (2007) is Shown here in fig.10.
Coal with carbon sequestration is 15 times as costly, and solar is up to 70 times as costly. So, from the discussion above it is crystal clear that, though initial installment of nuclear plant is high, after implementing it is cost effective and apposite reason for taking it as a future energy alternative. So, from the discussion cost factor, it is easily comprehend that, cogitating about the economy, nuclear power can be a better option for the developing countries.

3.2 Comparative Economic Studies of Fossil Fuels and Nuclear

Price Arising of Fossil fuels is a great concern to the developing and least developing countries. International fuel prices diversely affect generating costs. In the last 4 years gas price has more than doubled and it adds 19 euro per MWh and it adds CO2 cost. Coal price has increased by 60% in recent 3 years it adds 7 euro per MWh and adds CO2 cost. Uranium price has been tripled it adds 1 euro per MWh, but production cost remains stable. Based on costs of supply from Russia or from Middle East, the gas price in world could remain around 3.6 euro/GJ, but it will more likely remain bound to oil, up to 5 euro/GJ.If anticipated replacement of operating coal plants, then nuclear would be 3 times cheaper than gas per ton of avoided CO2 and this cheaper nuclear production cost will influence the developing countries to go towards nuclear. The following figures arise for the costs of electricity production in newly constructed power plants in 2010. For economic competitiveness of a Gas Cooled fast Reactor (GFR) is cooled by supercritical CO2 in a direct Brayton cycle power conversion system (PCS) is designed. Because of its compact PCS, 10% of capital costs are saved. A reduction of 5% in busbar costs is achieved because of the higher thermal efficiency of the S-CO2 cycle. Economic prospects of Advanced Nuclear Reactor are also attractive features for the developing and least developing countries.

3.3 The Financial Model for Gen-4 Nuclear Power

The underlying assumption here is that the adoption decision is made by a dynamically optimization economic agent who must choose between a fossil fuel and a nuclear plant to minimize the expected generating cost. It is assumed that the nuclear power plant project contains no risk and produces a deterministic and known cost. We denote the value of the nuclear project equals the electricity price minus the constant production cost. However, we consider that the cost of a fossil fuel power plant follows a geometric Brownian motion of the form:

$$\frac{\delta C}{C} = \xi \delta t + \phi \delta z \qquad (6)$$

The variable unit cost of a fossil fuel power plant is the only source of uncertainty in our model, the value of the investment option is function of this cost C. By a standard arbitrage argument, the project value can be satisfied the following differential equation:

$$Q(P - C) + (r - \delta)V_{GC}C = V_G - 0.5\phi^2 C^2 V_{GCC} \qquad (7)$$

The general solution to this,

$$V_{GC} = A1C^{\chi 1} + A2C^{\chi 2} \qquad (8)$$

Where,

$$\chi 1 = [(r - \delta)/\phi^2 - 0.5^2]^{1/2} - (r - \delta)/\phi^2 + 0.5$$

$$\chi 2 = -[(r - \delta)/\phi^2 - 0.5^2]^{1/2} - (r - \delta)/\phi^2 + 0.5$$

We denote by F(C) the value of the option to invest in a fossil fuel power plant. we can write write dF as:

$$\delta F = F_C \delta C + 0.5 F_{CX} (\delta C)^2 \qquad (9)$$

A riskless portfolio can be made by assuming that the option value F(C) satisfies its lemma and that the market to completely hedge the price risks exists. Then the following differential equation is obtained:

$$rF = rCF_C + 0.5\phi^2 C^2 F_{CX} \quad (10)$$

The general solution to this

$$F(C) = B_1 C^{\chi 1} + B_2 C^{\chi 2} \quad (11)$$

Equations above must be solved to get must be solved to get B_1, B_2.

$$B_1 = V_{N\chi 2} \frac{C^{-H\chi 1}}{\chi 2 - \chi 1}$$

$$B_2 = -V_{N\chi 2} \frac{C^{-H\chi 2}}{\chi 2 - \chi 1}$$

By using this financial model to study sensitivities, overnight costs of $1,200, $1,500, and $1,800 per kW are used.

4. Environmental Aspects of Gen-4 Nuclear Power (EAGN)

4.1 Environmental Impacts and Radiotoxic Dosage of Fossil Fuels

The efflorescence environmental effects ensuing from the use of fossil fuels are the discharge, during the burning action, of contents like brown ash, CO2, all oxides of nitrogen, SO2 and traces of heavy materials. Carbon dioxide (CO2), methane (CH4), nitrogen oxide (NO2) and two Chloro-Fluoro-Carbons (CFCl3 and CF2Cl2) make the ambiance hold heat and thus lead to greenhouse warming. Contamination from fossil fuels is darned for 24,000 early deaths each year in the U.S. alone. However, as with all energy sources, there is some defilement related with defend actions such as manufacturing and expatriation. In figure 11, radiotoxic dosage of fossil fuels and shielding has shown.

The National Council on Radiation Protection and Measurements (NCRP) reckoned the average out radioactivity per short ton of coal is 17,100 mill curies/4,000,000 tons in terms of net radioactive discharge . With 154 coal plants in the U.S.A, this quantities to expelling of 0.6319 TBq per year for a scoop plant, which still does not straightaway equate to the fixes on nuclear plants, as coal emissions hold long lived isotopes and have different dispersion .In terms of dosage to a human living nearby, coal plants release 100 times the radio toxicity of nuclear plants. NCRP reports estimated the dot to the population from 1000 MW coal and nuclear plants at 490 personae/ year and 4.8 person-rem/year respectively. The Environmental Protection Agency (EPA) estimates an added dose of 0.03 milli-rem per year for living within 50 miles (80km) of a coal plant and 0.009 milli-rem for a nuclear plant for annually irradiation dosage estimation. Unlike coal-fired or oil-fired generation, nuclear power generation does not directly bring forth any sulfur dioxide, nitrogen oxides, or mercury. So, for the countries where environmental contamination is of grave concern incorporated with cost factor, nuclear can be a better energy option for them.

4.2 Protecting Environment: Gen-4 Nuclear Option

Abstracted of nuclear power plants, electric alternative emanations of NOx would be 2 million tons per year higher. Nuclear energy also extends an alleviation of the globular carbon dioxide (CO2) disoblige that the world can do without. About 1,600 million tons of CO2 yearly emanations would have ensued if 16 percent of the world electricity now generated by nuclear power were to have been generated using coal Sulfur dioxide emissions would be 5 million tons a year higher. In France, for example, from 1980 to 1986, in the

power sectors, SO2 and NOx emissions were contracted by 71% and 60% respectively, causing diminutions of 56% respectively, in total SO2 and NOx emissions in France. Through the fission of uranium, nuclear energy plants develop electricity, not by the burning of fuels. In figure 12, Protecting environment by reducing confinement times via Gen-4 Tech is shown.

Another crucial gain that nuclear rendered energy has on our environment is that the wastes acquired are completely insulated from the environs. Some of these noxious heavy metals include arsenic, cadmium, lead,Sources of emission free electricity in Percentage and mercury. Though the radioactive wastes produced by nuclear energy may be life threatening for thousands of years, part of the waste caused by the burning of coal remains dangerous forever. In advanced nuclear, for generating electricity a High Efficiency and Environment Friendly nuclear Reactor(HEER) is designed to enable efficient fuel utilization and as it exhibits longer fuel cycle, thus need less refueling. For a safe environment, a 1000 MW liquid salt cooled reactor was designed that is fully environmental friendly and for that purpose, the reactor uses the binary salt NaF-BeF2 as the primary coolant and it uses U-Zr-H as fuel which are fully clean. As concerning about the environment, nuclear is a clean and environmental friendly energy.

5. Nuclear Power for Developing Countries (NPDC)

At present the developing countries account for approximately 80% of the worlds population. By 2050 it is predicted that the figure will rise to about 86%. Inadequate supply of energy hinders the socio-economic development in these countries to a great extent. At present, the energy usage in Bangladesh is 90% gas-based and a greater 42% of this limited resource is being utilized for electricity generation as depicted in Fig. 5 drawn on the basis gas consumption in different sectors of Bangladesh on a particular day in May 2009. According to an estimate, electricity demand is likely to grow by 15% in the next 15 years, meaning the country will have to increase the capacity to 8,000 MW by 2025. Present day gas resources suggest that the country will face deficit of 142 million cubic feet per day (mmcfd) in 2011 and it will rise to 1714 mmcfd by 2019-20. The country will need to add 19,000 MW of additional power, causing the gas demand to spiral up to 4,567 mmcfd by 2019- 20.Even if Bangladesh's GDP growth remains as low as 5.5 percent till 2025. Hence dependence on gas would further exhaust this natural resource in the years to come, which would in the long run impede industrial growth and economic development. Energy from conventional sources should be searched on priority basis in developing countries. Electricity generation should be based on a source that can support large scale production, long term security and environment friendly solutions. As had been discussed in the previous sections, productive utilization of nuclear energy has minimal impact on environmental pollution and also the costs are low as far as long term solutions are concerned. So nuclear power generation is the ultimate solution for the least developed countries to meet the growing demand of energies in the years to come.

6. Conclusion

Speculating about diverse viewpoints, it is clear that, succeeding energy for the world is nuclear. For having a carbon emission free environment, nuclear is a just alternative. Considering the cost of energy generation, electricity production and for replenishment of energy crisis, energy future lie down towards nuclear. Our analyze settles that in order to obtain a long term solution to the ongoing energy crisis, it is important for the world to formulate frameworks for nuclear energy based electricity generation in the near future. In spite of the environs well-disposed nature and renewability of sources like solar, wind, biomass or geothermal energy resources, these sources cannot serve as a long term cost effective nostrum to energy crisis in the years to come. By devising and comparing about cost factors, environmental issues, power generation efficacy and fossil fuel replacement benefits, nuclear can be good option as a energy source for developing countries. Appropriate safety measures with complimentses to nuclear power can emphatically and unquestionably provide environment friendly, cost effective, sustainable solutions to the problem of energy crisis and thereby help the world to excise its future energy exact.

References

Energy Information Administration (EIA)s, Annual Report, 2006.

World Energy Outlook , Annual Report, 2006-2008.
C. Flavin and M. H. Aeck, “Energy for development the potential role of renewable energy in meeting the millennium development goals” in Worldwatch Institute, 2007.
A. Burgio, N. Scordino, Members, IEEE, “Energy Resources And Environmental Protection: The Nuclear Option”, in Seminar on Population Growth, Sustainable Development, 2008.
W. Turner and J. W. Nuclear , “Nuclear Energy five Role In A More Sustainable Future Electricplc”, United Kingdom.
P. Riley, “Nuclear Energy: A Sustainable Future”,in IEEE conference on Energy & Power.
The WIKIPEDIA (2011) website [online], Available: http://en.wikipedia.org/
The European Energy Forum Website [Online], Available: http://www.europeanenergyforum.eu/
R. Azuma, Y. Baillot, R. Behringer, S. Feiner, S. Julier, B. MacIntyre, “Recent advances in augmented reality”in IEEE ComputerGraphics and Applications, vol. 21, issue no. 6, 2001, pp. 34-47.
Bjorn Wahlstrom, Bernhard Wilpert, Sue Cox, Rosario Sola, Carl Rollenhagen, “Learning Organizations for Nuclear Safety” in IEEE 7th Human Factors Meeting Scottsdale Arizona, 2002.
Rheinisch-Westflischen Institute for Economic Research -RWI, Report on 2007.
The European Energy Forum Website [Online], Available: http://www.europeanenergyforum.eu/
Andreas Eursch, “Increased Safety for Manual Tasks in the Field of Nuclear Science Using the Technology of Augmented Reality” in IEEE Nuclear Science Symposium Conference, 2007.
Syed Bahauddin Alam, Hussain Mohammed Dipu Kabir, A B M Rafi Sazzad, Khaled Redwan, Ishtiaque Aziz, Imranul Kabir Chowdhury, Md. Abdul Matin, Can Gen-4 Nuclear Power and Reactor Technology be Safe and Reliable Future Energy for Developing Countries? In 2010 IEEE International Power and Energy Conference, PECON 2010, pp. 95-100, Malaysia, 29 Nov, 2010.

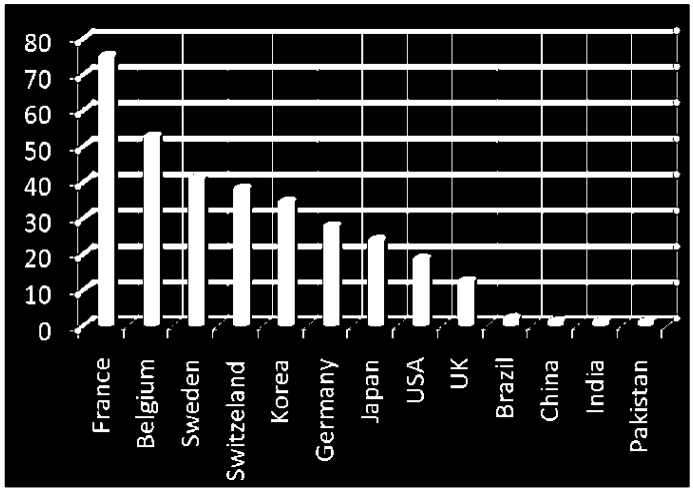

Fig.1. Percentage Use of Nuclear Power for electricity generation in different countries

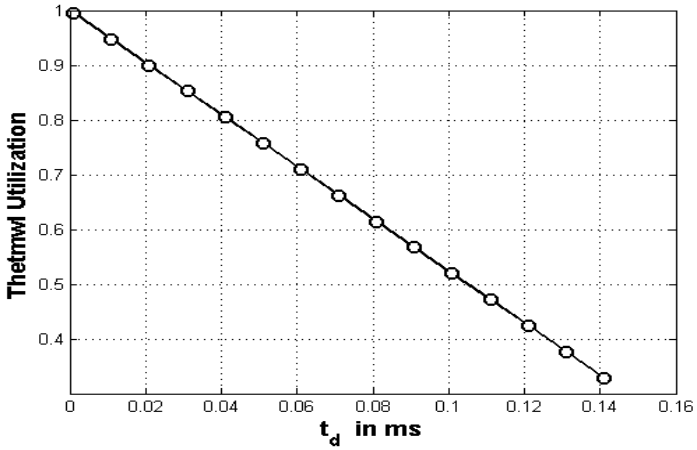

Fig.2. Thermal utilization

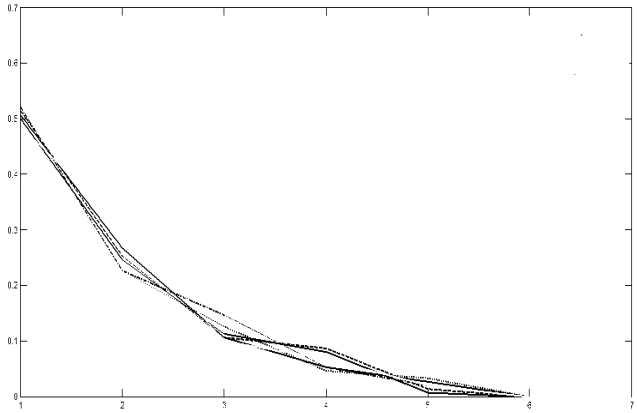

Fig.3. Decay of neutron lifetime

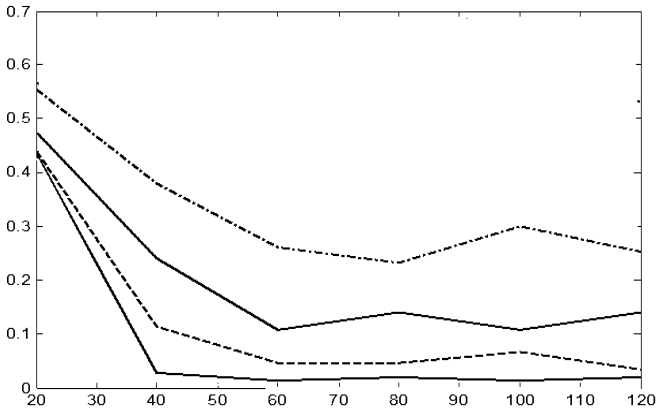

Fig.4. Radioactive decay for heavy particles via kinetics model

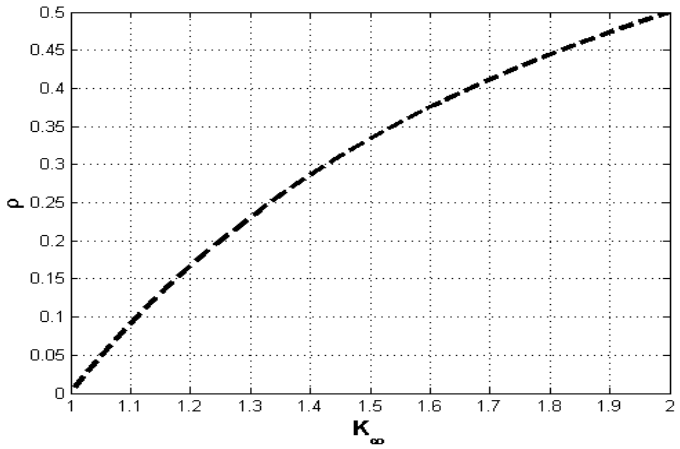

Fig.5. Reactor Kinetics for Delayed neutrons

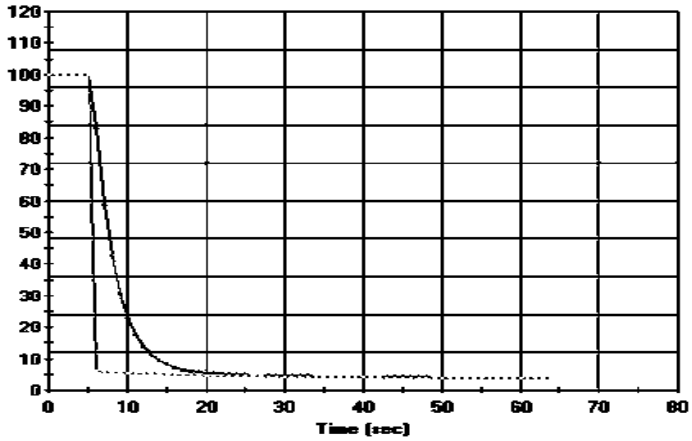

Fig.6. Loss of electric load

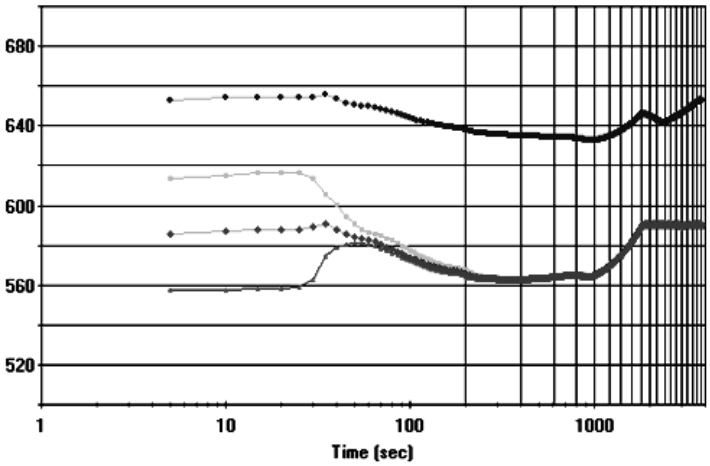

Fig.7. Loss of normal feed water in Log scale

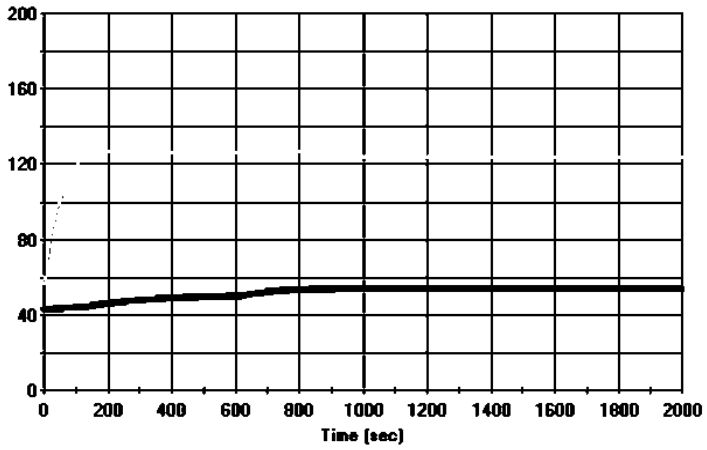

Fig.8. Boundary case of main steam line breaks

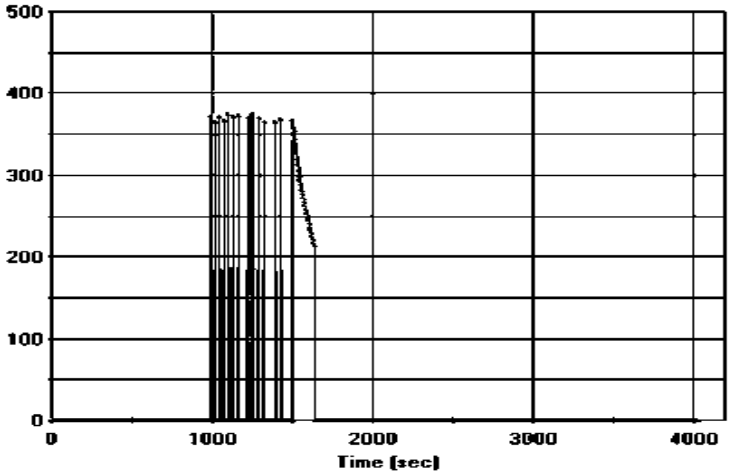

Fig.9. Steam generator Tube Rupture

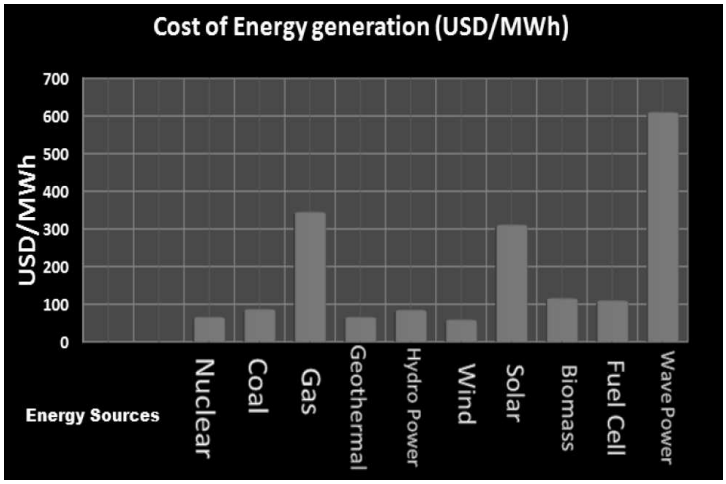

Fig.10. Levelised Energy Cost for Different Generation Technologies

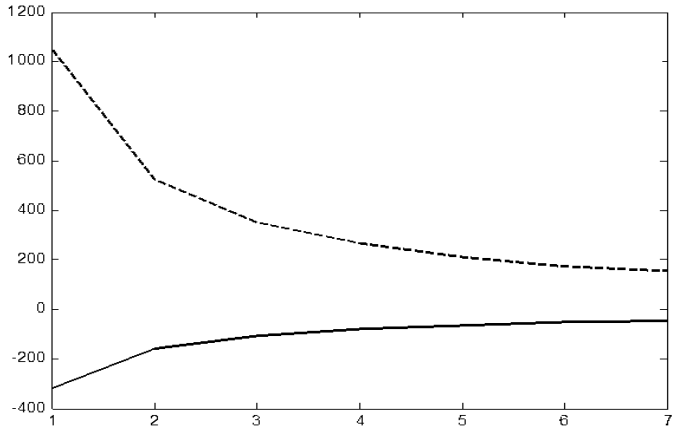

Fig.11. Radiation shielding

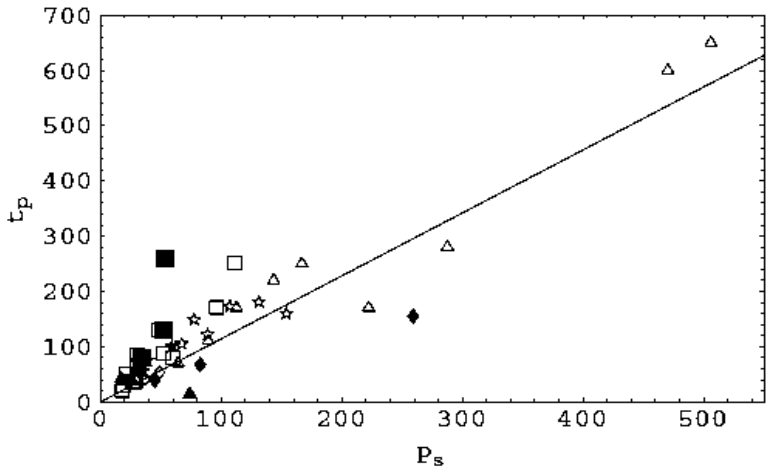

Fig.12. Loss of confinement times

Journal of Energy Technologies and Policy
ISSN 2224-3232 (Paper) ISSN 2225-0573 (Online)
Vol.2, No.1, 2011

Design, Modeling and Performance Investigation of GC PVGS

K.Rajambal, G.Renukadevi, N.K.Sakthivel
Department of Electrical Electronics Engg , Pondicherry Engineering College , Pondicherry ,India
* E-mail of the corresponding author: renunila_1977@yahoo.com

Abstract

This paper proposes a new topology for the power injection system that is based on the parallel association of two voltage source inverters: one is operated using a quasi-square voltage waveform strategy and the other operates with a PWM based strategy. The aim of this topology is that the quasi-square inverter injects the power from the photovoltaic generation system and the PWM inverter controls the current quality. The proposal optimizes the system design, permitting reduction of system losses and an increase of the energy injected into the grid.

Keywords: quasi square wave inverter, pulse width Modulation inverter, photo voltaic power system, modulation Index (M).

1. Introduction

Since the start of the industrial age more than 150Years ago, the world economy was running on fossil fuels, which were cheap as there was no cost associated with their Production, but only with their extraction and transportation. The negative effects on the environment became visible only in the last 30 years. Renewable energy resources will be increasingly important part of power generation in the new Millennium. Besides assisting in the reduction of the emission of greenhouse gases, they add the much needed flexibility to the energy resource mix by decreasing the dependence on Fossil fuels. Due to their modular characteristics, ease of the Installation and because they can be located closer to the user photovoltaic (PV) systems have great potential as distributed power source to the utilities. PV systems are installed on the roof of the residential buildings and connected directly to the grid.(called grid-tie or grid-connected). A grid-tied PV system consists of two main stages a PV module and power injection System as shown in Figure. 1. In these PV systems , power Conditioning system (PCS) should have high efficiency and Low cost The power generated from the renewable energy systems are tied to the utility grid (Doumbia 2004) and (Jih-heng Lai 2003). In remote places where there is less/no feasibility of utility grids, renewable energy Systems provides electricity to the isolated region. These isolated renewable energy systems can be employed to power residential applications. For renewable energy sources, the output voltage and power typically depends on a variety of uncontrollable factors. for example: radiation intensity determines the obtainable voltage and power output of a solar panel, wind speed determines voltage and power of a wind electrical generator; and the output Voltage and power of a fuel cell changes with the operating temperature, fuel and air flow rates (Detrick 2005) to (DeSouza 2006). To obtain the required voltage output for varying input conditions, power conditioning Systems (PCS) are introduced as interfacing scheme between the PV panels and grid . The existing power conversion topologies used in power conditioning system consist of boost converter and a pulse width modulation inverter or a multi level inverter. The boost converter enhances the low voltage output from the renewable energy sources during low input conditions And the inverter converts the dc power into ac of required voltage and frequency. The two stage conversion system also increases the system cost and decreases the efficiency of the system. In this project, an inverter topology without the intermediate dc-dc converter has been presented. This scheme reduces the system losses and increases the efficiency and increase of the

energy injected into the grid. The proposed inverter is designed for a kW photovoltaic generation system. Photovoltaic generation scheme along with the inverter is simulated in MATLAB/Simulink. Simulation is carried out to study the power flow characteristics for varying solar intensities and modulation indices and the results are presented.

2. Description of the Pvgs with QSWI-PWM Inverter

Fig.1 shows the inverter topology. This Photovoltaic Generation system presents a topology of the power injection system (PIS) that has the function of injecting the power produced by the photovoltaic cell groups, converting the energy from the original DC form to the final AC form with the desired electrical characteristics. The part of the PIS that carries out this conversion is the inverter (Carrasco 2006) .Usually, Pulse width modulation (PWM) based inverters (Kwon 2006) or multilevel topology inverters are used (Gupta 2006). In this paper a new topology for the PIS is presented based on the parallel association of two voltage source inverters. (VSI): one is operated using a quasi-square voltage waveform strategy (quasi-square waveform inverter, QSWI).It can be operated with the operating frequency of grid frequency (50Hz) and the other operates with a PWM based strategy (high-switching-frequency inverter, HSFI).and this inverter can be operated as high switching frequency of 20kHz.The general purpose of the QSWI is to inject the power generated by the PVGS into the grid. In order to achieve this, controlling the fundamental component of the inverter and that of the HSFI is to be responsible for controlling the quality of the current injected into the grid. The mathematical modeling of the various system components are discussed below:

(a) Modeling Of PV Cell

The characteristics of a solar cell relating the cells voltage to current are expressed by the equations, that are given below ,The PV cell output current is given as,

$$I_{pv} = I_{ph} - I_0[\exp(\frac{q(V_{pv} + I_{pv}R_s}{AKT}) - 1] \quad \text{..... (1)}$$

The PV cell output voltage is given as,

$$V_{pv} = \frac{AKT}{q}\ln(\frac{I_{ph} - I_{pv} + I_0}{AKT}) - I_{pv}R_s \quad \text{……..(2)}$$

The light generated current is given as,

$$I_{ph} = [I_{scr} + K_i(T - 298)]\lambda / 100 \quad \text{…… (3)}$$

The saturation current is given as,

$$I_0 = I_{or}(\frac{T}{T_r})^3 \exp[\frac{qE_{go}}{BK}(\frac{1}{T_r} - \frac{1}{T})] \quad \text{…….. (4)}$$

(b) Power Injection System

A direct connection to the inverters without a previous DC/DC converter has been chosen. The upper inverter in the figure.1 (inverter 1) is the Quasi Square Wave Inverter and the lower inverter (inverter 2), is the High Switching Frequency Inverter. Both inverters share the same DC bus, which is connected to the PVGS. The capacitor between the PVGS and the PIS must absorb the active power fluctuations (that always exist in a single-phase system). Therefore it achieves constant power extracted from the PVGS, by

keeping the DC voltage at the output terminal of the PVGS constant under these power fluctuations. The QSWI is responsible for injecting the energy produced by the PVGS. This inverter deals with high currents but at low switching frequency (50-60 Hz), resulting in lower losses than if the inverter is operated with a PWM technique. This inverter injects a current with a high total harmonic distortion (THD) into the grid. The PWMI is connected in parallel with the QSWI and working as a part of the PIS and its corrects the current produced by the QSWI improving its THD.The PWMI (working as APF) not only can correct the QSWI current, but also correct the current demanded by a non-linear load connected to the same point of common coupling (PCC) than the PVGS. (Usually between 10 to 20 kHz).

(C) Design of Inductance

The QSWI inductance value (L1) must be selected to permit the injection of the maximum power That the PVGS can generate (which depends on the irradiance and temperature conditions).The power injected into the grid from the PVGS (neglecting the PIS losses),

$$P_S = V_S I_{S,1} = P_{PVGS} \quad \text{…….…….. (5)}$$

As the current is in phase with the grid voltage. The RMS fundamental current component injected by the QSWI (I1) can be determined by ,

$$I_1 = \frac{\sqrt{V_1^2 - V_S^2}}{L_1 \omega} \quad \text{…..…….…… (6)}$$

From that two equations we get,

$$L_1 = \frac{V_S}{\omega P_{PVGS}} \sqrt{V_1^2 - V_S^2} \quad \text{…….…….. (7)}$$

The inductance with proposed DC voltage is given by,

$$L_1 = \frac{V_S}{\omega P_{PVGS}} \sqrt{(0.9 V_{dc} \cos\frac{\pi}{6})^2 - V_S^2} . \quad \text{…… (8) and,}$$

$$L_2 = \frac{V_{dc} - \sqrt{2} V_S}{i_{2,slope}} \quad \text{..…..…… (9)}$$

The coupled inductors enable the advantage of, output ripple current reduction due to AC magnetic field cancellation within the inductor core. Improved efficiency due to lower peak currents. Reduction in required output capacitance. Faster transient response due to the ability to use lower effective inductance values. Reduced overshoot or undershoot during load transients. Frequency range up to 2 MHZ.

3. Simulation Results

The individual models of the PV array and inverters are simulated and their characteristics are studied. Then the models of PV array and inverters are integrated along with grid and simulation is carried out to study the power flow characteristics for varying solar intensities. The effect of modulation index is studied

and the optimum modulation is identified for different solar intensities for maximizing the power output. The simulation results are discussed below,

(a) Characteristics of the PV module.

The model equations (1) - (4) of the PV cell detailed in section II (a) are used to obtain the I-V characteristics of the PV module given in appendix. Figure.2 shows the I-V characteristics for varying solar intensities at constant temperature of 25°C.It observed that the current increases with increase in intensity thereby increasing the power output of the solar cell. It is observed that the PV array generates 550V Voltage and 8.8A current at the rated intensity of 100mW/cm² with 34 modules in series and 2 modules in parallel. Figure.3 shows that I-V characteristics for varying temperature at rated intensity of 100mW/cm².It is observed that the current variation for marginal temperature variation from 25°C to 65°C.The output power versus power characteristics of the PV array for different intensity is shown in Figure.4 It is observed that the power increases with increasing voltage and reaches a maximum value and starts decreasing for any further increase in voltage. It is also seen that the output power increases with increasing intensity.

(b) PIS results

The quasi square wave inverter and pulse width modulation inverter are modeled in MATLAB-SIMULINK. The performance of the grid connected PIS which includes PWM and QSW Inverters are studied for different modulation indices. Figure.5 shows the firing pulses for Quasi Square Wave Inverter. A reference sine wave of 50Hz is compared with constant dc voltage to generate the firing pulse. The output voltage is varied by controlling the width of the pulse. In this switching scheme, the positive and negative half cycles are present for an interval less than the half the period of the output frequency. The QSWI is responsible for injecting the energy produced by the PVGS. The steady state voltage and current waveforms of the inverter are presented in Figures.6&7. It is seen that peak current of the QSWI is about 17 A without the controller. A reference sine wave of 50Hz is compared with triangular wave of 20 kHz to generate the firing pulse. The width of each pulse varies as a sine fashion. The frequency of the reference determines the output frequency of the inverter. The number of pulses in each half cycle depends on the carrier frequency. The output voltage is controlled by adjusting the modulation index. The PWMI is connected in parallel with the QSWI and working as a part of the PIS and its corrects the current produced by the QSWI improving its THD are seen from Figure.11. The main advantage of the proposed system is the inverter loss decrease, because the QSWI has low losses which are due principally to conduction. The switching losses are small because the switching frequency matches the grid frequency, near 50Hz. The conduction losses could be even further reduced if a low ON- voltage semiconductor is selected, since no high speed switching semiconductors are needed for this inverter. But also losses in the HSFI (principally due to the switching losses) decrease notably, because the current levels for this inverter are lower than those produced if it was working alone (without the QSWI cooperation). This can be observed in Figure.10. Where the maximum instantaneous current value is lower than 3 A, a value that is significantly lower than the maximum value of 15 A for the total injected current, Figure.11. If one assumes that the switching losses are proportional to the maximum instantaneous current value, these losses will be reduced to approximately 20%. Therefore the high switching semiconductors used in this inverter will have a current ratio of about five times lower than the semiconductor used in a conventional PWM inverter for the same task. The reduction in losses allows one to use a smaller aluminium radiator. Furthermore, the QSWI inductor can be built with a conventional core coil designed for a working frequency of 50 Hz (ferromagnetic core and conventional cupper wire), and the HSFI inductor can be built with an air core coil with smaller section cupper wire (usually special cupper wires must be used due to the high switching frequency), because the RMS current value is smaller than if it operates alone.

4. Control system

The PIS control can be divided into the blocks shown in the schematic diagram of Figure. 12.

(a) Maximum Power Point Tracking (MPPT) block:

The objective of this block is to set and to maintain the PVGS at its maximum power point (MPP). When the PVGS is working at this point, one hast that,

$$\frac{dP_{PVGS}}{dV_{PV}} = 0 \qquad \text{…….. (10)}$$

The MPPT scheme is shown in Figure. 13. In the proposed system, this condition is achieved by considering the power derivative as the error input of a proportional integral (PI) controller. In this way if the PI controller is well-designed, the power derivative will become zero in the steady state and the MPP will be tracked. A saturation function has been included to prevent the improper operation of the integral part of the controller during start-up transients. A low-pass filter is included to eliminate the components in the power derivative due to the switching frequency.

(b) Reference Supply Current Generation Block

This is the principal block of the proposed control system, because it guarantees that the current extracted from the PVGS is the desired one and so the MPP is tracked. The RMS value of the fundamental current component that must be injected into the grid is determined by neglecting the PIS losses:

$$I_{S,ref} = \frac{V_{PV} I_{PV,ref}}{V_S} \qquad \text{…….. (11)}$$

This reference current value is tuned by the output of an additional PI whose input is the error between the reference current that must be extracted from the PVGS(determined by the MPPT block) and the actual one(measured from the system). The aim of this tuning is to compensate the system losses that have not been considered in (11).The RSCG block contains a synchronization module in fig.14. that generates two sinusoidal signals with unity RMS value, which are in phase (the first one) and in quadrature (the second one) with the fundamental grid voltage component, and an RMS grid voltage fundamental component calculation module .As a result the reference supply current is a sinusoidal wave in phase with the grid voltage, and its RMS value is equal to that given by (11).

(c) Signal Generation for Inverter 1

This block implements the collaboration between the two inverters and their principle of operation was described in above. Figures 15 and 16 shows the schematic diagram for each inverter. In Figure.15 the function block “Fcn” implements equation (11) , and the function block “Fcn1” is used to avoid values greater than 1 for the arc cosine function of this equation.

(d) Switching Signal Generation for Inverter 2

The QSWI is operated in a quasi-open-loop obtaining the value of β from the reference supply current (determined in part B), not its measured value. The HSFI switching signals are generated based on the error existing between the reference supply current and the measured one, by using a hysteresis band that compares the error with zero for a fixed sample period (Figure.16).

5. Controller results:

The closed loop control systems are simulated with the parameters given in Appendix. The simulation results of the PVGS and Inverter are studied individually and the overall system performance for varying solar intensities and modulation indices are observed. From Figure.17 to 21 shows that the performance of the PVGS and the grid connected system results of the both inverter currents are simulated at rated intensity of 100mW/cm². The main advantage of the proposed system is the inverter loss decrease, because the QSWI has low losses which are due principally to conduction. The switching losses are small because the switching frequency matches the grid frequency, near 50Hz. The conduction losses could be even further reduced if a low ON- voltage semiconductor is selected, since no high speed switching semiconductors are needed for this inverter. But also losses in the HSFI (principally due to the switching losses) decrease notably, because the current levels for this inverter are lower than those produced if it was working alone (without the QSWI cooperation). This can be observed in Figure. 21. Where the maximum instantaneous current value is lower than 3 A, a value that is significantly lower than the maximum value of 15 A for the total injected current shown in Figure.22. If one assumes that the switching losses are proportional to the

maximum instantaneous current value, these losses will be reduced to approximately 20%. Therefore the high switching semiconductors used in this inverter will have a current ratio of about five times lower than the semiconductor used in a conventional PWM inverter for the same task. The reduction in losses allows one to use a smaller aluminium radiator. Furthermore, the QSWI inductor can be built with a conventional core coil designed for a working frequency of 50 Hz (ferromagnetic core and conventional cupper wire), and the HSFI inductor can be built with an air core coil with smaller section cupper wire (usually special cupper wires must be used due to the high switching frequency), because the RMS current value is smaller than if it operates alone. The total inductor losses will be lower: (a) the electric losses in inductor of inverter 1 decrease because it has a lower resistance (R1) then if it had been built with air core coils (because far fewer turns of copper wire are needed). Ferromagnetic losses will be small since the operation frequency is 50 Hz.(b) the electric losses in inductor of inverter 2 decrease too, because the RMS of the current that flows through it(I 2) is reduced by five times Although the cost could seem to increase due to the more complex topology and control and to the higher number of semiconductors needed, others factor related to cost should be taken into account: decrease in losses and so decrease in the size of the aluminium radiator, possibility of using ferromagnetic core inductors for filtering the greater fraction of the current (this inductors are about 30% less expensive than air core inductors), possibility of using slower semiconductors (so cheaper devices) for the greater current fraction, and using lower rating high frequency semiconductors (because they operate with a lower current fraction).

6. Experimental results:

The prototype model of this scheme has been implemented in hardware. The prototype model has been tested with a laboratory Prototype (Figure.23) solar module (supplying 12 VDC) is connected to a four branches inverter (MOSFET-IRF840) and it can be connected into the load. The results are shown in Figure. 24 to 29.The proposed PIS behaves as in the simulation setup. The output voltage of the 15W PV module is found to vary from 15.07V to 18.09Volt over a day. The corresponding output voltages of the inverter voltage are varying from 11.8V to 13.2Volt.The output voltage and current waveform are observed and presented. The hardware results are compared with the simulation results. It is found that the hardware a result closely matches with the simulation results, thus validating the simulation model of the grid connected PVGS.

7. Conclusion

The power characteristics of the photovoltaic generation system is investigated for varying solar intensisties.The power output of the photovoltaic module, the voltage and currents of the inverters and the power export to the grid are observed for different intensities. The effect of modulation index is studied and the optimum modulation is identified for every solar intensities for maximizing the power output. A closed loop control is designed to maximize the power output for varying intensities. The proposed system optimizes the system design, permitting the reduction of the system losses (conduction and switching losses, and Joule effect losses in inductors) and so increases the energy effectively injected into the grid. There will consequently be an increase in profit when selling this energy.

APPENDIX

PV Generation System

Parameter	Value

Number of series connected cells	34
Number of parallel connected cells	2
Photovoltaic cell reference	SHELL BP150-P
MPP current (25°C, 100mW/cm²)	8.8A
MPP voltage (25°C, 100mW/cm²)	550V
Power rating at rated intensity of 100(mW/cm²)	3kW

Power Injection System

Filter inductance L1	50mh ×2
Filter inductance L2	25mH ×2
Switching frequency	20 kHz

REFERENCES:

Doumbia.M.l.,Agbossou, K.;Bose, T.K.(2004), “Islanding protection evaluation of inverter-based grid-connected hybrid renewable energy system, Electrical and Computer Engineering",1081-1084

Jih-heng Lai (2003), “Power Electronics applications in renewable energy system”, Industrial Electronics Society, IECON.

Detrick, A. Kimber, and L.Mitchell (2005), “Perfomance Evaluation Standards for Photovoltaic Modules and Systems,” proceedings of the 31th IEEE Photovoltaic Specialists Conference, Lake Buena Vista, FL.

Armenta-Deu.C (.2003) “Prediction of battery behaviour in SAPV applications Renewable Energy” 28:1671-1684.

K.C.A.deSouza,O.H.Goncalves,D.C.martins(2006). “study and optimization of two dc-dc power structures used in a grid- connected photovoltaic system”,power electronics specialists conference,PESC06,pp.1-5

Carrasco. J.M, Franquelo, L.G, Bialasiewicz. J.T, Galvan, E, Portillo-Guisado. R.C, Prats.M.A.M, Leon., J.I, Moreno-Alfonso.N (2006), “Power-Electronic Systems for the Grid Integration of Renewable Energy Sources: A Survey”. IEEE Transactions on Industrial Electronics, vol. 53, issue 4, pages:1002 - 1016.

Weidong Xiao, Ozog, N.; Dunford.W.G (2007) “Topology Study of Photovoltaic Interface for Maximum Power Point Tracking”. IEEE Transactions on Industrial Electronics, vol 54, issue 3, pages 1696 – 1704.

Kwon.J.-M, Nam.K.-H, Kwon.B.H (2006), “Photovoltaic Power Conditioning System with Line Connection”. IEEE Transactions on Industrial Electronics, vol. 53, issue 4, pages 1048- 1054.

Gupta.A.K, Khambadkone.A.M (2006). “A Space Vector PWM Scheme for Multilevel Inverters Based on Two-Level Space Vector PWM”. IEEE Transactions on Industrial Electronics, vol. 53, issue 5, pages 1631 – 1639.

Rico, Amparo,Cadaval, Enrique Romero; Montero, Maria Isabel Milanes (2007) “Power Injection Control System and Experimental Model based on Manufacturer Characteristic Curves for a Photovoltaic Generation System”. Compatibility in Power Electronics,CPE '07, pages 1 – 7. May 29 2007.

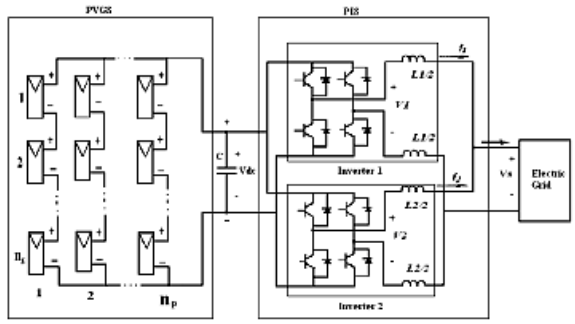

Figure.1. Power Conditioning System for a Grid connected Photovoltaic System

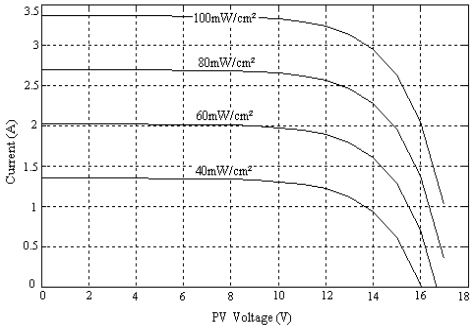

Figure.2 I-V characteristics of PV module for varying solar intensities at rated cell temperature

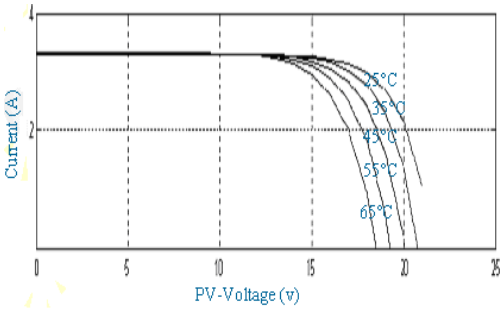

Figure.3 I-V characteristics of PV module for different cell temperature at rated intensity

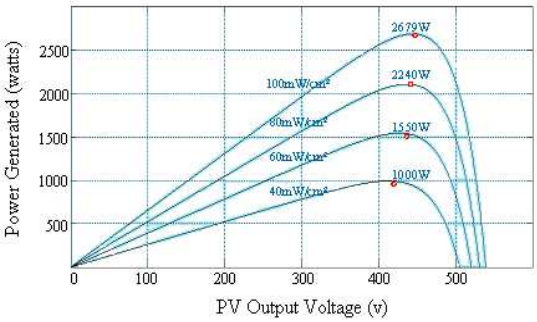

Figure .4 Power characteristics for various solar intensities at rated cell temperature

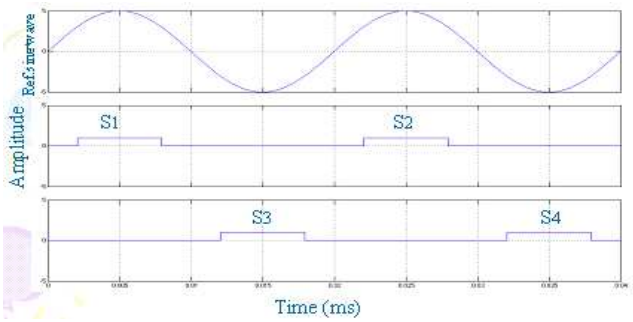

Figure.5. Firing pulse for QSWI

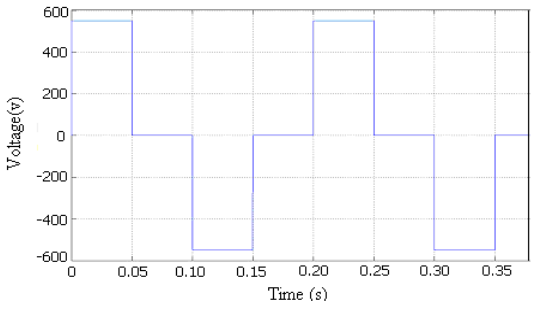

Figure.6. Quasi Square Wave Inverter Voltage

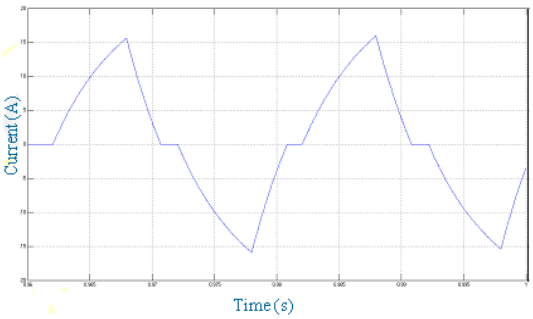

Figure.7. Quasi Square Wave Inverter Current

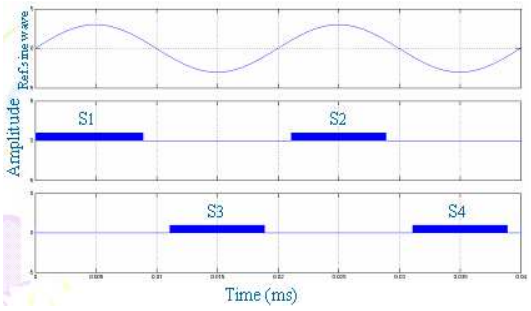

Figure.8. Firing pulse for PWMI

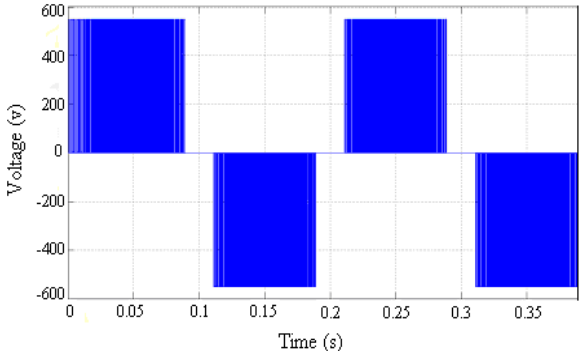

Figure.9.Pulse Width Modulation Inverter Voltage

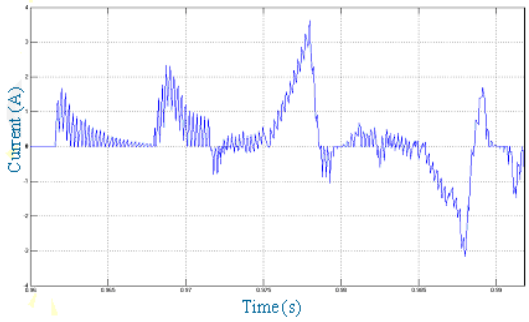

Figure.10. High Switching Frequency Inverter

Current

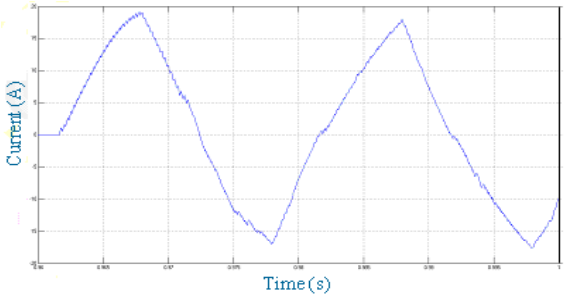

Figure.11. Current Injected into the grid

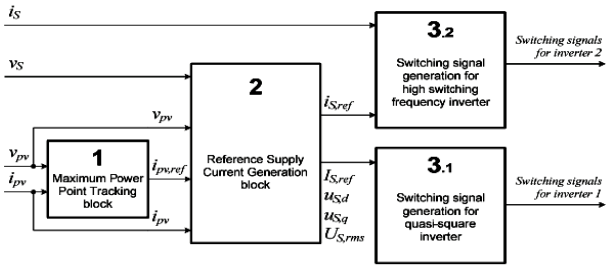

Figure.12 Maximum Power Point Tracking (MPPT)

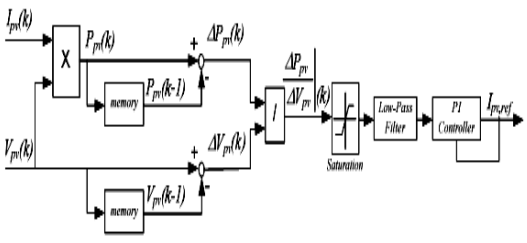

Figure.13 MPPT scheme

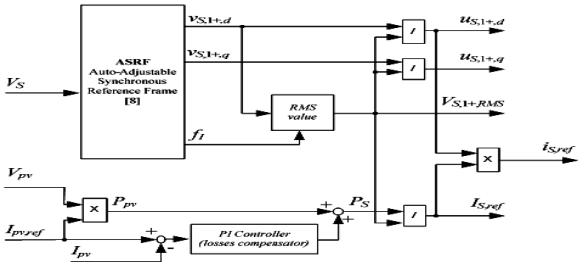

Figure.14.RSCG block contains a synchronization module

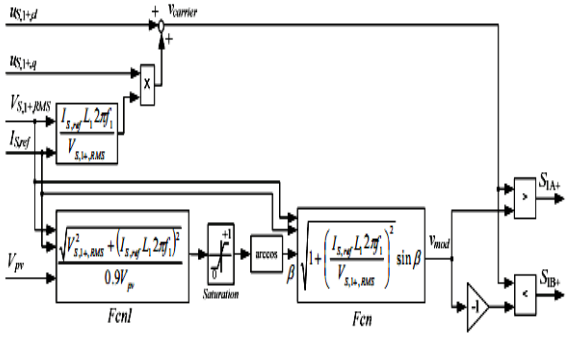

Figure.15. Inverter Switching

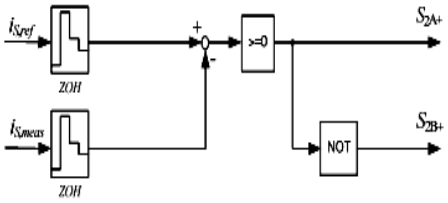

Figure.16. Inverter Switching

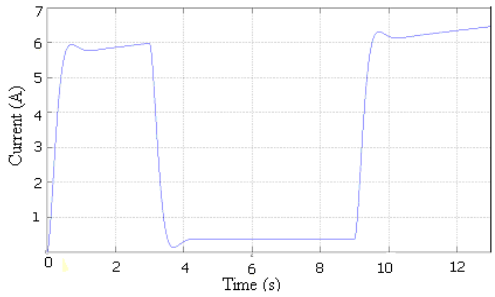

Figure.17 PVGS Current at 100mW/cm²

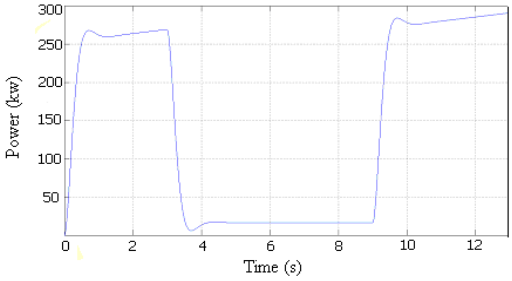

Figure.18 Power Extracted from the PVGS

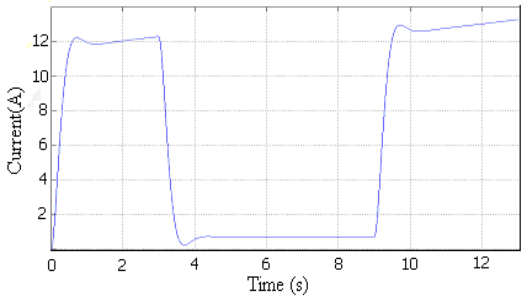

Figure.19 Supply reference current rms

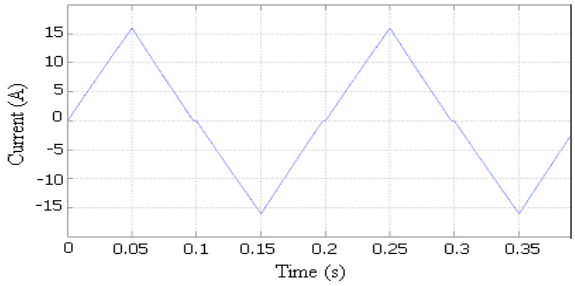

Figure.20.Quasi Square Wave Inverter Current

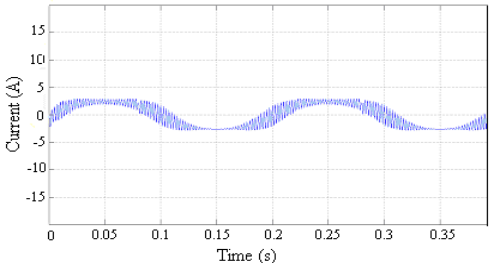

Figure.21. High Switching Frequency Inverter Current

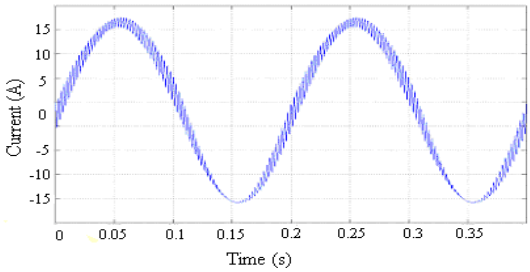

Figure.22.Current Injected into the grid

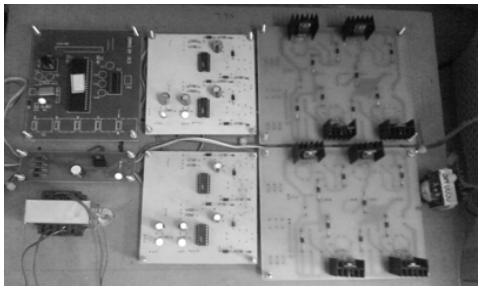

Figure.23. Hardware setup

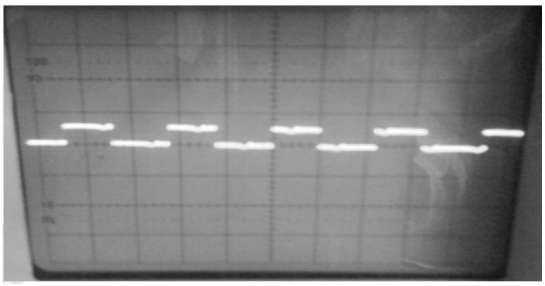

Figure.24. Firing pulse for QSWI

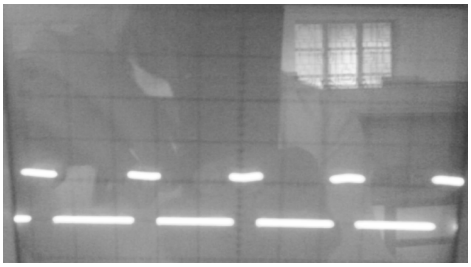

Figure.25. Firing pulse for PWMI

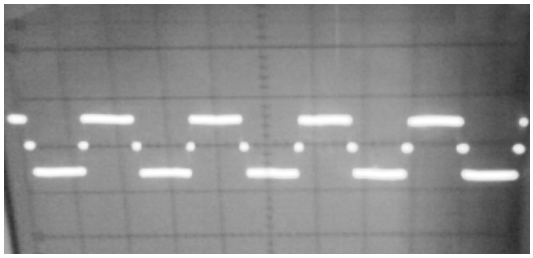

Figure.26. Quasi Square Wave Inverter Voltage

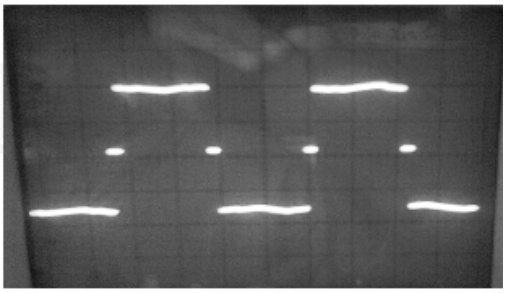

Figure.27. Pulse Width Modulation Inverter Voltage

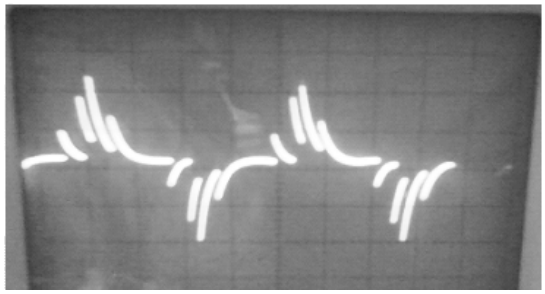

Figure.28. High Switching Frequency Inverter Current

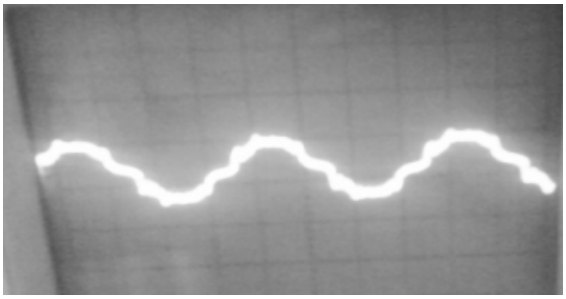

Fig.29. Load Voltage

Table 1

DC VOLTAGE	AC VOLTAGE	CURRENT	POWER
15	12.2	0.51	6.22
16	12.8	0.65	8.32
17	12.9	0.67	8.64
18	13.5	0.69	9.31

Table 2

TIME	DC VOLTAGE	AC VOLTAGE (Peak)	AC VOLTAGE (Rms)	CURRENT	POWER
9.30 am	15.07	16.68	11.8	0.49	5.78
10.30 am	15.19	17.53	12.4	0.54	6.69
11.30 am	16.16	18.10	12.8	0.62	7.93
12.30 pm	16.27	18.24	12.9	0.64	8.25
1.30 pm	18.09	18.66	13.2	0.66	8.71
2.30 pm	17.92	17.67	12.5	0.64	8.00
3.30 pm	15.08	16.68	11.8	0.60	7.08
4.30 pm	11.83	11.03	7.8	0.5	3.9

Bibliography of authors

K.Rajambal received her Bachelor of Engineering in Electrical & Electronics, Master of Engineering in power electronics and Ph.D in Wind Energy Systems in 1991, 1993 and 2005 respectively from Anna University, Chennai, India. She is working as a Associate professor in the Department of Electrical and Electronics in Pondicherry Engineering College,Pondicherry, India. Her area of interest includes in the fields of Wind Energy systems and Photovoltaic Cell, Power Converter such as DC-DC Converters, AC-AC Converters and Multilevel Inverters with soft switching PWM schemes and power electronics application towards power systems. She has published papers in national, international conferences and journals in the field of non renewable energy sources and power electronics.

G.Renukadevi received her Undergraduate Degree in Electrical Engineering from The Institution of Engineers, India in 2006 and Master of technology in Electrical Drives and Control from Pondicherry Engineering College, Pondicherry, India in 2009. Now pursuing Ph.D in Pondicherry Engineering College, Pondicherry, India. Her field of interest is power electronics, Drives and control, Modeling, AI techniques and control systems.

N.K.Sakthivel received Master of technology in Electrical Drives and Control in 2010 from Pondicherry Engineering College, Pondicherry, India in 2009.His field of interest is power electronics, renewable energy and control systems.

Journal of Energy Technologies and Policy
ISSN 2224-3232 (Paper) ISSN 2225-0573 (Online)
Vol.2, No.1, 2011

Dynamic linkages between transport energy and economic growth in Mauritius – implications for energy and climate policy

Riad Sultan

Department of Economics and Statistics, University of Mauritius, Reduit, Mauritius

Email: r.sultan@uom.ac.mu

Abstract

The consumption of fossil fuels in the transport sector represents the fastest growing source of greenhouse gases in the world – a major source leading to global warming. While action is needed to restrict the use of fossil fuels, such a conservation policy relies on the relationship between energy and economic growth. The paper investigates the causal relationship between economic growth and transport energy in Mauritius for the period 1970-2010 using an aggregate production framework with real investment. Gasoline and diesel are analyzed separately. The bounds test cointegration approach is applied and the error correction representation concludes that there is a unidirectional Granger causality running from economic growth to transport energy in the long-run. A rise in transport energy is, therefore, expected with economic progress. This result is attributed to discretionary mobility arising from high standard of living. However, bi-directional causality is found between transport energy and real investment. Restricting transport energy may therefore be detrimental to real investment and long-run growth in Mauritius.

1. Introduction

The society is currently dumping around 800 tonnes of carbon dioxide - the most important greenhouse gases (GHGs) - into the atmosphere each and every second, and forecasts indicate that the rate will increase to 1600 tonnes a second by about 2050 (Palmer 2008). Given the slow atmospheric carbon absorption, such emissions act as a stock pollutant and its concentration is likely to raise the earth average temperatures (Boko *et al*. 2007). Evidence from the Intergovernmental Panel on Climate Change (IPCC) clearly shows that changes in climatic conditions are expected as greenhouse gases accumulate (IPCC 2007). Greenhouse gases come mostly from the use of energy which is central to economic activity. There is, in fact, an overwhelmingly scientific consensus that action is needed to restrict the use of fossil fuels (Chapman 2007). The transport sector is among the main sectors which represent the fastest growing source of GHGs, partly because it plays an important role in economic activities (Wright & Fulton 2005; Abmann & Sieber 2005).

Given the role of the transport sector in the economy, development strategists face a dilemma since economic growth is desirable but not its negative effects. Sustainable transport strategy must take into account the rising demand for fossil fuels and the negative effects of carbon emissions at the same time (Abmann & Sieber 2005). Various measures have been proposed for sustainable transport to be in line with climate policy. Options for sustainable transport as reviewed by Abmann & Sieber (2005) include the use of renewable energy, such as bio-fuels, and the restriction of transport demand through economic instruments such as fuel or carbon taxes. In short, strategies for sustainable transport can be broadly classified into two policy measures –renewable energy development versus energy reduction. Both have one common aspect - they both come at a cost. However, as far as restricting energy is concerned, its implication relates to the effects of reducing fossil fuels on economic growth.

Policy makers are expected to be fully aware of the nexus between transport energy and economic growth for both energy and environmental policy (Oh & Lee 2004). If transport energy, such as gasoline and diesel, spurs economic growth, then restricting its use may impede economic growth. However, if such

causality direction runs from economic growth to transport energy, then a conservation policy may be desirable. A bi-directional relationship would imply that a careful and selected policy instruments should be used to reduce energy without affecting growth.

The energy-economic growth nexus can be enlightened by analyzing the causal relationship between transport energy and economic growth. Using econometric tools and the Granger representation theorem, this paper investigates the dynamic relationship between transport energy and growth in a multivariate framework using an aggregate production function. Gasoline and diesel are analysed separately. The Autoregressive Distributed Lag (ARDL) bounds test is used to investigate the long-run relationship between transport energy and economic growth for a small island open economy, Mauritius, for the period 1970-2010. Policy issues which are related to energy and climate policy are eventually discussed.

The paper is organized as follows: in section 2, a brief review of literature on the energy-economic growth nexus is provided; section 3 gives a picture of economic development and transport energy in Mauritius; the methodological issues, data and econometrics framework are detailed in section 4 and section 5 provides the results. Section 6 presents the policy implications.

2. Economic growth and the transport sector in Mauritius

Mauritius is an island of approximately 1860 km^2 with a population of 1.24 million (CSO 2010). Investigating the relationship between energy and economic growth for the Republic of Mauritius provides an important case experiment mainly due to its strong economic performance and economic diversification since independence in 1968. Faced with deteriorating terms of trade and a rapidly growing population and labour force in the early 1970s, the island implemented various initiatives to diversify the economy and to raise the standard of the people (Wellisz & Saw 1994). Following the report of James Meade in the 1960s, the import substitution strategy and the establishment of an export-oriented manufacturing sector in the 1970s had contributed to the recovery of the economy. The island shifted from an agriculture mono-crop economy to an economy based on manufacturing sector in the 1980s, especially textile through the Export Processing Zone. Finally, the state developed a multi-sector base economy at the turn of the 21st century, with emphasis on service sectors such as tourism and Information Communication Technology (ICT). Table 1 shows the transformation of the economy from 1960 to 2010.

The Mauritian case is highlighted by many development economists and its record of sustained growth inspires many countries (Vandermoortele & Bird 2010). Since the 1970, economic growth rose to 5 percent per-annum on average and since the early 1980s growth rates have increased slightly to an average of 6 percent per-annum (Figure 1).

Alongside with economic development, the demand for transport has increased dramatically. Personal travel and vehicle ownership has been on the rise. There has also been a growing demand for movement of goods. This eventually led to an increase in gasoline and diesel consumption in the transport sector. Figure 2 shows the fuel consumption in the transport sector for the period 1970-2010 for gasoline and diesel. A number of factors may have contributed to the rise in demand for fuel, including the rise in population, an increase in household income, migration of the middle classes from rural to urban areas and greater participation of women in the labour force (Enoch 2003). The rise in fuel consumption in the transport sector is also linked with the rise in ownership of private vehicles which has more than quadrupled since the 1980s.

3. Energy and economic growth nexus: a brief review of literature

Energy economists have long been interested with whether energy is a stimulus to generate GDP (Chontanawat *et al*. 2010; Toman & Jemelkova 2003). The theoretical foundation of considering energy as a determinant of real output can be found in the Solow growth model (Solow 1956) with exogenous technical progress. This is commonly referred to as the growth hypothesis of energy (Ozturk 2010) which postulates that energy is a causal factor to economic growth and restrictions on the use of energy may adversely affect economic growth. The growth hypothesis suggests that energy consumption plays an

important role in economic growth both directly and indirectly in the production process as a complement to labour and capital. However, this causal relationship relies on the interaction of energy with other variables such as capital and labour.

The relationship between transport energy and economic growth provides another facet of the dilemma and the direction of the causation between the two variables. Mobility is an important element for economic activities to take place. Following the theoretical foundation of Becker's theory of allocation of time, transport is intimately related to both consumption and the allocation of time among discretionary activities (Baker 1965). Hence, travelling and consequently the use of energy is a derived demand emanating from consumption and production activities. However, this fails to account of a fact that travelling can itself be regarded as an activity (Anas 2007). With economic growth, income increases and the demand for product variety grows. Consequently, consumers seek a larger diversity of opportunities to shop, purchase services and engage in recreation or leisure-related activities. Car ownership also increases and the availability of multiple private vehicles allows more discretionary mobility to take place. This eventually leads to a rise in transport energy. Based on the above reasoning, the causal relationship runs from economic growth to energy consumption.

From an empirical point of view, a number of studies aimed at finding causal relationship between energy and economic growth. The study of Kraft & Kraft (1978) is among the pioneers to test whether energy use causes economic growth or vice-versa. Over the last three decades, the energy-economic growth analysis has witnessed many different variations. Studies can be classified into whether aggregate energy or disaggregate energy is used. For instance, Masih & Masih (1996), Glasure & Lee (1997), Akinto (2008), and Odhiambo (2009) analyse aggregate energy consumption while Ziramba (2009), Fatai *et al*. (2004) examine disaggregate energy such as coal, gas, electricity separately. Studies such as Masih & Masih (1996), Fatai *et al*. (2004) and Odhiambo (2009) employ strictly two variables, energy consumption and income proxied by GDP in a dynamic econometric framework. Others such as Narayan & Smith (2005) and Wolde-Rufael (2010) have augmented the econometric analysis to account for more variables such as capital and employment in the analysis. The latter is referred to as the production-side analysis.

Results have been inconclusive. For the US, Yu & Choi (1985) find no causality between energy and GDP while Soytas & Sari (2006), using multivariate co-integration and ECM, find a unidirectional relationship running from energy to GDP. Bi-directional causality has been found for Venezuala and Columbia by Nachane *et al*. (1988), for Pakistan by Masih & Masih (1996), for Phillipine and Thailand by Asafu-Adjaye (2000), among others. Soytas & Sari (2006) also find bi-directional causal relationship for Canada, Italy, Japan and UK and Wolde-Rufael (2005) for Gabon and Zambia. Oh & Lee (2004) employs a VECM to test for Granger causality in the presence of cointegration among aggregate energy, GDP and real energy price for Korea for the period 1980-2000 and conclude that there is no causality between energy and GDP in the short-run and a uni-directional causal relationship from GDP to energy in the long-run. It also implies that a sustainable development strategy may be feasible with lower level of CO2 emissions from fossil fuel combustion. Odhiambo (2009) uses the bounds test approach to cointegration and concludes that for both the short-run and long-run, there is a uni-directional causality running from energy to GDP for South Africa and Kenya while casualty runs from GDP to energy for Congo (DRC).

4. Empirical investigation: data, methodology and models

4.1 Theoretical formulation

Studies which examine the energy consumption-economic growth nexus have used reduced-form time-series models to test for causal relationship (Bartleet & Grounder 2010). In our analysis, transport energy namely gasoline and diesel, is considered as an input in an aggregate production function. Following the conclusion of Stern & Cleveland (2004), that the empirical assessment must be free of specific structural linkages, this study examines the relationship between transport energy and economic growth by incorporating a capital stock variable. The neo-classical one-sector aggregate production model where capital formation as well as energy, are treated as separate factors of production, is shown as follows:

$$Y_t \equiv f(E_t, K_t, L_t) \quad (1)$$

Where Y_t is aggregate output or real GDP, K_t is the capital stock, L_t is the level of employment and E_t is energy. The subscript *t* denotes the time period. Dividing by labour, we postulate the following

$$y_t \equiv f(x_t, e_t, k_t) \tag{2}$$

Where $y_t = \frac{Y_t}{L_t}, e_t = \frac{E_t}{L_t}, k_t = \frac{K_t}{L_t}$

Taking the log linear form of Eq. (2), we can obtain:

$$\ln y_t \equiv \beta_0 + \beta_1 \ln e_t + \beta_2 \ln k_t + \varepsilon_t \tag{3}$$

Where the logarithmic form of the variables means that the variable is now in a growth rate form. The coefficients $\beta_1, \beta_2,$ and β_3 refers to the elasticity of output with respect to energy and capital stock, respectively.

The relationship between aggregate real output, capital stock, and energy described by the production function in Eq.(2) indicates that in the long-run, real output, capital, and energy may move together (Soyta & Sari 2007). Hence, there may be a long-run equilibrium relationship between the variables of concern, and can be easily examined using tests for multivariate cointegration and Granger-causality (Wang *et al*. 2011). The estimation procedures rest on two basics: the cointegration techniques and the short and long-run dynamics.

4.2 Econometric formulation - The ARDL Cointegration approach

The ARDL bounds testing approach is employed to examine long-run equilibrium relationship among the three variables (all variables are in logarithms), namely real GDP (*LRGDP*), real investment (*LRINV*), and energy used in transport, i.e., gasoline (*LGAS*) and diesel (*LDIE*). All variables are in per capita level. An ARDL model is a general dynamic specification, which uses the lags of the dependent variable and the lagged and contemporaneous values of the independent variables, through which the short-run effects can be directly estimated, and the long-run equilibrium relationship can be indirectly estimated. Unlike other cointegration techniques, the ARDL does not impose a restrictive assumption that all the variables under study must be integrated of the same order. In other words, the ARDL approach can be applied regardless of whether the underlying regressors are integrated of order one [*I(1)*], order zero[*I(0)*] or fractionally integrated. The ARDL test is suitable even if the sample size is small and the technique generally provides unbiased estimates of the long-run model and valid t-statistics even when some of the regressors are endogenous (Harris & Sollis 2003).

The ARDL technique involves estimating the following unrestricted error correction model (UECM):

Model 1: Gasoline and economic growth nexus

$$\Delta LRGDP_t = a + \sum_{i=0}^{m} b_{igdp}\, \Delta LGAS_{t-1} + \sum_{i}^{q} c_{igdp}\, \Delta LRGDP_{t-i} + \sum_{i=0}^{n} d_{igdp}\, \Delta LRINV_{t-1} + \eta_{1gdp}\, LRGDP_{t-1} + \eta_{2gdp}\, LGAS_{t-1} + \eta_{3gdp}\, LINV_{t-1} + \varepsilon_{gdp,t} \tag{4}$$

$$\Delta LGAS_t = a_1 + \sum_{i=0}^{m} b_{igas}\, \Delta LGAS_{t-1} + \sum_{i}^{q} c_{igas}\, \Delta LRGDP_{t-i} + \sum_{i=0}^{n} d_{igas}\, \Delta LRINV_{t-1} + \eta_{1gas}\, LRGDP_{t-1} + \eta_{2gas}\, LGAS_{t-1} + \eta_{3gas}\, LINV_{t-1} + \varepsilon_{gas,t} \tag{5}$$

$$\Delta LINV_t = a_{inv} + \sum_{i=0}^{m} b_{iinv}\, \Delta LGAS_{t-1} + \sum_{i}^{q} c_{iinv}\, \Delta LRGDP_{t-i} + \sum_{i=0}^{n} d_{iinv}\, \Delta LRINV_{t-1} + \eta_{1inv}\, LRGDP_{t-1} + \eta_{2inv}\, LGAS_{t-1} + \eta_{3inv}\, LINV_{t-1} + \varepsilon_{inv,t} \tag{6}$$

Model 2: Diesel and economic growth nexus

$$\Delta LRGDP_t = a + \sum_{i=0}^{m} f_{igdp}\, \Delta LDIE_{t-1} + \sum_{i}^{q} g_{igdp}\, \Delta LRGDP_{t-i} + \sum_{i=0}^{n} h_{igdp}\, \Delta LRINV_{t-1} + \mu_{1gdp}\, LRGDP_{t-1} + \mu_{2gdp}\, LGAS_{t-1} + \mu_{3gdp}\, LINV_{t-1} + \zeta_{gdpt} \tag{7}$$

$$\Delta LDIE_t = a + \sum_{i=0}^{m} f_{idie}\,\Delta LDIE_{t-1} + \sum_{i}^{q} g_{idie}\,\Delta LRGDP_{t-i} + \sum_{i=0}^{n} h_{idie}\,\Delta LRINV_{t-1} + \mu_{1die}\,LRGDP_{t-1} + \mu_{2die}\,LGAS_{t-1} + \mu_{3die}\,LINV_{t-1} + \zeta_{die,t} \quad (8)$$

$$\Delta LINV_t = b_{inv} + \sum_{i=0}^{m} f_{iinv}\,\Delta LDIE_{t-1} + \sum_{i}^{q} g_{iinv}\,\Delta LRGDP_{t-i} + \sum_{i=0}^{n} h_{iinv}\,\Delta LRINV_{t-1} + \mu_{1inv}\,LRGDP_{t-1} + \mu_{2inv}\,LGAS_{t-1} + \mu_{3inv}\,LINV_{t-1} + \zeta_{inv,t} \quad (9)$$

The cointegration analysis is carried out by testing the joint significance of the lagged levels of the variables using the *F*-test where the null of no cointegration is defined by $H_o : \eta_{1j} = \eta_{2j} = \eta_{3j} = \eta_{4j} = 0$ (*for j=gdp, gas, inv, emp)* for the gasoline system equation and $H_o : \mu_{1j} = \mu_{2j} = \mu_{3j} = \mu_{4j} = 0$ for (*j=gdp, die, inv, emp)* for the diesel system equation. The alternative is that $H_1 : \eta_{1j} \neq \eta_{2j} \neq \eta_{3j} \neq \eta_{4j} \neq 0$ and $H_1 : \mu_{1j} \neq \mu_{2j} \neq \mu_{3j} \neq \mu_{4j} \neq 0$.

The asymptotic distribution of the *F*-statistic is non-standard under the null hypothesis and it is originally derived and tabulated in Pesaran *et al*. (2001) but modified by Narayan (2005) to accommodate small sample sizes. Two sets of critical values are provided: one which is appropriate when all the series are *I(0)* and the other for all the series that are *I(1)*. If the computed *F*-statistic falls above the upper critical bounds, a conclusive inference can be made regarding cointegration without the need to know whether the series were *I(0)* or *I(1)*. In this case, the null of no cointegration is rejected. Alternatively, when the test statistic falls below the lower critical value, the null hypothesis is not rejected regardless whether the series are *I(0)* or *I(1)*. In contrast, if the computed test statistic falls inside the lower and upper bounds, a conclusive inference cannot be made unless we know whether the series were *I(0)* or *I(1)*. Causality tests in this framework can be undertaken as a first step of the ARDL approach.

An Error Correction Model provides two alternative channels of the interaction among our variables: short-run causality through past changes in the variable, and long-run causality through adjustments in equilibrium error. The ECM for our three variables case can be written as follows:

For gasoline

$$\begin{bmatrix} \Delta LRGDO_t \\ \Delta LGAS_t \\ \Delta LRINV_t \end{bmatrix} = \begin{bmatrix} a_1 \\ a_2 \\ a_3 \end{bmatrix} + \sum_{i=1}^{p} (1-L) \begin{bmatrix} b_{11}b_{12}b_{13} \\ b_{21}b_{22}b_{23} \\ b_{31}b_{32}b_{34} \end{bmatrix} \cdot \begin{bmatrix} \Delta LRGDO_{t-i} \\ \Delta LGAS_{t=i} \\ \Delta LRINV_{t-i} \end{bmatrix} + \begin{bmatrix} \varphi_1 \\ \varphi_2 \\ \varphi_3 \end{bmatrix} \begin{bmatrix} ECT_{t-1} \\ ECT_{t=1} \\ ECT_{t-1} \end{bmatrix} + \begin{bmatrix} \xi_1 \\ \xi_2 \\ \xi_3 \end{bmatrix} \quad (10)$$

For diesel

$$\begin{bmatrix} \Delta LRGDO_t \\ \Delta LDIE_t \\ \Delta LRINV_t \end{bmatrix} = \begin{bmatrix} c_1 \\ c_2 \\ c_3 \end{bmatrix} + \sum_{i=1}^{p} (1-L) \begin{bmatrix} d_{11}d_{12}d_{13} \\ d_{21}d_{22}d_{23} \\ d_{31}d_{32}d_{34} \end{bmatrix} \cdot \begin{bmatrix} \Delta LRGDO_{t-i} \\ \Delta LDIE_{t=i} \\ \Delta LRINV_{t-i} \end{bmatrix} + \begin{bmatrix} 1 \\ 2 \\ 3 \end{bmatrix} \begin{bmatrix} ECT_{t-1} \\ ECT_{t=1} \\ ECT_{t-1} \end{bmatrix} + \begin{bmatrix} \varepsilon_1 \\ \varepsilon_2 \\ \varepsilon_3 \end{bmatrix} \quad (11)$$

ξ_i, ε_i (for i=1, 2, 3) are serially uncorrelated random error terms. The error correction terms denoted by $ECT_{r,t-1}$ are the cointegrating vectors and φ_i, (for *i=1,..3*) are the adjustment coefficients, showing how much disequilibrium is corrected. The deviation from long-run equilibrium is gradually corrected through a series of short-run adjustments. The size and statistical significance of $ECT_{r,t-1}$ is a measure of the extent to which the left hand side variable in each equation returns in each short-run period to its long-run equilibrium in response to random shocks.

Once the long-run relationships have been identified and an ECM is estimated, the next step is to examine the short-run and long-run Granger causality between the two proxies for transport energy and real output. The traditional Granger's definition of causality is based on the notion that the future cannot cause the past but that the past can cause the future. According to Granger's definition of causality, a time series X, causes another time series Y, if Y can be predicted better (in a mean-squared-error sense) using past values of X than by not doing so. That is, if past values of X significantly contribute to forecasting Y, then X is

said to Granger cause Y (Odhiambo 2010). An error correction model enables one to distinguish between long- and short-run causality in addition to bringing the lost information due to differencing back into the system through the error correction terms. The Granger causality test can therefore be conducted from an error correction representation.

4.3. Variables specification and data sources

This study utilises time series data for the period 1970-2010 for gasoline and for diesel, from the Statistics office, Mauritius. For key variables, such as economic activities, we take as proxy the real GDP per capita (RGDP) and for energy, we take total gasoline (*GAS*) and total diesel (*DIE)* consumption in the transport sector in per capita unit. Data on GDP, deflators, capital formation and population were all obtained from the National Accounts, Statistics Office, Mauritius. Data on energy was obtained from the Digest of Energy statistics, Statistics Office, Mauritius. We use gross capital formation to proxy the stock of physical capital following the work of Soytas & sari (2006), Wolde-Rufael (2009) and Ouedraogo (2010). It is argued that since in the perpetual inventory method, the rate of depreciation is assumed to be constant, changes in investment are closely related to changes in capital stock.

5. Results and discussion

Table 2 provides tests of unit roots in level and first difference of the variables: *LRGAS* , *LDIE* , *LRGDP* and *LRINV* using the Augmented Dicker-Fuller (ADF) method and the Phillip-Perron (PP) test. We see that diesel and investment time series are *I(0)* from the ADF test but the PP test fails to reject the null hypothesis of unit roots in the level for all the variables above. The two tests are then applied to the first difference of the time series and the results are shown in table 2. We conclude that all variables are first-difference stationary and proceed to tests of cointegration.

The bounds test is appropriate for this study given that there is a mixture of *I(0)* and *I(1)* series and that no series are *I(2)*. The results are shown in table 3 and 4 for gasoline and diesel respectively. The basis for conducting the test relies on the Unrestricted Error Correction Model (UECM). The UECM models pass the diagnostic tests with respect to the Lagrange multiplier test for residual serial correlation, the Ramsey RESET test for functional form, the Jarque-Berra test of normality and the White hetrocedasticity test. The real GDP equation and real investment however shows a problem of functional form as depicted by the RESET test at 10%. For the diesel system analysis, the real GDP equation exhibits a normality problem. Various specifications were attempted, however, the problem persists. It is therefore important to interpret the economic growth causality with care. The critical values for the bounds test are taken from Narayan (2005) and table 3 and 4 show the lower bound and upper bound for 5% level of significance.

Table 3 concludes that a cointegration relationship exists when gasoline and investment are taken as dependent variables while table 4 shows the cointegration results for the diesel regression. The bounds test to cointegration can also be used to provide insight on the long-run causation between the variables. In the long-run, the causality runs from economic growth and real investment to gasoline and diesel. The results also show that real investment is endogenous for both the gasoline and diesel equation, adjusting to shocks in the long-run equilibrium.

The Granger causality analysis, based on an ECM within the ARDL is presented in table 5 and 6. The Wald test concludes that gasoline adjusts to changes in the long-run equilibrium – the coefficient of the error term has the correct sign and is highly significant (table 5). This is consistent with the bounds test results. Hence, it can be concluded that the real GDP per capita and real investment per capita Granger-cause gasoline consumption in the long-run. This result was rather consistent with the rise in mobility as a consequence of higher standard of living. Since private cars operate mostly with gasoline fuel, enhanced mobility for discretionary purposes leads to a rise in the consumption of fossil fuel.

In the short run, only per capita real investment influences gasoline consumption. Real GDP is Granger-caused by gasoline in the short-run but not in the long-run. The results conclude that gasoline is not a major input in the aggregate production function of the economy. Its effect can be traced from the

investment regression where gasoline is found to Granger-caused real investment in the long-run and as well as in the short-run.

Table 6 gives the econometric result for the diesel regression and similar linkages are found. Growth is found to Granger-caused diesel consumption. Since the public bus transport system operates with diesel, such conclusion is also reflecting the rise in mobility of the population. As can be seen from table 6, bi-directional causality is found between real investment and transport energy in the long-run - consistent with the bounds test result - as well as in the short run. The Wald statistics concludes that the null-hypothesis of no causality can be rejected given the level of significance of coefficients.

The results suggest that with economic progress, the enhanced standard of living is likely to increase transport energy. Such conclusion is consistent with Anas (2007)'s concept of discretionary mobility that transport should not be viewed as only a derived demand. Mobility may be an end in itself. The important conclusion is the complementary between investment and energy. If a carbon or energy tax is imposed as part of climate policy to restrict the rise in fossil fuel consumption, economic growth may be affected through the effect of energy on investment. This policy will be detrimental to real investment and a negative shock to real investment is expected.

6. **Conclusions and policy implications**

The conclusions from the Granger causality tests reveal that gasoline and diesel have similar linkages in the economy. The cointegration relationships suggest that transport energy, real GDP per capita and real investment per capita form a long-run equilibrium. Both gasoline and diesel readjusts shocks to the equilibrium condition. This implies that we should expect a rise in transport energy as the economy progresses and as wealth is generated. In both the long-run and short-run, we also found that there is a bi-directional causality between the two types of transport energy and investment. Hence, we conclude that Mauritius exhibits an energy dependence economy such that an adequate supply of diesel and gasoline are essential for real investment.

The study shows the dilemma which is implied in the design of energy and climate policy. Policy makers can be trapped in reducing fossil fuels used in the transport sector, through restricting mobility as a climate and energy policy. For a small island state, Mauritius, a conservative strategy for transport energy would prove detrimental to investment and long-run economic growth. Policy instruments such as energy tax must be carefully analysed. The Granger-causality test concludes that energy and climate policies which are devoted towards a reduction in GHGs should emphasise the use of alternative sources rather than exclusively attempt to reduce overall energy consumption. The development of bio-fuels is, therefore, a promising avenue to ensure an adequate supply of energy to sustain economic performance.

We attribute the result that economic growth takes precedence over diesel and gasoline to discretionary mobility which is due to higher standard of living. Hence a change in behaviour towards sustainable mobility is vital. Since the population is expected to be highly mobile especially with higher participation of women in the labour force, the improvement of public transport could be a way to lessen the rise in private vehicles usage.

Such conclusion does not imply that a reduction in energy resulting from a shift of less efficient vehicles is not suitable. Studies have shown that efficient vehicles may raise energy productivity and hence, may establish a stimulus rather than an obstacle to economic development. In the transport sector, this may require the replacement of old and inefficient vehicles by new and efficient ones. Our analysis has been restricted through the availability of data on energy in Mauritius. A longer time period would definitely enhance the robustness of the analysis. Alternatively, the study has focused on an inbound causality relationship. Outbound causal studies using the Impulse Response Function and the Variance Decomposition Model may be possible avenues for further research.

References

Abmann, D. & Sieber, N. (2005), "Transport in developing countries: Renewable Energy versus Energy

reduction?", *Transport Reviews* **25**(6), 719-738.

Akinto, A. E. (2008), "Energy consumption and economic growth: evidence from 11 Sub-Sahara African countries", *Energy Economics* **30**(5), 2391–2400.

Anas, A. (2007), "A unified theory of consumption, travel and trip chaining", *Journal of Urban Economics* **62**, 162–186.

Asafu-Adjaye, J. (2000), "The relationship between energy consumption, energy prices and economic growth: time series evidence from Asian developing countries", *Energy Economics* **22**, 615–625.

Barleet, M. & Gounder, M. (2010), "Energy consumption and economic growth in New Zealand: Results of trivariate and multivariate models", *Energy Policy* **28**, 3508-3517.

Becker, G.. S. (1965), "A theory of the allocation of time", *Economic Journal* **LXXV**, 493–508.

Boko, M., Niang, I., Nyong, A., Vogel, C., Githeko, A., Medany, M., Osman-Elasha, B., Tabo, R. & Yanda, P. (2007), Africa. Climate Change 2007: Impacts, Adaptation and Vulnerability. *Contribution of Working Group II to the Fourth Assessment Report of the Intergovernmental Panel on Climate Change*. Eds. M.L. Parry, O.F. Canziani, J.P. Palutikof, P.J. van der Linden and C.E. Hanson, 433-467. Cambridge University Press, Cambridge UK.

Chapman, L. (2007), "Transport and climate change: a review", *Journal of Transport Geography* **15**, 354-367.

Chontanawat, J., Hunt, L. C. & Pierse, R. (2008), "Does energy consumption cause economic growth? Evidence from a systematic study of over 100 countries", *Journal of Policy Modeling* **30**, 209-220.

CSO (2010) National Accounts, Central Statistics Office, Statistics Office, Mauritius.

Enoch, M. P. (2003), "Transport practice and policy in Mauritius". *Journal of Transport Geography* **11**, 297–306..

Fatai, K. Oxley, L. & Scrimgeour, F. G. (2004), "Modelling the causal relationship between energy consumption and GDP in New Zealand, Australia, India, Indonesia, The Philippines and Thailand", *Mathematics and Computers in Simulation* **64**, 431-445.

Glasure, Y.U. & Lee, A.R. (1997), "Cointegration, error correction, and the relationship between GDP and electricity: the case of South Korea and Singapore", *Resource and Energy Economics* **20**, 17–25.

IPCC. (2007). *Climate Change 2007: Synthesis Report. An Assessment of the Intergovernmental Panel on Climate Change*. Cambridge University Press, Cambridge.

Kraft, J. and Kraft, A. (1978), "On the relationship between energy and GNP", *Journal of Energy and Development* **3**, 401–403.

Masih, A. M. M. & Masih, R. (1996). "Energy consumption, real income and temporal causality: results from a multi-country study based on cointegration and error-correction modeling techniques". *Energy Economics* **18**, 165-183.

Nachane, D.M., Nadkarni, R.M., & Karnik, A.V., (1988), "Co-integration and causality testing of the energy–GDP relationship: a cross-country study", *Applied Economics* **20**, 1511–1531.

Narayan, P.K. (2005), "The saving and investment nexus for China: evidence for cointegration tests". *Applied Economics* **37**, 1979–1990.

Narayan, P.K. & Smyth, R. (2005), "Electricity consumption, employment and real income in Australia: evidence from multivariate Granger causality tests", *Energy Policy* **33**, 1109–1116.

Odhiambo, N. M. (2009), "Energy consumption and economic growth nexus in Tanzania: An ARDL bounds testing approach", *Energy Policy* **37**, 617-622.

Oh, W. & Lee, K. (2004), "Energy consumption and economic growth in Korea: testing the causality relation", *Journal of Policy Modelling* **26**, 973-981.

Ouedraogo, M. I. (2010), "Electricity consumption and economic growth in Burkina Faso A cointegration analysis", *Energy Economics* **32**, 524-531.

Ozturk I. (2010), "A literature survey on energy-growth nexus", *Energy Policy* **38**, 340–349.

Palmer, A. (2008), Transport, energy and global climate change. *The IES Journal Part A: Civil & Structural Engineering* **1**(2), 163-170.

Pesaran, M.H., Shin, Y., & Smith, S. (2001), "Bounds testing approach to the analysis of level relationships", *Journal of Applied Econometrics* **16**, 289–326.

Solow R. M. (1956), "A contribution to the theory of economic growth", *Quarterly Journal of Economics* **70**, 65-94

Soytas, U., & Sari, R. (2006), "Energy consumption and income in G-7 countries", *Journal of Policy Modelling* **28** (7), 739–750.

Soytas, U. & Sari, R. (2007). The relationship between energy and production: evidence from Turkish manufacturing industry. *Energy Economics* 29, 1151–1165.

Stern, D.I. & Cleveland, C.J. (2004), "Energy and economic growth", *Rensselaer Working Papers in Economics* 0410, Rensselaer Polytechnic Institute, New York.

Toman, M. A., & Jemelkova, B. (2003), "Energy and economic development: An assessment of the state of knowledge", *The Energy Journal* **24,** 93–112.

Wang, Y., Wang, Y., Jing, Z., Zhu., X. & G. Lu (2011), "Energy consumption and economic growth in China: A multivariate causality test", *Energy Policy* **39,** 4399-4406.

Wellisz, S. & Saw , P. L. S. (1994), *A World bank comparative study -The Political Economy of Poverty, Equity and Growth, Five small Open economies*, Edited by R. Findlay and S. Wellisz. The World Bank Ocford University Press.

Wolde-Rufael, Y. (2009), "Energy consumption and economic growth: the African experience revisited", *Energy Economics* **31**, 217–224.

Wolde-Rufael, Y. (2010), Bounds test approach to cointegration and causality between nuclear energy consumption and economic growth in India. *Energy Policy* **38**, 52-58.

Wright, L. & Fulton, L. (2005), "Climate Change Mitigation and Transport in Developing Nations", *Transport Reviews* **25**(6), 691-717.

Vandemoortele, M. & Bird, C. (2011), *Progress in economic conditions: sustained success against the odds in Mauritius*. Overseas Development Institute, ODI publications, 111 Westminster Bridge Road, London SE1 7JD, UK.

Ziramba, E. (2009), "The demand for residential electricity in South Africa", *Energy Policy* **36**, 3460–3466.

Figure 1 :Growth in real GDP per capita

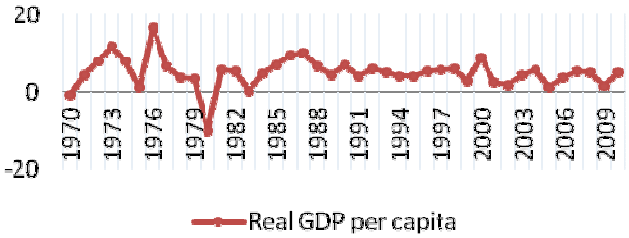

Source: Computed from the data from Statistics Office, Mauritius, World Bank Indicators and International Financial Statistics

Table 1: Sector distribution of GDP in Mauritius 1960-2010					
	1960	1980	1990	2000	2010
	%	%	%	%	%
Agriculture	31.3	15.1%	11.8	6.7	3.6
Industrial	24.7	25.6	34.1	29.5	20.1
Services	44	59.3	54.1	63.8	76.3
Source: National Accounts of Mauritius CSO publication					

Figure 2: Fuel consumption in the Transport sector

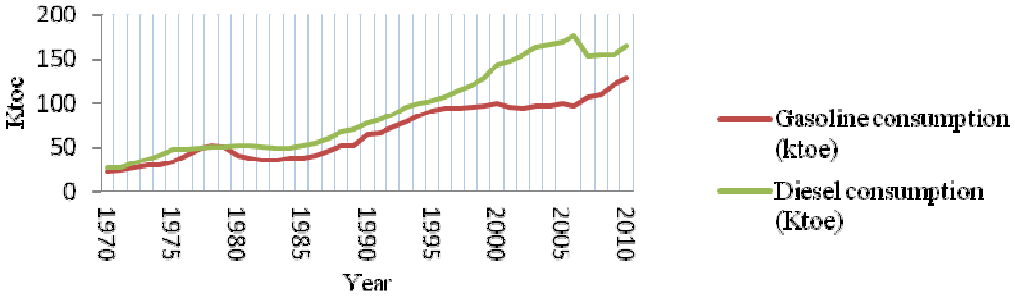

Source: Computed from the Digest of Energy Statistics, Statistics Office, Mauritius

Table 2. Unit root test result from the ADF and PP methods in annual data at level form and first difference form

Variables	Augmented Dicker Fuller test		Philip-Perron test (PP)	
Level form	ADF test statistics	Critical Values (LL)	PP test (Z(rho))	BW(LL)
$LRGAS_t$	-3.514	-3.539(2)	-2.327	-12.980(3)
$LDIE_t$	-3.781	-3.539(3)	-1.705	-12.980(3)
$LRGDP_t$	-3.405	-3.539(3)	-1.536	-12.980(3)
$LRINV_t$	-4.427	-3.539(3)	-4.161	-12.980(3)
First difference				
$\Delta LRGAS_t$	-3.504	-2.947(0)	-21.884	-12.948(3)
$\Delta LDIE_t$	-3.408	-2.947(1)	-30.658	-12.948(3)
$\Delta LRGDP_t$	-3.436	-2.947(1)	-50.545	-12.948(3)
$\Delta LRINV_t$	-3.296	-2.947(1)	-33.571	-12.948(3)

The null hypothesis for the ADF and PP tests is that the time series exhibit a unit root. The optimal lag length on the variables in ADF test equations are selected by Schwarz Information Criterion. The bandwidth for the PP test is selected with the Newey-West Barlett kernel method.
*, **, *** denote significance at 10% level, 5%, and 1% respectively.

Source: Computed from *Microfit 4.0*

Table 3. Results of the bounds tests: gasoline equation

Equation	Estimated F-statistics	5% critical value bounds		Evidence of cointegration
		I(0)	*I(1)*	
$F_{LRGDP}(LRGDP_t/,LGAS_t,LRINV_t)$	0.230	3.100	4.088	No
$F_{LGAS}(LGAS_t/,LRGDP_t,LRINV_t)$	4.607	3.100	4.088	Yes
$F_{LRINV}(LRINV_t/,LRGDP_t,LGAS_t)$	8.716	3.100	4.088	Yes

Notes: Critical values are for the model with intercept but no trend with k=3 regressors

Source: computed from *Microfit 4.0*

Table 4. Results of the bounds tests: diesel equation

Equation	Estimated F-statistics	5% critical value bounds		Evidence of cointegration
		I(0)	*I(1)*	
$F_{LRGDP}(LRGDP_t/,LDIE_t,LRINV_t)$	0.263	3.100	4.088	No
$F_{LDIE}(LDIE_t/,LRGDP_t,LRINV_t)$	5.0221	3.100	4.088	Yes
$F_{LRINV}(LRINV_t/,LRGDP_t,LDIE_t)$	6.17	3.100	4.088	Yes

Notes: Critical values are for the model with intercept but no trend with k=3 regressors

Source: Computed from *Microfit 4.0*

Table 5.Results from the Granger causality tests – gasoline and real output

Dependent variables	Type of Granger causality				
	Short-run				Long-run
	$\Delta LGAS_t$	$\Delta LRDGP_t$	$\Delta LINV_t$		ECT_{t-1}
	Wald F-statistics				t-statistics

$\Delta LGAS_t$		0.532	13.193***		-0.316(0.067)***-
$\Delta LRDGP_t$	0.842		39.482***		-0.036(-0.065)
$\Delta LINV_t$	12.712***	28.662***			-0.822(0.112)***
Source: Computed from *Microfit 4.0*					

Table 6.Results from the Granger causality tests- diesel and real output					
Dependent variables	Type of Granger causality				
	Short-run				Long-run
	$\Delta LDIE_t$	$\Delta LRDGP_t$	$\Delta LINV_t$		ECT_{t-1}
	Wald F-statistics				t-statistics
$\Delta LDIE_t$		0.002	7.768***		-0.161(0.006)***
$\Delta LRDGP_t$	0.059		16.737***		0.914(0.368)
$\Delta LINV_t$	0.387	16.216***			-0.467(0.103)***
Source: Computed from *Microfit 4.0*					

Journal of Energy Technologies and Policy
ISSN 2224-3232 (Paper) ISSN 2225-0573 (Online)
Vol.2, No.1, 2011

Speed Torque characteristics of Brushless DC motor in either direction on load using ARM controller

M.V.Ramesh[1], J.Amarnath[2], S.Kamakshaiah[3], B.Jawaharlal[4], Gorantla.S.Rao[5]

1. Department of EEE, P.V.P Siddhartha Institute of Technology, Vijayawada, A.P, India.

2. Department of EEE, J N T U H College of Engineering, Hyderabad, A.P., India.

3. Department of EEE, Vignan Institute of Technology and Science, Hyderabad, India.

4. Scientist, DRDO-RCI, Hyderabad.

5. Department of EEE, Vignan University, Vadlamudi, India.

vrmaddukuri@gmail.com

Abstract

This paper presents the speed torque characteristics of BLDC motor on load in forward and reverse direction. The Hall sensors of the BLDC motor is bestowed as the input to the ARM controller. The PWMs are produced depending upon the input of the controller. In order to convert DC to three phase AC, three phase bridge inverter with MOSFET as switches is used. The generated PWMs are inputted to the gate of the MOSFETs in the inverter. The output of the inverter is the energization sequence of BLDC motor and only two phases energizes at once. Dynamometer is used for encumbering the motor. The results are acquired for variable load torque and Speed torque characteristics are observed.

Keywords: BLDC motor, PWM, MOSFET and dynamometer.

1. Introduction

Since 1980's new prototype concept of permanent magnet brushless motors has been built. The Permanent magnet brushless motors are categorized into two kinds depending upon the back EMF waveform, Brushless AC (BLAC) and Brushless DC (BLDC) motors [2]. BLDC motors have trapezoidal back EMF and quasi-rectangular current waveform. BLDC motors are quickly becoming famous in industries like Appliances, HVAC industry, medical, electric traction, automotive, aircrafts, military equipment, hard disk drive, industrial automation equipment and instrumentation because of their high efficiency, high power factor, silent operation, compact, reliability and low maintenance [1].In the event of replacing the function of alternators and brushes, the BLDC motor requires an inverter and a position sensor that exposes rotor position for appropriate alternation of current. The rotation of the BLDC motor is built on the feedback of rotor position that is gained from the hall sensors. BLDC motor generally utilizes three hall sensors for deciding the commutation sequence. In BLDC motor the power losses are in the stator where heat can be easily shifted through the frame or cooling systems are utilized in massive machines. BLDC motors have many benefits over DC motors and induction motors. Some of the benefits are better speed versus torque characteristics, high dynamic response, high efficiency, long operating life, noiseless operation, higher speed ranges [2].Till now, over 80% of the controllers are PI (Proportional and integral) controllers because they are facile and easy to comprehend [3].

The speed controllers are the conventional PI controllers and current controllers are the P controllers to

achieve high performance drive. Fuzzy logic can be considered as a mathematical theory combining multi-valued logic, probability theory, and artificial intelligence to simulate the human approach in the solution of various problems by using an approximate reasoning to relate different data sets and to make decisions. It has been reported that fuzzy controllers are more robust to plant parameter changes than classical PI or controllers and have better noise rejection capabilities. In this paper, hardware implementation of the BLDC motor is done by using ARM controller. We propose the Speed Torque characteristics of the BLDC motor drive rotating not only in forward but also in reverse direction. We used dynamometer with hysteresis brake to load the motor. The torque and speed of the BLDC motor is measured in dynamometer and basing on the readings Speed Torque characteristics ware drawn. The paper is organized as follows: Section II explains about construction and operating principle of BLDC motor, Section III elaborates the modelling of BLDC motor, Section IV presents the hardware implementation of BLDC motor. The hardware results are presented in detail in Section V and Section VI concludes the paper.

2. Construction and Operating Principle

BLDC motors are a kind of synchronous motor. This indicates the magnetic field produced by the stator and the magnetic field produced by the rotor twirls at the same frequency. BLDC motors do not experience the “slip” that is normally observed in induction motors. BLDC motor is built with a permanent magnet rotor and wire wound stator poles.

1.1. Stator

The stator of a BLDC motor as shown in Fig.1 comprises of stacked steel laminations with windings kept in the slots that are axially cut along the inner periphery as shown in Figure 1. Most BLDC motors have three stator windings linked in star fashion. Each of these windings is assembled with various coils interconnected to derive a winding. One or more coils are kept in the slots and they are interconnected to form a winding. Each of these windings is distributed over the stator periphery to form an even numbers of poles.

1.2. Rotor

The rotor is formed from permanent magnet and can alter from two to eight pole pairs with alternate North (N) and South (S) poles. The suitable magnetic material is selected to form the motor depending upon the required field density in the rotor. Ferrite magnets are used to make permanent magnets. Now a day, rare earth alloy magnets are gaining popularity.

Fig. 1 Stator of a BLDC motor

1.3. Hall Sensors

The commutation of a BLDC motor as shown in Fig.2 is in check electronically. In order to rotate the BLDC motor, the stator windings ought to be energized in an order. It is essential to understand the rotor position in order to know which winding will be energized following the energizing sequence. Rotor position is perceived using Hall effect sensors embedded into the stator on the non-driving end of the motor as shown in fig. . Whenever the rotor magnetic poles pass near the Hall sensors, they give a high or low signal, suggesting the N or S pole is passing near the sensors. The exact order of commutation can be estimated, depending upon the combination of these three Hall sensor signals.

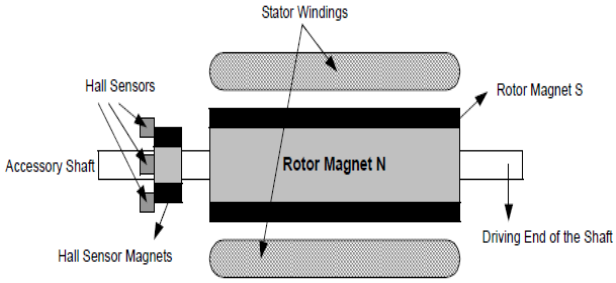

Fig. 2 Rotor and Hall sensors of BLDC motor

1.4. Theory of operation

Each commutation sequence has one of the windings energized to positive power, the second winding is negative and the third is in a non-energized condition. Torque is engendered because of the interaction between the magnetic field generated by the stator coils and the permanent magnets. Ideally, the peak torque takes place when these two fields are at 90° to each other and goes down as the fields move together. In order to place the motor running, the magnetic field generated by the windings should shift position, as the rotor moves to catch up with the stator field [9].

1.5. Commutation Sequence

The commutation sequence, for every 60 electrical degrees of rotation, one of the Hall sensors changes the state. It takes six steps to finish an electrical cycle. In Synchronous, with every 60 electrical degrees, the phase current switching ought to be renovated. However, one electrical cycle may not agree to a complete mechanical revolution of the rotor. The number of electrical cycles to be repeated to complete a mechanical rotation is dictated by the rotor pole pairs. One electrical cycle is completed for each rotor pole pairs. Hence, the number of electrical cycles equals the rotor pole pairs. A three phase bridge inverter is used to balance the BLDC motor. There are six switches and these switches should be switched depending upon Hall sensor inputs. The Pulse width modulation techniques are used to switch ON or OFF the switches. In order to vary the speed, these signals should be Pulse Width Modulated (PWM) at a much higher frequency than the motor frequency. The PWM frequency should be at least 10 times that of the maximum frequency of the motor. When the duty cycle of PWM is differed within the sequences, the average voltage supplied to the stator reduces, thus lowering the speed. Another benefit of having PWM is that, if the DC bus voltage is much greater than the motor rated voltage, the motor can be controlled by limiting the percentage of PWM duty cycle corresponding to that of the motor rated voltage. This adds plasticity to the controller to assemblage motors with various rated voltages and matches the average voltage output by the controller, to the motor rated voltage, by controlling the PWM duty cycle. The speed and torque of the motor hinge upon the strength of the magnetic field generated by the energized windings of the motor that depend on the current through them. Hence the adjustment of the rotor voltage (and current) will change the motor speed.

2. Modelling of BLDC Motor

The flux distribution in BLDC motor is trapezoidal and hence the d–q rotor reference frames model is not suitable. It is shrewd to derive a model of the PMBLDC motor in phase variables when if is given the non-sinusoidal flux distribution. The derivation of this model is depends on the postulations that the induced currents in the rotor due to stator harmonic fields, iron and stray losses are neglected. The motor is taken to have three phases even though for any number of phases the derivation procedure is true to life. Modeling of the BLDC motor is done applying classical modeling equations and therefore the motor model is highly adaptable. These equations are illustrated depending upon the dynamic equivalent circuit of BLDC motor. The assumptions made for modelling and simulation purpose are the common star connection of stator windings, three phase balanced system and uniform air gap. The mutual inductance between the stator phase windings are uncountable when compared to the self-inductance and so neglected in designing the model [3].

Dynamic model equation of motion of the motor is described in the form of equations (1) to (9).

$$W_m = (T_e - T_l) / J_s + B \qquad (1)$$

T_e – electromagnetic torque, T_l– load torque, J – moment of inertia, B – friction constant

Rotor displacement can be found out as,

$$\Theta_r = (P/2)\, W_m /s \qquad (2)$$

whereP – Number of poles

Back EMF will be of the form,

$E_{as} = k_b f_{as}(\Theta_r) W_m$ (3) $E_{bs} = k_b f_{bs}(\Theta_r) W_m$ (4) $E_{cs} = k_b f_{cs}(\Theta_r) W_m$ (5)

where K_b -back EMF constant

Stator phase currents are estimated as,

$i_a = (V_{as} - E_{as}) / (R+Ls)$ (6) $i_b = (V_{bs} - E_{bs}) / (R+Ls)$ (7) $i_c = (V_{cs} - E_{cs}) / (R+Ls)$ (8)

where R – resistance per phase, L – inductance per phase

Electromagnetic torque developed,

$$T_e = (E_{as}i_{as} + E_{bs}i_{bs} + E_{cs}i_{cs}) / W_m \quad (9)$$

3. HARDWARE CONFIGURATION

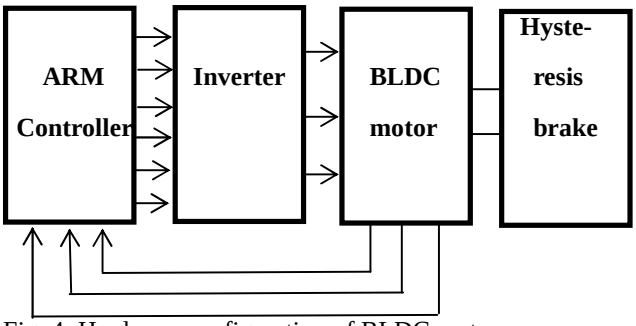

Fig. 4: Hardware configuration of BLDC motor

The hardware configuration of BLDC motor with loading arrangement is shown in Fig.4. The block diagram comprises ARM controller, three phase bridge Inverter, BLDC motor and hysteresis brake. The hall sensor output of BLDC motor is provided as the input to ARM controller and the PWMs are generated which are provided as the input to inverter. The inverter converts DC to three phase AC and the AC supply is given to the BLDC motor. The load is applied to the BLDC motor by coupling hysteresis brake with the BLDC motor. When the load on the BLDC motor increases, the speed decreases.

3.1. INVERTER

The circuit of three phase bridge inverter is shown in fig. 5. A three phase inverter is applied to transfer DC to three phase AC. Here six MOSFETs are used as the switches. P-channel MOSFET is linked with the upper arm and N-channel MOSFET is linked with the lower arm of the inverter. The symbol and ratings of N-channel MOSFET is shown in fig. 6. Among them, two of the six MOSFETs are energized at once. At this situation, one switch from the upper arm and one from the lower arm are turned on. Therefore, two phases will be energized. The current will flow into the motor from upper arm turn on switch and return from bottom arm turn on switch.

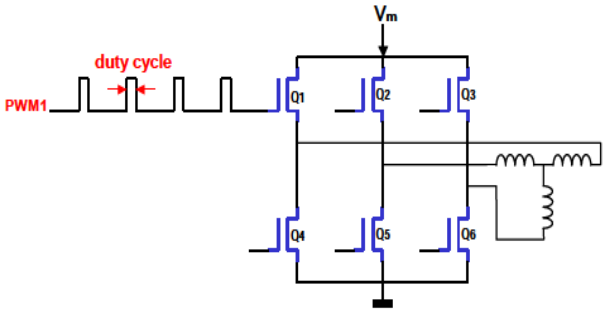

Fig. 5: Three phase Inverter circuit

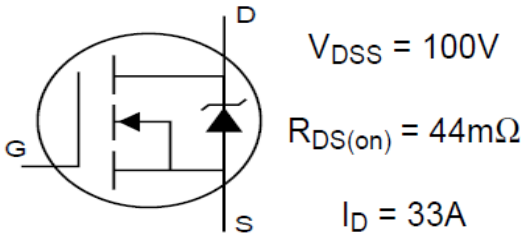

Fig. 6: Symbol and Ratings of MOSFET

HPCL 3120 MOSFET drivers are used to drive the switches. MOSFET driver is the opto-coupler for cutting off the microcontroller from inverter circuit. The HCPL-3120 comprises a GaAsP LED optically coupled to a built-in circuit with a power output stage. This opto-coupler is ideally fit for driving power IGBTs and MOSFETs applied in motor control inverter applications. The high operating voltage range of the output stage furnishes the drive voltages necessary by gate controlled devices. The voltage and current supplied by this opto-coupler makes it ideally fit for directly driving IGBTs with ratings up to 1200V/100A.PWM is given as the input to the driver of the concerned switches. The output of the three phase inverter is the trapezoidal waveform because one from the upper arm and one from the lower arm will conduct. The functional diagram of HPCL 3120 is shown in fig. 7.

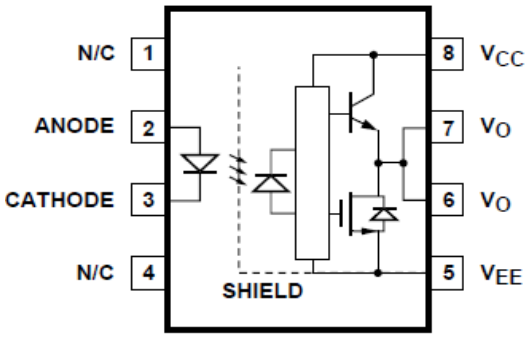

Fig. 7: Functional diagram of HPCL 3120

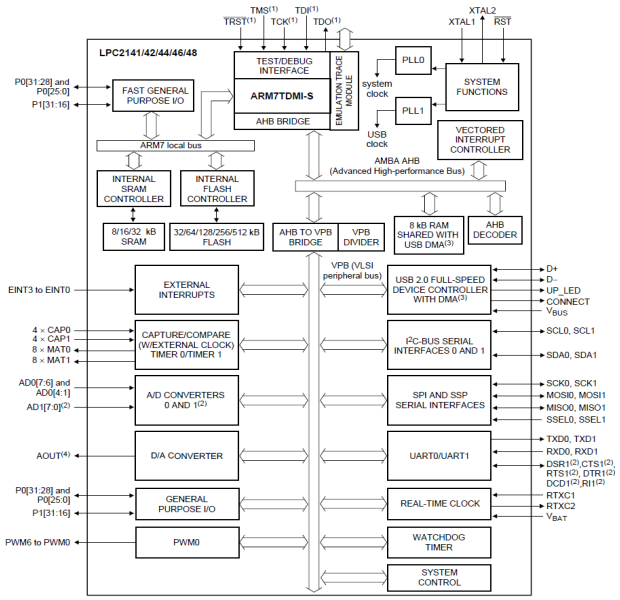

Fig. 8: Architecture of ARM controller

3.2. CONTROLLER

ARM 2148 controller is 16/32-bit, 8 to 40 KB of on-chip static RAM and 32 to 512 KB of on-chip flash program memory, 128 bit wide interface/accelerator enables high speed 60 MHz operation, USB 2.0 Full Speed compliant Device Controller, 8KB of on-chip RAM accessible to USB by DMA, two 10-bit A/D converters, two 32-bit timers/external event counters PWM unit and watchdog, low power real-time clock with independent power and dedicated 32 kHz clock input, On-chip integrated oscillator operates with an external crystal in range from 1 MHz to 30 MHz and with an external oscillator up to 50 MHz, Processor wake-up from Power-down, Single power supply chip with Power-On Reset (POR) and BOD circuits: CPU operating voltage range of 3.0 V to 3.6 V (3.3 V ± 10 %) with 5 V tolerant I/O pads. The architecture of ARM 2148 is shown in fig. 8.

3.3. *DYNAMOMETER*

The loading structure of the BLDC motor is constructed by applying dynamometer. It comprises of hysteresis brake with torque and speed controller. The BLDC motor is burdened by applying the brakes. The torque, speed and power can be measured. TM 302 In-line torque transducer is used to measure the torque and power. The features of torque transducer are Integrated Torque and Speed Conditioning 0.1 Nm to 20 Nm, Accuracy< 0.1%, Overload Capacity of 200%, Overload Limit of 400%, Non-Contact, No Electronic Components in Rotation, High Electrical Noise Immunity, Single DC Power Supply of 20Vdc to 32Vdc, Immediate Speed Detection, Adjustable Torque Signal Frequency Limitation, Built-in Test Function, Stainless Steel Shaft, EMC Susceptibility Conforms to European Standards. The torque transducer diagram is shown in fig.9.

Fig. 9: Diagram of Torque transducer.

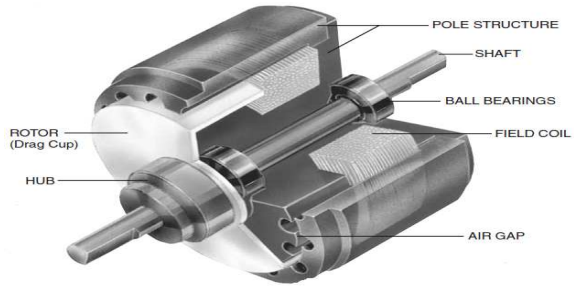

Fig. 10: Model diagram of Hysteresis brake

AHB-1 model Series Compressed-air-cooled Hysteresis Brake is used to employ brakes on BLDC motor. The features of hysteresis brake are ideal for low-torque/high speed applications with phenomenal power ratings, Torque of 1 Nm to 24 Nm, Speed up to 25,000 rpm, Power up to 5300 W, Compressed-air cooling offers excellent heat dissipation, Allowable input air pressure of up 95 PSI eliminates the need for a regulator and provides precise torque control independent of shaft speed. The model diagram of hysteresis brake is shown in fig. 10.

4. Simulation and Experimental Results

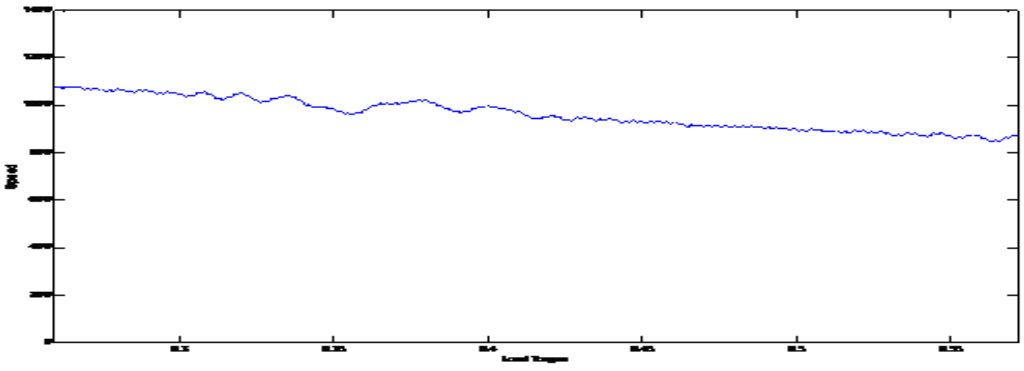

Fig. 11: Simulated Speed torque characteristics of BLDC motor in forward direction.

The simulation was done in MATLAB/Simulink and the Speed Torque characteristics in both forward as

well as reverse direction were drawn as shown in the figure. The load torque is continuously varying and the variation of the Speed is observed in both forward and reverse direction. The Speed-Torque characteristic in the forward direction is shown in fig. 11. The Speed-Torque characteristic in the forward direction is shown in fig. 12.

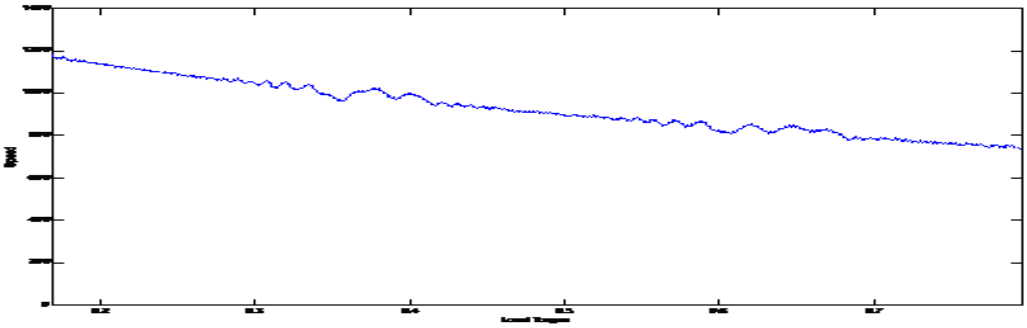

Fig. 12: Simulated Speed torque characteristics of BLDC motor in reverse direction

Fig. 13: Hardware Implementation

The Experiment is done on BLDC motor by connecting inverter with ARM controller. Dynamometer is linked with the BLDC motor and hysteresis brake is applied to the BLDC motor. When the brake is applied, the load torque increases and therefore the speed of the motor decreases. The BLDC motor is rotated in both forward as well as reverse direction. The reading of Speed, torque and power is taken from the dynamometer. The Speed-Torque characteristics of the BLDC motor are drawn individually for forward and reverse directions. Fig.11 shows the Speed-Torque characteristics of the BLDC motor in forward direction. Fig.12 shows the Speed-Torque characteristics of the BLDC motor in reverse direction. The Speed-Torque characteristics of the BLDC motor are compared when the BLDC motor is rotated in both forward as well as reverse direction. Fig.13 shows comparison of the Speed-Torque characteristics of the BLDC motor in forward as well as reverse direction.

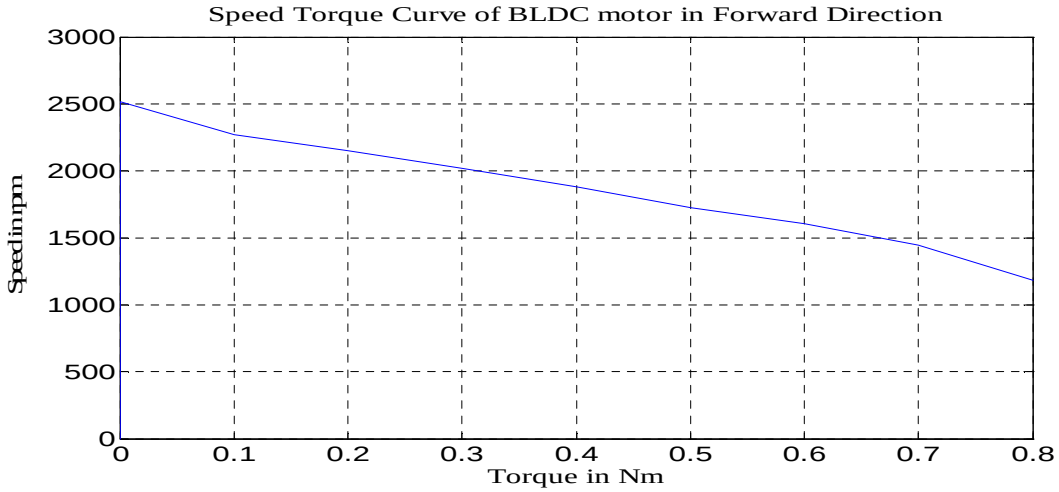

Fig. 14: Speed torque characteristics of BLDC motor in forward direction.

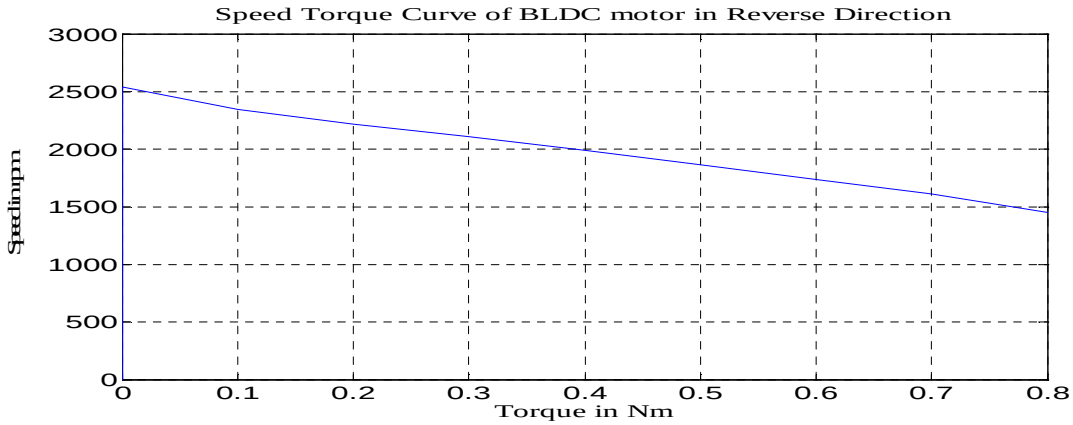

Fig. 15: Speed torque characteristics of BLDC motor in reverse direction.

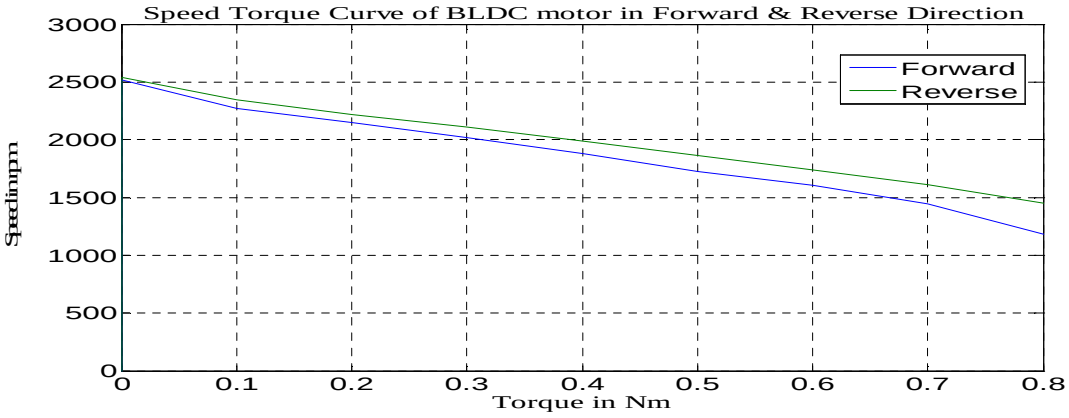

Fig. 13: Speed-Torque characteristics of BLDC motor in both forward as well as reverse direction.

From fig. 13 we can observe that the Speed Torque characteristics of BLDC motor has some difference in

dropping characteristics when it rotates in forward and reverse direction. The simulated and experimental results for the Speed-Torque characteristics of BLDC motor drive in forward and reverse direction are presented. The Specifications of Motor are shown in Table.1

5. Conclusions

In this paper, the BLDC motor is restrained by utilizing ARM controller. The MOSFETs are used in three phase bridge inverter for converting DC to three phase AC. HPCL 3120 driver is used to drive the MOSFETs and also to isolate the inverter circuit from ARM controller. The speed of the BLDC motor can be differed by changing the turn on time of the PWM. The hall sensor output of the BLDC motor is inputted to the ARM controller. The loading arrangement of the BLDC motor is given by dynamometer. The load torque of the BLDC motor is varied by applying the torque sensor. The speed, torque and power of the BLDC motor are measured and the Speed-Torque characteristics are drawn when the motor is rotating not only in forward but also in reverse direction. The simulated values of the BLDC motor can be compared with the experimental results.

Table 1: Motor ratings

Specifications	Units
No. of poles	4
Moment of inertia, J	0.00022 Kg-m^2
Flux density, B	0
Stator resistance, R	0.7
Stator Inductance, L	5.21mH
Terminal Voltage, V	24
Motor constant	0.10476

References

P.Pillay and R.krrishnan. “Modelling , simulation and analysis of a Permanent magnet brushless DC motor drive”, *IEEE Transaction on Industrial Applicantions*, Vol26, pp124-129,2002.

“AN885 - Brushless DC (BLDC) Motor Fundamentals” 2003 Microchip Technology Inc.

IRF540N Advanced HEXFET® Power MOSFETs from International Rectifier.

AHB-1 Series Compressed-air-cooled Hysteresis brake datasheet from Magtrol.

TM 301-308 In-line Torque Transducer datasheet from Magtrol.

HPCL-3120 2Amps Output Current IGBT/MOSFET Gate driver Optocoupler datasheet from Hewlett Packard.

2N2222 NPN switching Transistor datasheet from Discrete Semiconductors.

UM10139, LPC214x User Manual from Philips Semiconductors.

"AN10661, Brushless DC motor control using the LPC 2141", an application note from Philips Semiconductors.

"AN885 - Brushless DC (BLDC) Motor Fundamentals", 2003 Microchip Technology Inc.

M.V.Ramesh received the B.Tech degree in Electrical and Electronics Engineering from Nagarjuna University in the year 1998 and M.S (Electrical Engineering) from German university in the year 2002. Since June 2003 working as an Assistant Professor at P.V.P.S.I.T Engineering College, Vijayawada. His research interests include Power electronics and drives, Power system automation, Hybrid Vehicle Design and Reactive power compensation. He published several papers at the national and international conferences.

J. Amarnath graduated from Osmania University in the year 1982, M.E from Andhra University in the year 1984 and Ph.D from J.N.T. University, Hyderabad in the year 2001. He is presently Professor in the Department of Electrical and Electronics Engineering, JNTU College of Engineering, Hyderabad, India. He presented more than 60 research papers in various national and international conferences and journals. His research areas include Gas Insulated Substations, High Voltage Engineering, Power Systems and Electrical Drives.

S. Kamakshaiah graduated from Osmania University. He obtained M.E (HV) from IISc, Bangalore and Ph.D also from IISc, Bangalore He is former professor & Head of Electrical & Electronics Engineering and chairman of Electrical science J.N.T.University, Hyderabad. He is presently Professor in the Department of Electrical and Electronics Engineering, Vignan college of Engineering, Hyderabad, India. He presented many research papers in various national and international conferences and journals. His research areas include Electrical Machines, High Voltage Engineering, Power Systems, and Electromagnetic Fields.

B.Jawaharlal received the B.Tech degree in Electrical and Electronics Engineering from Andhra University in the year 1998 and M.E from IISc Bangalore in the year 2000. From 2001-2007 worked as Scientist in DRDO/NSTL, Vishakapatnam and at present working as Scientist in DRDO/RCI, Hyderabad.

Journal of Energy Technologies and Policy
ISSN 2224-3232 (Paper) ISSN 2225-0573 (Online)
Vol.2, No.1, 2011

Interoperability Framework for Data Exchange between Legacy and Advanced Metering Infrastructure

Mini S. Thomas
Department of Electrical Engineering, Jamia Millia Islamia
New Delhi, India
Tel: +91-9810424609 E-mail: min_st@yahoo.com

Ikbal Ali
Department of Electrical Engineering, Jamia Millia Islamia
New Delhi, India
Tel: +91-9891478481 E-mail: Iqali_in@yahoo.com

Nitin Gupta
Department of Electrical Engineering, Jamia Millia Islamia
New Delhi, India
Tel: +91-9891960129 E-mail: nitin_ias@yahoo.co.in

Abstract

Performance of Advanced Metering Infrastructure (A MI) is improving due to the introduction of International Electrotechnical Commission's (IEC) 61850 standard based smart meters and Intelligent Electronic Devices (IEDs). Whereas, legacy metering infrastructure and devices can not be ignored due to their wide spread use and substantial capital investment, but at the same time advance technology based smart meters are forcing utilities to adopt new technology in metering. Middle path, before complete transformation takes place, seems to be to make legacy and AMI interoperable. This paper proposes a solution where applications from different manufacturers can access a standard interoperable metered data. A novel solution is also provided for accessing the meter metadata without manually inputting the address parameters of a particular meter to reduce the development time involved in deploying the AMI head-ends.

Keywords: AMI, AMI Head-end, IEC 61850, Interoperability, Metadata, Smart Grid, XML Database

1. Introduction

Smart Grid is becoming popular day by day where utilities, manufacturers, and solution providers are exploring ways and means to improve and implement the technology for leveraging the existing power generation, transmission, distribution and metering infrastructure. A number of smart-grid advances in distribution management are expected where integration means, protocol standards, open systems, standard databases and data exchange interfaces will allow flexibility in the implementation of the head-end applications [1]. Further critical technologies like advanced visualization capabilities, measurement based stability analysis etc. are needed to achieve the vision of smart control center for providing reliable, economical, and sustainable delivery of electricity [2], [3]. To achieve the vision, utilities and solution providers have to develop and integrate the necessary technologies. Javier described the concept,

characteristics, and benefits of implementing a smart grid [4]. Considering multi-manufacturer devices in an infrastructure, utilities have limited capabilities for enabling the integration across the applications to perform functions like system planning, power delivery and customer operations. In most of the cases, users of one department can not access the applications or data of other departments because of integration and interoperability issues. It is estimated that the utilities allocates programming budget of 35-40% for developing, maintaining and updating the programs especially for exchanging the information between legacy systems and databases [4]. In some cases, it was found that the lack of acceptable standards has delayed or stopped the deployment of smart grid technologies [5]. Thus smart grid society should be aware of guidelines and best practices that the electric utility is using in integration of energy infrastructure. Smart grid solutions suite using industry standards such as IEC61850, IEC61968, IEC61970, Common Information Model (CIM), and web services can help in data exchange amongst different applications [6]. IEC 61850 is a standard that provides an ability to achieve interoperability between multi-vendors IEDs installed in a substation [7]. IEC 61850 provides a comprehensive model that organizes data in a manner that is consistent across all types and brands of IED's.

Javier pointed out that the brand of one manufacturer does not always work with the brand of another manufacturer and identified this as a problem of flying monkeys [4]. Various strategies adopted by the utilities to overcome this problem are described by Steven in [8], where utilities try to give tender to a single manufacturer, who can complete the job from designing to erection and commissioning with proper documentation and training. With this solution, still, the utilities are dependent on the solution providers to carry out an integration task. Dependency on a particular solution provider is not a wise decision when the utilities look it from future perspectives.

Interoperability is a property which enables heterogeneous systems and organizations to work together for exchanging or sharing the information. Thus interoperability enables seamless end-to-end integration of hardware and software components in a system. Infrastructure or systems providing interoperability will be more productive through automation and enable smooth data and information exchange. Interoperability also enables users to choose between features and vendors rather than technologies. A checklist is provided by Alison et al. that help utilities to determine whether they have the characteristics or capabilities to contribute to the interoperability [9].

2. AMI and Smart Grid

Grid is not a single entity but a combination of multiple networks comprising of varying levels of devices, the communications and co-ordination among them are mostly manually controlled. By adding digital intelligence to the existing grid infrastructure, the grid can be made smarter. Automatic meter reading (AMR) is the technology of automatically polling the electricity usage reading from electric meters and transferring the readings to a central station for billing purposes. AMR technologies reduced the cost of reading the power meters by eliminating the involvement of man power. Thus AMR help utilities to overcome the challenges involved in meter-reading. Due to one way communication, AMR alone can not satisfy the objectives of today's environment. AMI comprising smart meters with two-way communication is becoming an emerging technology growing from AMR where meter readings are gathered intelligently at reduced cost [10]. AMI as a subset of smart grid acts as a solid interface between the grid and the consumers. Earlier, the electricity outages in a particular area were identified via the customer calls. By utilizing an AMI, the utilities can identify when, where, and why an outage occurs. Leveraging AMI infrastructure is an emerging research area where suitable strategies need to be adopted for realizing the smart grid. To know the load profile, power consumption or demand of a particular area, AMI plays a critical role in delivering the electricity usage. AMI with two way communication enables time stamping of metered data, outage detection and other functions like real-time pricing, load profile detection, on-off switching of registered home appliances etc. A cost effective and flexible GSM based AMI system is described by Huibin et al. where distributed structure of the AMI system makes it easy to be adopted in different sizes of utility systems [10].

In AMI systems, most of the time, there exist heterogeneous software/hardware components in the same network. Moreover, they are tightly coupled with each other and make interaction and integration job

tedious for a system integrator or a solution provider. A service oriented AMI is discussed by Shudong et al. where smart meter reading is performed by calling the distributed meter reading services on the smart meters but the solution does not incorporate the digital meters having one way communication called as legacy meters installed in the network [11]. Ronald, in [12], described a software package using Open Database Connectivity (ODBC) and Dynamic Data Exchange (DDE) protocol for exchanging the data with the power systems, which is generic with Microsoft technologies only. Considering a scenario of TCP/IP Modbus networks in smart grid, various applications like SCADA, Energy Management system (EMS), and AMI creates their own proprietary databases and some of the databases are not in the standard format. For example, Schneider Electric SCADA Vijeo Citect 6.0 stores the tag values in .hst files whose format is not a standard format [18]. Therefore, without using translating or converting mechanisms, applications of different vendors can not access these .hst files or proprietary databases. Keeping heterogeneous nature of application's databases in mind, the domain of data engineering is under extensive research [13-15].

It is observed that by incorporating the IEC 61850 based smart meters and IEDs, web services, CIM, and Service-Oriented Architecture (SOA) technologies, interoperability can be achieved. But the problem arises when legacy infrastructure is integrated with the advanced infrastructure. This paper is an attempt to provide a mechanism for integrating the plurality of TCP/IP Modbus metering networks.

While developing the AMI head-ends, users or system integrators have to refer power meter manual for knowing the parameters address called as metadata. This is a manual task which becomes cumbersome when there are varieties of multi-vendor meter models installed in an AMI network. Referring power meter manuals involves human intervention which increases the overall development time of AMI head-end applications. This paper provides a novel mechanism of automatically extracting the metadata from a power meter and thus eliminates the need of inputting the parameters address manually.

Further the paper is organized as follows. Section 3 describes the current scenario of data exchange in a traditional metering infrastructure. Section 4 describes the proposed methodology for interoperable framework for data exchange between legacy and advanced metering infrastructure. An interoperable framework for metering infrastructure and its advantages are described in Section 5, whereas conclusions are given in section 6.

3. Data Exchange in Traditional AMI Network

Figure 1 illustrates the two AMI networks, comprising multi-vendor meters, where Application2 is required to fetch the data from a Database1 existing in Network1. Because of the different database architecture, i.e. schema and data types, translating or converting software components need to be incorporated as an interface between Database1 and Application2 to help Application2 for accessing the data from Database1 [12]. Application developers have to spend more time in understanding the architecture of database and modify the application accordingly. This problem becomes tedious to handle if a large number of AMI network databases need to be integrated. Therefore, a new methodology is proposed in this paper by which any of the AMI applications can access the database without requiring any translation or conversion of data.

4. Modified AMI Network Architecture

The architecture, as shown in Figure 2, consists of multiple AMI networks, each comprising at least one or more digital Modbus TCP/IP power meters, having one way communication means and smart meters having two way communication means at level1 as depicted M1, M2…, Mn. AMI head-end, AMI proprietary database, and XML database in parallel with proprietary database at level2, whereas Level3 is the higher level comprising applications like ERP system, and SCADA historian server, running on a remote station or local station. In the modified architecture, XML database running in parallel not only helps in achieving the interoperability but also provides redundancy in case of failure of AMI proprietary database. Thus by creating a XML database in each AMI network help applications, running at level2 or level3, for exchanging the metered data. Working of the proposed methodology for the modified AMI network architecture, as shown in Figure 2, is depicted in Figure 3.

"Parameter Extraction Routine" accepts two inputs named as "Meter Model Make" and "Meter Slave ID" and sends a read request for finding the address of parameters from a central repository. After extracting the parameters address, "Meter Polling Routine" polls the meters for extracting the metered values which are further used by the "Data Storage Routine" for storing the metered data in XML format.

In the modified architecture, ModSim32 tool is used to virtualize the functionality of a physical power meter installed at level1. ModSim32, as shown in Figure 4, simulates data from one or more Modbus slave devices instead of having the physical meters or slave devices [16]. ModSim32 can be connected to a Modbus TCP/IP master application via TCP/IP protocol. ModSim32 supports multiple simultaneous communications with master application and the data is accessed via any connected COM port or TCP/IP network connection. Figure 4 shows the screenshot for configured parameters (i.e. voltage, current, frequency, kW, kVA, kVAR, and kWhr) in ModSim32 for which data is scanned in AMI head-end. Thus effectively, a test setup is created where head-end application is shown in Figure 5 and a virtual physical meter with which this head-end application exchanges data is shown in Figure 4.

The created AMI head-end, as shown in Figure 5, is different from the existing meter head-ends, e.g. System Manager Software (SMS) from Schneider [17] or any other SCADA systems, because it does not need manual entry of the parameters addresses because the parameters are extracted automatically. The framework of achieving interoperability for data exchange in the AMI networks and parameter extraction from digital meters are described in the next section.

5. Interoperable Framework Implementation for AMI Network

For fetching the parameters value from a power meter, AMI head-end application needs to be configured with addresses of those parameters. Configuring the head-end application with parameter address, discussed in [17], or any other SCADA system is a manual task. This requires a user to enter the addresses of the parameters for each meter connected with AMI head-end application. Moreover, user has to refer a specific power meter manual for looking the address parameters.

5.1 Automatic extraction of parameter address

In the proposed methodology, the manual user intervention is eliminated by providing an XML file (i.e. called as "Rule File") containing the metadata, or parameter address information, for a particular meter. The XML rule file is required to be stored in the name of meter's model in a shared repository. For example, this paper has considered a virtual Win-tech meter, whose XML rule file called as "ModSim32-Sim.xml", is stored in the repository representing Win-tech meter model "ModSim32-Sim". Once all the XML rule files by different meter manufacturers for all the meter models are placed in one repository, the head-end application, as shown in Figure 5, scans each XML rule file for extracting the addresses of the parameters. For example, for finding the address of parameters like voltage, current etc. of Win-tech meter model ModSim32-Sim, the head-end application first searches an XML file "ModSim32-Sim.xml" placed in the repository. On the identification of "ModSim32-Sim.xml" file, a file handle is created, which extracts the address of the parameter (i.e. voltage, current, frequency, kW, kVA, kVAR, and kWhr) from the "ModSim32-Sim.xml" file. The mechanism for searching the XML rule files and extracting the addresses of parameters from the XML rule file is made automatic and one time process, which is executed at the time of initialization of the head-end application. The implemented AMI head-end application, as shown in Figure 5, consists of two windows. Left side window is called as "Meter Parameter Values", displaying the meter readings, and right side window is called as "Meter Connection Settings", in which configuration settings for a meter model are entered.

In "Meter Connection Settings", only "Slave Node ID" and "Slave Meter Make" fields are entered by the user and rest of the process for searching the XML rule file and parameter address extraction is performed by the head-end application automatically. "Slave Node ID" is the slave identifier assigned to a particular power meter installed in a metering network at level1 of Figure 2.

The value assigned to the "Slave Node ID" field needs to be a unique integer value for each power meter in the same network. "Slave Meter Make" field provides the information about the make of a meter model to the head-end application. This information enables the head-end application to refer to a particular XML rule file for extracting the addresses of parameters. The workflow of the head-end application is shown in Figure 6.

5.2 XML Data Storage

AMI is a network of heterogeneous systems comprising of multi-vendor meter head-end applications and databases. The data offered by these applications is not always compatible when exchanging the data with other vendor's applications. The proposed methodology uses an XML format to overcome the problem of data incompatibility so that any of the vendor's application can access it. XML data is stored in plain text format. Data extracted from a meter is wrapped into tags, which is software or hardware independent.

Data Storage Routine, as depicted in Figure 3, stores the meter readings in the XML format. Figure 7 displays the part of the stored data in XML form, where data is stored with the following information (i) Date, (ii) time stamp, (iii) meter model, (iv) location of the installed meter, and (v) parameter's value. Date and time stamping along with the parameter's value are used for tracking the historical values of any parameter of interest. Thus the history record of logged parameters enables the utilities to generate bills or do analysis for taking certain actions.

In case of a faulty situation, meter model and location information, stored in the XML file, enables the user to easily track the location of the installed meter. XML format storage thus enables the head-end applications interoperable and allows any meter manufacturer's application to access the XML databases without the need of any driver or protocol translator/converter. Moreover, using the XML data makes it easier to upgrade and integrate with new applications and systems without the cooperation from different vendors. Hence, leveraging the existing AMI becomes possible.

5.3 Rules

"Rule File" stores the metadata in XML format for a particular meter model. For example Figure 8 displays one of the rule file and provides the information related to the meter's manufacturer name, meter model, meter serial number, parameters addresses (i.e. voltage, current, power etc.), bytes required to store the parameter's value.

Advantages of creating the XML rules and database are as follows:

i) Automatic Address Extraction:

The automatic parameter address extraction eliminates the need of referring the meter manual for finding the address of the parameters.

ii) Fast AMI Deployment:

In case of hundreds of thousands of meters installed in an AMI network, proposed methodology makes the AMI head-end deployment faster due to its automatic address extraction property.

iii) User Friendly:

Users can customize the XML rule file as per their requirements to create their own tags as per the power meter specifications without taking technical help from solution provider.

iv) Adaptable:

In any of the monitoring applications, data storage plays an important role. If data is easily available or accessible, third-party applications can easily work on this data without wasting the time and efforts in knowing how to extract the data from proprietary data storage. Thus the use of storing the data in XML format enables third party applications adaptable to the storage means.

v) High Availability:

As the XML data storage is redundant to existing AMI database, any failure or corruption of AMI database will not hamper the work of other applications as XML database is still available. Thus redundant database makes the data available at any time. Moreover, queries for extracting the data will be executed on XML database instead of executing on AMI proprietary database.

Methodology, proposed in this paper, intends to relieve the utilities of worrying too much on integration issues and thus provides a solution for leveraging the legacy metering infrastructure by integrating it with the AMI. Once the AMI infrastructure is integrated, the overall system can provide much improved information of electricity usage and grid status seamlessly, that further enables utilities to make better decisions about system improvements and service offerings. The proposed architecture is not limited to only electric meters rather it can be used for water and gas digital meters as well.

5. Conclusion

Paper has proposed the XML format based interoperability framework for data exchange between legacy and AMI infrastructure and successfully demonstrates the implementation of the two important aspects, automatic parameter address extraction and data storage in XML format, related to interoperability and for integrating the legacy and AMI infrastructure

References

[1] Hassan Farhangi, “The Path of the Smart Grid,” IEEE Power & Energy Magazine, vol. 8, no.1, pp. 18-28, January-February 2010.

[2] Pei Zhang, Fangxing Li, N. Bhatt, "Next-Generation Monitoring, Analysis, and Control for the Future Smart Control Center," IEEE Transactions on Smart Grid, vol. 1, no. 2, pp. 186-192, Sept. 2010.

[3] Fangxing Li, Wei Qiao, Hongbin Sun, Hui Wan, Jianhui Wang, Yan Xia, Zhao Xu, and Pei Zhang “Smart Transmission Grid: Vision and Framework,” IEEE Transactions on Smart Grid, vol. 1, no. 2, pp. 168-177, September 2010.

[4] Javier Rodríguez Roncero, “Integration Is Key to Smart Grid Management,” CIRED Seminar 2008: Smart Grids for Distribution, Frankfurt, paper no. 9, pp. 23-24, June 2008.

[5] S. Rahman, “Smart grid expectations,” IEEE Power and Energy Magazine, vol. 7, no. 5, pp. (88, 84-85), Sept.-Oct. 2009.

[6] Andrea Mercurio, Alessandro Di Giorgio, and Pierfrancesco Cioci “Open-Source Implementation of Monitoring and Controlling Services for EMS/SCADA Systems by Means of Web Services—IEC 61850 and IEC 61970 Standards,” IEEE Transactions on Power Del., vol. 24, no.3, pp. 1148-1153, July 2009.

[7] M. S. Thomas, D. P. Kothari, and Anupama Prakash “Design, Development, and Commissioning of a Substation Automation Laboratory to Enhance Learning,” IEEE Transactions on Education, vol. 54, no. 2, pp. 286-293, May 2011.

[8] S. E. Collier, “Ten steps to a smarter grid,” IEEE Rural Electric Power Conference, pp. B2 - B2-7, 26-29 April 2009.

[9] Alison Silverstein, Richard Schomberg, “Highlighting Interoperability: How to design a new metering-system architecture,” Public Utilites Fortnightly, vol. 145, no. 6, pp. 78-82, 2007.

[10] Huibin Sui, Honghong Wang, Ming-Shun Lu, and Wei-Jen Lee “An AMI System for the Deregulated Electricity Markets,” IEEE Transactions on Industry Applications, vol. 45, no. 6, pp. 2104-2108, November/December 2009.

[11] Shudong Chen, J. Lukkien, Liang Zhang "Service-oriented Advanced Metering Infrastructure for Smart Grids," Asia-Pacific Power and Energy Engineering Conference, pp. 1-4, 28-31, March 2010.

[12] R. H. Simpson, "Power System Data Base Management," IEEE Transactions on Industry Applications, vol. 37, no. 1, pp. 153-157, Jan.-Feb. 2001.

[13] Sally McClean, Bryan Scotney "A Scalable Approach to Integrating Heterogeneous Aggregate Views of Distributed Databases," IEEE Transactions on Knowledge and Data Engineering, vol. 15, no. 1, pp. 232-236, Jan.-Feb. 2003.

[14] L. Caroprese, S. Greco, and E. Zumpano, "Active Integrity Constraints for Database Consistency Maintenance," IEEE Transactions on Knowledge and Data Engineering, vol. 21, no. 7, pp. 1042-1058, July 2009.

[15] W. Meier, "eXist: An Open Source Native XML Database," In Web, Web-Services, and Database Systems LNCS (Springer), vol. 2593, pp. 169-183, 2003.

[16] "ModSim32-Application Description," [Online]. Available: http://www.win-tech.com/html/modsim32.htm

[17] "System Manager Software," [Online]. Available: http://sedatacenters.com/products/power/power_monitoring/system_ma nagersoftware/

[18] "Vijeo Citect- 10 things you should know about SCADA," [Online]. Available: http://www.globaldownload.schneiderelectric.com/85257578007E5C8A/all/BD60E019EB44EF318525759F 00692DB4/$File/vijeocitect_1_en.pdf

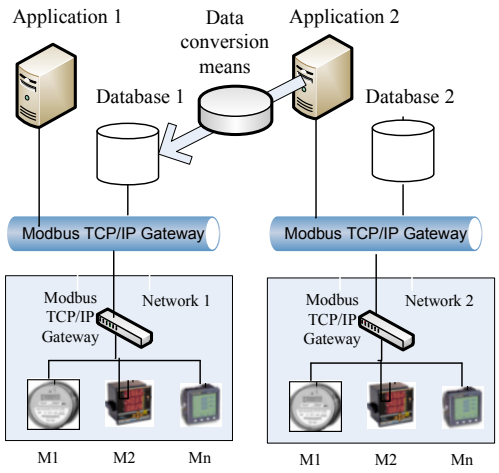

Figure 1. Two Different AMI Network Trying to Exchange the Meter Database

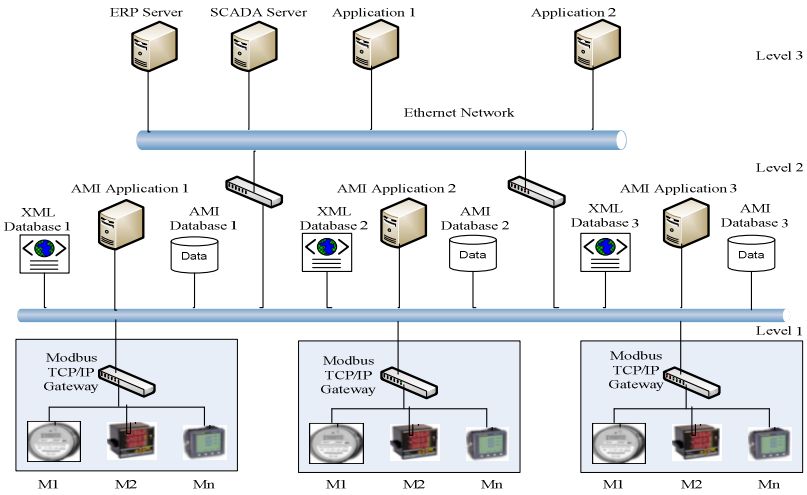

Figure 2. Modified AMI Architecture

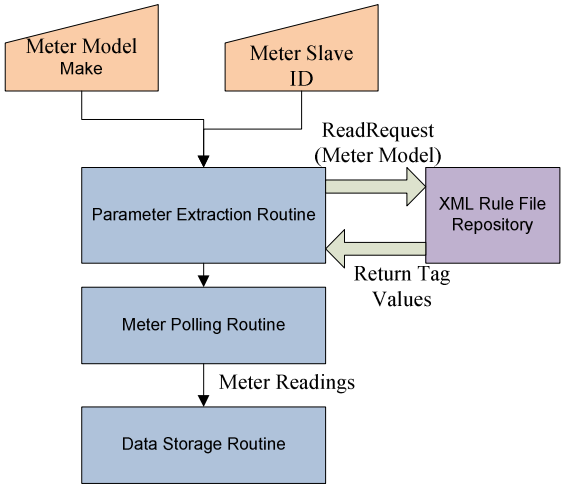

Figure 3. Modified Architecture Internals

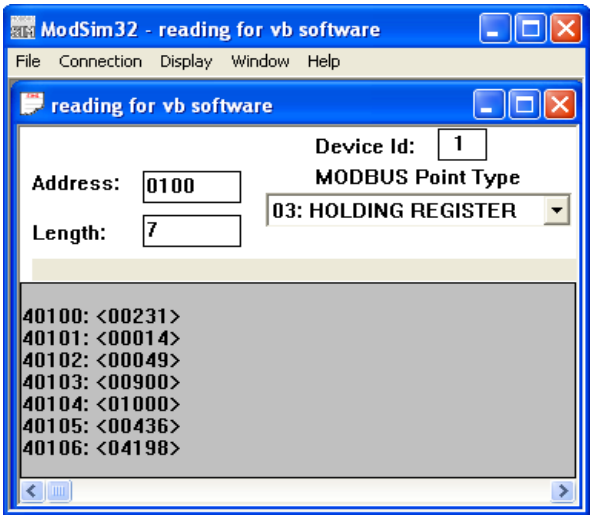

Figure 4. ModSim32 Software Virtualizing a Physical Meter

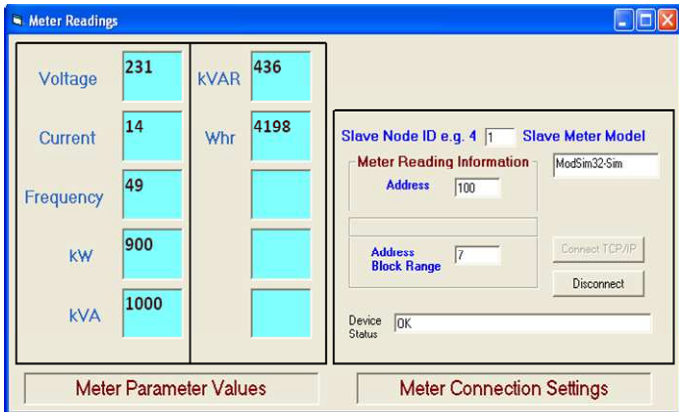

Figure 5. AMI Head-End User Interface

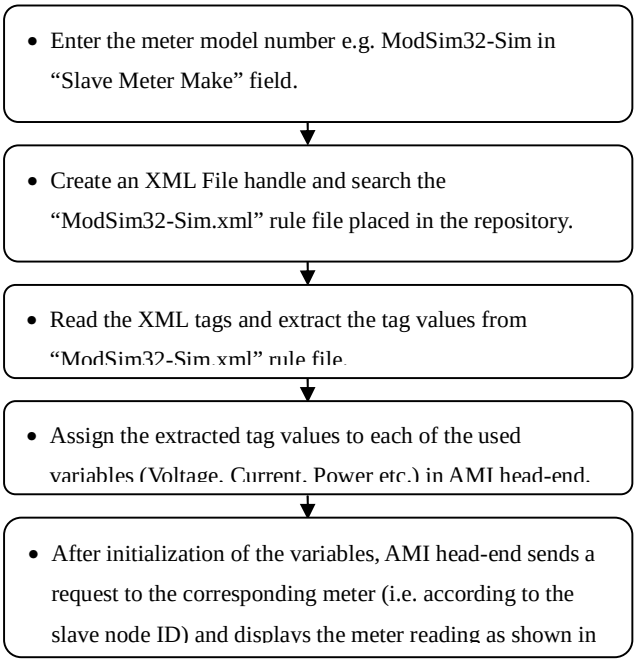

Figure 6. AMI Head-end Framework Steps


```
<?xml version="1.0" encoding="UTF-8" ?>
- <Meter_Database>
  - <Meter_Reading>
      <Date>9/12/2011</Date>
      <Time>10:43:07 PM</Time>
      <Meter_ID>M1-ModSim32-Sim</Meter_ID>
      <Meter_Location>Loc1</Meter_Location>
      <Meter_Voltage>231</Meter_Voltage>
      <Meter_Current>14</Meter_Current>
      <Meter_Frequency>49</Meter_Frequency>
      .  .
      .  .
      .  .
      .  .
    </Meter_Reading>
  </Meter_Database>
```

Figure7. Data Storage in XML Form

```
<?xml version="1.0" encoding="utf-8" ?>
- <Policy>
  - <Meter_Parameters>
      <Meter_Make>Win-tech</Meter_Make>
      <Meter_Model>ModSim32-Sim</Meter_Model>
      <Meter_SrNo>12345</Meter_SrNo>
      <Meter_Voltage>100</Meter_Voltage>
      <Meter_Voltage_Byte>1</Meter_Voltage_Byte>
      <Meter_Current>101</Meter_Current>
      <Meter_Current_Byte>1</Meter_Current_Byte>
      <Meter_Frequency>102</Meter_Frequency>
      <Meter_Frequency_Byte>1</Meter_Frequency_Byte>
      <Meter_KW>103</Meter_KW>
      <Meter_KW_Byte>1</Meter_KW_Byte>
      <Meter_KVA>104</Meter_KVA>
      <Meter_KVA_Byte>1</Meter_KVA_Byte>
      <Meter_KVAR>105</Meter_KVAR>
      <Meter_KVAR_Byte>1</Meter_KVAR_Byte>
      <Meter_WH>106</Meter_WH>
      <Meter_WH_Byte>1</Meter_WH_Byte>
    </Meter_Parameters>
  </Policy>
```

Figure 8. XML Rule File

Mini S. Thomas (M'88–SM'99) received the Bachelor's degree from the University of Kerala, Kerala, India, and the M.Tech. degree from the Indian Institute of Technology (IIT) Madras, Chennai, India, both with gold medals, and the Ph.D. degree from IIT Delhi, Delhi, India, in 1991, all in electrical engineering. Her employment experiences were at the Regional Engineering College Calicut, Kerala, India; the Delhi College of Engineering, New Delhi, India; and currently as a Professor with the Faculty of Engineering and Technology, Jamia Millia Islamia, New Delhi, India. She has published 60 papers in international/ national journals and conferences. Her current research interests are in SCADA systems, intelligent protection of power systems, and the smart grid. Prof. Thomas received the prestigious Career Award for young teachers, instituted by the Government of India.

Ikbal Ali (M'04, SM'11) received B.Tech. degree from Aligarh Muslim University, Aligarh, India and the M.Tech. degree from the Indian Institute of Technology, Roorkee, India. Currently, he is Senior Assistant Professor in the Department of Electrical Engineering, Jamia Millia Islamia, New Delhi. His current research

interests are the SCADA/ Energy Management Systems, IEC 61850-based substation automation systems, substation communication networks architecture, power system communication, and smart grid.

Nitin Gupta received the Bachelor's degree in Instrumentation engineering from Sant Longowal Institute of Engineering and technology (SLIET), Sangrur, Punjab India, in 2002, and the M.Tech. degree in Computer Science and Engineering from Guru Jambheshwar University, Hisar, Haryana India, in 2004. He is currently pursuing PhD from the department of Electrical Engg., Jamia Millia Islamia, New Delhi, India.

Journal of Energy Technologies and Policy
ISSN 2224-3232 (Paper) ISSN 2225-0573 (Online)
Vol.2, No.1, 2011

Minimizing Rental Cost under Specified Rental Policy in Two Stage Flowshop Set Up time, Processing Time Each Associated with Probabilities Including Break-down interval and Job Block Criteria

Sameer Sharma

Department of Mathematics, Maharishi Markandeshwar University, Mullana, Ambala, India

* E-mail of the corresponding author: samsharma31@yahoo.com

Abstract: This paper is an attempt to study two stage flow shop scheduling problem in which the processing times and independent setup times each associated with probabilities of the jobs are considered to minimize rental cost under specified rental policy including break-down interval and equivalent job-block criteria. The study gives an optimal schedule for the problem. The method is justified with the help of numerical example and a computer program.

Keywords: Equivalent-Job, Rental Policy, Makespan, Elapsed Time, Idle Time, Breakdown Interval, Utilization Time

1. Introduction

Practical machine scheduling problems are numerous and varied. They arise in diverse areas such as flexible manufacturing systems, production planning, computer design, logistics, communication etc. A scheduling problem is to find sequence of jobs on given machines with the objective of minimizing some function of the job completion times. A variety of scheduling algorithms have been developed over the past years to address different production system. In flow shop scheduling it is generally assumed that the jobs must be processed on the machines in the same technological or machine order. One of the earliest results in flow shop scheduling theory is an algorithm given by Johnson (1954). The work was developed by Ignall and Scharge (1965), Bagga. (1969), Szwarch (1977), Anup (2002), Singh (2005), Gupta (2006) by deriving the optimal algorithm for two, three or multistage flow shop problems taking into account the various constraints and criteria. The basic concept of equivalent job for a job – block has been investigated by Maggu & Das (1977) and established an equivalent job – block theorem. Breakdown of machine due to failure of electric current or due to non - supply of raw material or any other technical interruptions have a significant role in production concern. Adiri (1989), Akturk and Gorgulu (1999), Smith (1956), Szwarc (1983), Chandramouli (2005), Singh (1985) have discussed the various concepts of breakdown of machines.

Gupta & Sharma (2011) studied n× 2 flow shop problem to minimize rental cost under pre–defined rental policy in which probabilities have been associated with processing time including breakdown interval and job – block criteria. The present paper is an attempt to extend the study made by Gupta & Sharma (2011) by introducing the concept of set up time separated from processing time, each associated with probabilities including job block criteria and breakdown interval. We have developed an algorithm for minimization of utilization of 2^{nd} machine combined with Johnson's algorithm to solve the problem

2. Practical Situations

A lot of practical situations have been observed in real life when one has got the assignments but does not have one's own machine or does not want to take the risk of investing a huge amount of money to purchase, under such situation the machine has to be taken on rent to complete the assignment. As in the starting of

his professional career, the medical practitioner does not buy expensive machine say X-ray machine, ultrasound machine etc but instead makes a contract on rent basis. Renting enables saving working capital, gives option for having the equipment and allows upgradation of new technology. Sometimes priority of one job over other is preferred. It may be because of urgency or demand of its relative importance, the job block criteria become important. Another event which is most considered in models is breakdown of machines. . The break down of the machines (due to delay in material, changes in release and tails date, tool unavailability, failure of electric current, the shift pattern of the facility, fluctuation in processing times, some technical interruption etc.) have significant role in the production concern. Setup includes work to prepare the machine, process or bench for product parts or the cycle. This includes obtaining tools, positioning work-in-process material, return tooling, cleaning up, setting the required jigs and fixtures, adjusting tools and inspecting material and hence significant.

3. Notations

S : Sequence of jobs 1,2,3,...,n

M_j : Machine j, j=1,2,.....

A_i : Processing time of i^{th} job on machine A

B_i : Processing time of i^{th} job on machine B

A'_I : Expected processing time of i^{th} job on machine A

B'_I : Expected processing time of i^{th} job on machine B

p_i : Probability associated to the processing time A_i of i^{th} job on machine A

q_i : Probability associated to the processing time B_i of i^{th} job on machine B

S_i^A : Set up time of i^{th} job on machine A

S_i^B : Set up time of i^{th} job on machine B

r_i : Probability associated to the set up time S_i^A of i^{th} job on machine A

s_i : Probability associated to the set up time S_i^B of i^{th} job on machine B

S_i : Sequence obtained from Johnson's procedure to minimize rental cost

β : Equivalent job for job block

L : Length of breakdown interval

$A'_{\alpha i}$: Processing time of i^{th} job after breakdown effect on machine A

$B'_{\alpha i}$: Processing time of i^{th} job after breakdown effect on machine B

A''_I : Expected processing time of i^{th} job after breakdown effect on machine A

B''_I : Expected processing time of i^{th} job after breakdown effect on machine B

C_j : Rental cost per unit time of machine j

U_i : Utilization time of B(2^{nd}machine) for each sequence S_i

$t_1(S_i)$:Completion time of last job of sequence S_i on machine A

$t_2(S_i)$:Completion time of last job of sequence S_i on machine B

$R(S_i)$:Total rental cost of sequence S_i of all machines

$CT(S_i)$:Completion time of 1^{st} job of each sequence S_i on machine A

4. Problem Formulation

Let n jobs say $\alpha_1, \alpha_2, \alpha_3, \ldots\ldots, \alpha_n$ are processed on two machines A & B in the order AB. A job α_i (i=1, 2, 3, ...,n) has processing time A_i & B_i on each machines respectively with probabilities p_i & q_i s.t. $0 \le p_i \le 1$, $\sum p_i = 1$, $0 \le q_i \le 1$, $\sum q_i = 1$. Let S_i^A & S_i^B be there setup times separated from their processing times associated with

probabilities r_i & s_i s.t. $0 \le r_i \le 1$, $\sum r_i = 1$, $0 \le s_i \le 1$, $\sum s_i = 1$on each machine. Let an equivalent job block β is defined as (α_k, α_m) where α_k , α_m are any jobs among the given n jobs such that α_k occurs before job α_m in the order of job block (α_k, α_m) .Our objective is to find an optimal schedule of the jobs which minimize the utilization time of machine and hence the total rental cost of the machines.

5. Assumptions

1. We assume the rental policy that all machines are taken on rent as and when they are required and are returned as when they are no longer required for processing.
2. Job are independent to each other.
3. Machine breakdown interval is deterministic, i.e. breakdown intervals are well known in advance. This simplifies the problem by ignoring the stochastic cases where breakdown interval is random.
4. Pre-emption is not allowed, i.e. once a job is started on a machine, the process on that machine can't be stopped unless job is completed.
5. It is given to sequence k jobs i_1, i_2 ……..i_k as a block or group job in the order (i_1, i_2 ……i_k) showing priority of job i_1 over i_2 etc

6. Algorithm

To obtain optimal schedule we proceed as:

Step 1: Define expected processing time A'_i & B'_i on machine A & B respectively as follows :

$A'_i = A_i \times p_i - S_i^B \times s_i$

$B'_i = B_i \times q_i - S_i^A \times r_i$

Step 2: Define expected processing time of job block $\beta = (k,m)$ on machine A & B using equivalent job block given by Maggu & Das. i.e. A'_β and B'_β are as follows.

$A'_\beta = A'_k + A'_m - \min (B'_k, A'_m)$

$B'_\beta = B'_k + B'_m - \min (B'_k, A'_m)$

Step 3: Apply Johnson's (1954) technique to find an optimal schedule of given jobs.

Step 4: Prepare a flow time table for sequence obtained in step 3 and read the effect of break down interval (a,b) on different jobs on lines of Singh T.P (1985).

Step 5: Form a reduced problem with processing time $A'_{\alpha i}$ and $B'_{\alpha i}$ If breakdown interval (a,b) has effect on job i^{th} then .

$A'_{\alpha i} = A_i \times p_i + L$,

$B'_{\alpha i} = B_i \times q_i + L$ where $L = b - a$, length of break down interval.

If breakdown interval (a,b) has no effect on i^{th} job then.

$A'_{\alpha i} = A_i \times p_i$

$B'_{\alpha i} = B_i \times q_i$

Step 6: Find revised processing time after the effect of breakdown (6,10) ie

$A''_i = A'_{\alpha i} - S_i^B \times s_i$

$B''_i = B'_{\alpha i} - S_i^A \times r_i$

Step 7: Find the processing time A''_β and B''_β of job block β (k , m) on machine A and B using equivalent job block β as in step 2 .

Step 8: Now repeat procedure to obtain optimal schedule of given jobs as in step 3

Step 9: Observe processing time of 1^{st} job of S_i on 1^{st} machine A let it be α .

Step 10: Obtain all jobs having processing time on A greater than α . Put this job one by one in 1st position of sequence S_i in same order. Let these sequences be S_2 , S_3 , S_4 ,....., S_r .

Step 11: Prepare In-out flow table only for those sequences S_i (i=1,2,....,r) which have job block β (k,m) and evaluate total completion time of last job of each sequence ie t_1 (S_i) & t_2 (S_i) on machine A & B respectively.

Step 12: Evaluate completion time CT(S_i) of 1st job of each of above selected sequence S_i on machine A .

Step 13: Calculate utilisation time U_i of 2nd machine for each of above selected sequence S_i as :

$U_i = t_2(S_i) - CT(S_i)$ for i=1,2,3,....,r

Step 14: Find min {U_i} , i=1,2,....,r let it be corresponding to i = m .Then S_m is optimal sequence for minimum rental cost .

Min rental cost = $t_1(S_m) \times C_1 + U_m \times C_2$

Where C_1 & C_2 are rental cost per unit time of 1st & 2nd machines respectively.

7. Programme

```
#include<iostream.h>
#include<stdio.h>
#include<conio.h>
#include<process.h>
void display();
void schedule(int,int);
void inout_times(int []);
void update();
void time_for_job_blocks();

float min;int job_schedule[16];int job_schedule_final[16];int n;
float a1[16],b1[16],a11[16],b11[16],s11[16],s21[16];float a1_jb,b1_jb;
float a1_temp[15],b1_temp[15];int job_temp[15];int group[2];//variables to store two job blocks
int bd1,bd2;//break down interval
float a1_t[16], b1_t[16],a11_t[16],b11_t[16];float a1_in[16],a1_out[16];float b1_in[16],b1_out[16];
float ta[16]={32767,32767,32767,32767,32767},tb[16]={32767,32767,32767,32767,32767};
void main()
{

clrscr();int a[16],b[16],s1[16],s2[16];
float p[16],q[16],r[16],s[16];int optimal_schedule_temp[16];int optimal_schedule[16];
float cost_a,cost_b,cost;
float min; //Variables to hold the processing times of the job blocks
cout<<"How many Jobs (<=15) : ";cin>>n;
if(n<1 || n>15)
{cout<<"Wrong input, No. of jobs should be less than 15..\n Exitting";getch();exit(0);}
cout<<"Enter the processing time and their respective probabilities ";
```

```
for(int i=1;i<=n;i++)
{cout<<"\nEnter the processing time,set up time and their probability of "<<i<<" job for machine A : ";
cin>>a[i]>>p[i]>>s1[i]>>r[i];
cout<<"\nEnter the processing time and its probability of "<<i<<" job for machine B : ";
cin>>b[i]>>q[i]>>s2[i]>>s[i];
//Calculate the expected processing times of the jobs for the machines:
a11[i] = a[i]*p[i];b11[i] = b[i]*q[i];s11[i] = s1[i]*r[i];s21[i] = s2[i]*s[i];
a1[i] = a11[i]-s21[i];b1[i] = b11[i]-s11[i];}
for(i=1;i<=n;i++)
{cout<<"\n"<<i<<"\t\t"<<a1[i]<<"\t\t"<<b1[i];}
cout<<"\nEnter the two job blocks (two numbers from 1 to "<<n<<") : ";
cin>>group[0]>>group[1];cout<<"\nEnter the break down intervals : ";cin>>bd1>>bd2;
cout<<"\nEnter the Rental cost of machine A : ";cin>>cost_a;
cout<<"\nEnter the Rental cost of machine B : ";cin>>cost_b;
//Function for expected processing times for two job blocks
time_for_job_blocks();
int t = n-1;schedule(t,1);
//Calculating In-Out times
inout_times(job_schedule_final);
//Calculating revised processing times for both the machines
//That is updating a1[], and b1[]
update();
//Repeat the process for all possible sequences
for(int k=1;k<=n;k++)      //Loop of all possible sequences
{for(int i=1;i<=n;i++)
{optimal_schedule_temp[i]=job_schedule_final[i];}
int temp = job_schedule_final[k];optimal_schedule_temp[1]=temp;
for(i=k;i>1;i--)
{optimal_schedule_temp[i]=job_schedule_final[i-1];}
//Calling inout_times()
int flag=0;
for(i=1;i<n;i++)
{if(optimal_schedule_temp[i]==group[0] && optimal_schedule_temp[i+1]==group[1])
{flag=1;break;}}
if(flag==1)
{inout_times(optimal_schedule_temp);
ta[k]=a1_out[n]-a1_in[1];tb[k]=b1_out[n]-b1_in[1];
if(tb[k]<tb[k-1])
{//copy optimal_schedule_temp to optimal_schedule
for(int j=1;j<=n;j++)
```

```
{optimal_schedule[j]=optimal_schedule_temp[j];}}}}
float smalla = ta[1];float smallb = tb[1];
for(int ii=2;ii<=n;ii++)
{if(smalla>ta[ii])
smalla = ta[ii];
if(smallb>tb[ii])
smallb = tb[ii];}
clrscr();
cout<<"\n\n\n\n\n\n\n\n\t\t\t       #####THE SOLUTION##### ";
cout<<"\n\n\t**********************************************************************";
cout<<"\n\n\n\t       Optimal Sequence is : ";
for (ii=1;ii<=n;ii++)
{cout<<optimal_schedule[ii]<<"      ";}
cout<<"\n\n\t       The smallest possible time span for machine A is : "<<smalla;
cout<<"\n\n\t       The smallest possible time span for machine B is : "<<smallb;
cost = cost_a*smalla+cost_b*smallb;
cout<<"\n\n\t       Total Minimum Rental cost for both the machines is : "<<cost;
cout<<"\n\n\n\t**********************************************************************";
getch();}
void time_for_job_blocks()
{
//The expected processing times for two job blocks are
if(b1[group[0]]<a1[group[1]])
{min = b1[group[0]];}
else
{min = a1[group[1]];}
a1_jb = a1[group[0]]+a1[group[1]] - min; //(b1[k]<a1[m])?b1[k]:a1[m];
b1_jb = b1[group[0]]+b1[group[1]] - min; //(b1[k]<a1[m])?b1[k]:a1[m];
getch();}
void update()
{for(int i=1;i<=n;i++)
{if(a1_in[i]<=bd1 && a1_out[i]<=bd1 || a1_in[i]>=bd2 && a1_out[i]>=bd2)
{a1_t[i] =a1_t[i];a11[i] = a11[i];}
else
{a1_t[i] += (bd2-bd1);a11[i] += (bd2-bd1);}
if(b1_in[i]<=bd1 &&b1_out[i]<=bd1 || b1_in[i]>=bd2 && b1_out[i]>=bd2)
{b1_t[i] =b1_t[i];b11[i] = b11[i];}
Else
{b1_t[i] += (bd2-bd1);b11[i] += (bd2-bd1);}}
//Putting values of a1_t and b1_t into a1 and b1 with proper order of jobs
```

```
for(i=1;i<=n;i++)
{a1[job_schedule_final[i]] = a1_t[i];b1[job_schedule_final[i]] = b1_t[i];
a11[job_schedule_final[i]] = a11[i];b11[job_schedule_final[i]] = b11[i];}
time_for_job_blocks();
int t = n-1;schedule(t,1);}
void inout_times(int schedule[])
{for(int i=1;i<=n;i++)
{//Reorder the values ofa1[], a11[] and b1[], b11[] according to sequence
a1_t[i] = a1[i];b1_t[i] = b1[i];a11_t[i] = a11[i];b11_t[i] = b11[i];}
for(i=1;i<=n;i++)
{if(i==1)
{a1_in[i]=0.0;a1_out[i] = a1_in[i]+a11_t[i];b1_in[i] = a1_out[i];b1_out[i] = b1_in[i]+b11_t[i];}
else
{a1_in[i]=a1_out[i-1]+s11[i-1];a1_out[i] = a1_in[i]+a11_t[i];
if(b1_out[i-1]+s21[i-1]>a1_out[i])
{b1_in[i] = b1_out[i-1]+s21[i-1];b1_out[i] = b1_in[i]+b11_t[i];}
else
{b1_in[i] = a1_out[i];b1_out[i] = b1_in[i]+b11_t[i];}}}}
int js1=1,js2=n-1;
void schedule(int t, int tt)
{if(t==n-1)
{js1=1; js2=n-1;}
if(t>0 && tt==1)
{for(int i=1,j=1;i<=n;i++,j++) //loop from 1 to n-1 as there is one group
{if(i!=group[0]&&i!=group[1])
{a1_temp[j] = a1[i];b1_temp[j] = b1[i];job_temp[j] = I;}
else if(group[0]<group[1] && i==group[0])
{a1_temp[j] = a1_jb;b1_temp[j] = b1_jb;job_temp[j] = -1;}
Else
{j--;}}
//Finding smallest in a1
float min1= 32767;int pos_a1;
for(j=1;j<n;j++)
{if(min1>a1_temp[j])
{pos_a1 = j;min1 = a1_temp[j];}}
//Finding smallest in b1
float min2= 32767;int pos_b1;
for(int k=1;k<n;k++)
{if(min2>b1_temp[k])
{pos_b1 = k;min2 = b1_temp[k];}}
```

```
if(min1<min2)
{job_schedule[js1] = job_temp[pos_a1];js1++;a1_temp[pos_a1]=32767;b1_temp[pos_a1]=32767;}
Else
{job_schedule[js2] = job_temp[pos_b1];js2--;a1_temp[pos_b1]=32767;b1_temp[pos_b1]=32767;}}
else
if(t>0 && tt!=1)
{//Finding smallest in a1
float min1= 32767;int pos_a1;
for(int i=1;i<n;i++)
{if(min1>a1_temp[i])
{pos_a1 = i;min1 = a1_temp[i];}}
//Finding smallest in b1
float min2= 32767;int pos_b1;
for(i=1;i<n;i++)
{if(min2>b1_temp[i])
{pos_b1 = i;min2 = b1_temp[i];}}
if(min1<min2)
{job_schedule[js1] = job_temp[pos_a1];js1++;a1_temp[pos_a1]=32767;b1_temp[pos_a1]=32767;}
else
{job_schedule[js2] = job_temp[pos_b1];js2--;a1_temp[pos_b1]=32767;b1_temp[pos_b1]=32767;}}
t--;
if(t!=0)
{schedule(t, 2);}
//final job schedule
int i=1;
while(job_schedule[i]!=-1)
{job_schedule_final[i]=job_schedule[i];i++;}
job_schedule_final[i]=group[0];
i++;job_schedule_final[i]=group[1];i++;
while(i<=n)
{job_schedule_final[i]=job_schedule[i-1];i++;}}
```

8. Numerical Illustrations

Consider 5 jobs and 2 machine problem to minimize rental cost . The processing and set up time with their respective associated probabilities are given as follows. Obtain optimal sequence of jobs and minimum rental cost of complete set up , given that rental cost per unit time for machine M_1 & M_2 are 10 and 11 units respectively . Jobs 2,5 are to be processed as a group job (2,5) with breakdown interval (6,10) .

Jobs	Machine A				Machine B			
i	A_i	P_i	S_i^A	r_i	B_i	q_i	S_i^B	s_i
1	16	0.3	6	0.1	13	0.3	5	0.3

2	12	0.2	7	0.2	8	0.2	4	0.2
3	14	0.1	4	0.3	15	0.2	6	0.1
4	13	0.3	5	0.2	14	0.2	8	0.1
5	15	0.1	4	0.2	9	0.1	4	0.3

Table-1

Solution: Step 1: The expected processing time A'_i and B'_i are as shown in table 2.

Step 2: Using Johnson's two machine algorithm and job block criteria given by Maggu & Das (1977) , the optimal sequence S = 3 – 1 – 4 – β , .i.e. S= 3 – 1 – 4 – 2 – 5

Step 3: The in-out table for sequence S is as shown in table 3.

Step 5: On considering effect of breakdown interval (6, 10) revised processing times A''_i and B''_i of machines A & B are as shown in table 4.

Step 6: On repeating the procedure to get optimal sequence using Johnson's algorithm (1954) and Job block criteria by Maggu & Das (1977) ,We have the optimal sequence $S_1 = 3 – 1 – 4 – 2 – 5$.

Step 9: The processing time of 1^{st} job of $S_1 = \alpha_1 = 0.8$

Step 10: Other optimal sequence for minimizing rental cost are

$S_2 = 1 – 3 – 4 – 2 – 5$, $S_3 = 2 – 3 – 1 – 4 – 5$, $S_4 = 4 – 3 – 1 – 2 – 5$

Step 11: In-out tables for sequences S_1, S_2 ,S_4 having job block (2,5) are shown in tables 5,6,7,8.

For sequence $S_1 = 3 – 1 – 4 – 2 – 5$

Total elapsed time on machine A = $t_1(S_1) = 26.2$

Total elapsed time on machine B = $t_2(S_1) = 27.7$

Utilization time of 2^{nd} machine B = $U_1 = 27.7 – 1.4 = 26.3$ units

For sequence $S_2 = 1 – 3 – 4 – 2 – 5$

Total elapsed time on machine A = $t_1(S_2) = 26.2$

Total elapsed time on machine B = $t_2(S_2) = 28.7$

Utilization time of 2^{nd} machine B = $U_1 = 19.9$ units

For sequence $S_4 = 4 – 3 – 1 – 2 – 5$

Total elapsed time on machine A = $t_1(S_4) = 26.2$

Total elapsed time on machine B = $t_2(S_4) = 33$

Utilization time of 2^{nd} machine B = $U_1 = 33.0 – 7.9 = 25.1$ units

Total utilization time of machine A is fixed 26.2 units

Minimum utilization time of 2^{nd} machine B is 19.9 units for the sequence S_2. Therefore the optimal sequence is $S_2 = 1 – 3 – 4 – 2 – 5$

Minimum rental cost is = 10 x 26.2 + 11 x 19.9 = 262 + 218.9 = 480.9 units.

References

Adiri; I., Bruno, J., Frostig, E. and Kan; R.A.H.G(1989), "Single machine flow time scheduling with a single break-down", *Acta Information*, 26(7) : 679-696.

Anup (2002), "On two machine flow shop problem in which processing time assumes probabilities and there exists equivalent for an ordered job block", *JISSO* , XXIII No. 1-4, pp 41-44.

Akturk, M.S. and Gorgulu, E (1999), "Match up scheduling under a machine break-down", *European journal of operational research*: 81-99.

Bagga P.C. (1969), "Sequencing in a rental situation", *Journal of Canadian Operation Research Society.*7 152-153.

Chandramouli, A.B.(2005), "Heuristic approach for N job 3 machine flow shop scheduling problem involving transportation time, break-down time and weights of jobs", *Mathematical and Computational Application*, 10 (2), 301-305.

Chander Sekharan, K. Rajendra, Deepak Chanderi (1992), "An Efficient Heuristic Approach to the scheduling of jobs in a flow shop", *European Journal of Operation Research* 61, 318-325.

Gupta, D. & Sharma, S. (2011), "Minimizing Rental Cost under Specified Rental Policy in Two Stage Flow Shop, the Processing Time Associated with Probabilities Including Break-down Interval and Job – Block Criteria" , *European Journal of Business and Management*, 3(2), 85-103.

Gupta, D., Sharma, S., Gulati, N.& Singla, P.(2011), "Optimal two stage flow shop scheduling to minimize the rental cost including job- block criteria, set up times and processing times associated with probabilities", *European Journal of Business and Management*, 3(3), 268- 286.

Ignall E and Scharge, L(1965), "Application of branch and bound technique to some flow shop scheduling problems", *Operation Research* 13, 400-412.

Johnson S. M. (1954), "Optimal two and three stage production schedule with set up times included" ,*Naval Res Log Quart*, 1(1), 61-68.

Maggu, P.L & Dass. G (1977), "Equivalent jobs for job block in job sequencing", *Opsearch*, 14(4),. 277-281.

Narian L & Bagga P.C. (2005**), "**Scheduling problems in Rental Situation", *Bulletin of Pure and Applied Sciences: Section E. Mathematics and Statistics*, 24, ISSN: 0970-6577.

Smith, W.E. (1956), "Various optimizers for single stage production", *Naval Research logistic* 3, 89-66.

Szware W. (1977), "Special cases of the flow shop problems", *Naval Research Log, Quarterly* 24, 403-492.

Szwarc (1983), "The flow shop problem with mean completion time criterion", *AIIE Trans.* 15, 172-176.

Singh , T.P. (1985), "On n x 2 flow shop problem solving job block, Transportation times, Arbitrary time and Break-down machine times", *PAMS* . XXI, No. 1-2 .

Singh, T.P., Rajindra, K. & Gupta, D. (2005), "Optimal three stage production schedule the processing time and set up times associated with probabilities including job block criteria", *Proceeding of National Conference FACM*, 463-470.

Singh, T.P, Gupta, D. (2006), "Minimizing rental cost in two stage flow shop , the processing time associated with probabilities including job block", *Reflections de ERA*, 1(2), 107-120.

Remarks

1. In case set up times of each machine are negligible, the results tally with Gupta & Sharma (2011).
2. The study may be extended further for three machines flow shop, also by considering various parameters such as transportation time, weights of jobs etc.

Tables

Table 2: The expected processing time A'_i and B'_i are

Jobs	A'_i	B'_i
1	3.3	3.3
2	1.6	0.2
3	0.8	1.8

4	3.1	1.8
5	0.3	0.1

Table 3: The in-out table for sequence S is

Jobs	A	B
i	In – Out	In – Out
3	0 – 1.4	1.4 – 4.4
1	2.6 – 7.4	7.4 – 11.3
4	8.0 – 11.9	12.8 – 15.6
2	12.9 – 15.3	16.4 – 18.0
5	16.7 – 18.2	18.8 – 19.7

Table 4: The revised processing times A''_i and B''_i of machines A & B are

Jobs	A''_i	B''_i
1	7.3	7.3
2	1.6	0.2
3	0.8	1.8
4	7.1	1.8
5	0.3	0.1

Table 5: The In-out table for sequence S_1= 3 – 1 – 4 – 2 – 5

Jobs	A	B
i	In – out	In – out
3	0 – 1.4	1.4 – 4.4
1	2.6 – 11.4	11.4 – 19.3
4	12.0 – 19.9	20.8 – 23.6
2	20.9 – 23.3	24.4 – 26.0
5	24.7 – 26.2	26.8 – 27.7

Table 6: The In-out table for sequence S_2 = 1 – 3 – 4 – 2 – 5

Job	A	B
i	In – out	In – out
1	0 – 8.8	8.8 – 16.7
3	9.4 – 10.8	18.2 – 21.2
4	12 – 19.9	21.8 – 24.6

2	20.9 – 23.3	25.4 – 27.0
5	24.7 – 26.2	27.8 – 28.7

Table 7: The In-out table for sequence S_4 = 4 – 3 – 1 – 2 – 5

Job	A	B
i	In – out	In – out
4	0 – 7.9	7.9 – 10.7
3	8.9 – 10.3	11.5 – 14.5
1	11.5 – 20.3	20.3 – 28.2
2	20.9 – 23.3	29.7 – 31.3
5	24.7 – 26.2	32.1 – 33.0

Journal of Energy Technologies and Policy
ISSN 2224-3232 (Paper) ISSN 2225-0573 (Online)
Vol.2, No.1, 2011

Power Loss Reduction in Radial Distribution System by Using Plant Growth Simulation Algorithm

Sambugari Anil Kumar.
Department of Electrical and Electronics Engineering, G.Pulla Reddy Engineering College
Kurnool-518007, Andhra Pradesh. India.
E-mail: sanil.0202@gmail.com

Raguru Satish Kumar
Department of Electrical and Electronics Engineering, R.G..M Engineering College
Nandyal-518502, Andhra Pradesh, India
E-mail: satishraguru@gmail.com

Abstract

The availability of an adequate amount of electricity and its utilization is essential for the growth and development of the country. The demand for electrical energy has outstripped the availability causing widespread shortages in different areas. The distribution network is a crucial network, which delivers electrical energy directly to the doorsteps of the consumer. In India the distribution networks are contributing to a loss of 15% against total system loss of 21%. Hence, optimal capacitor placement in electrical distribution networks has always been the concern of electric power utilities. As Distribution Systems are growing large and being stretched too far, leading to higher system losses and poor voltage regulation, the need for an efficient and effective distribution system has therefore become more urgent and important. In this regard, Capacitor banks are added on Radial Distribution system for Power Factor Correction, Loss Reduction and Voltage profile improvement.

Reactive power compensation plays an important role in the planning of an electrical system. Capacitor placement & sizing are done by Loss Sensitivity Factors and Plant Growth Simulation Algorithm respectively. Loss Sensitivity Factors offer the important information about the sequence of potential nodes for capacitor placement. These factors are determined using single base case load flow study. Plant Growth Simulation Algorithm is well applied and found to be very effective in Radial Distribution Systems. The proposed method is tested on 33 and 34 bus distribution systems. The objective of reducing the losses and improvement in voltage profile has been successfully achieved. The main advantage of the proposed approach in relation to previously published random algorithms is that it does not require any external parameters such as barrier factors, crossover rate, mutation rate, etc. These parameters are hard to be effectively determined in advance and affect the searching performance of the algorithm.

Keywords: Distribution systems, Loss Sensitivity Factors, Capacitor placement, Plant growth simulation algorithm.

1. Introduction

Distribution systems are the networks that transport the electric energy from bulk substation to many services or loads, thus causes more power and energy losses. Hence there is a need to reduce the system losses. By minimizing the power losses, the system may acquire longer life span and has greater reliability.

Loss minimization in distribution systems has assumed greater significance recently since the trend towards distribution automation will require the most efficient operating scenario for economic viability. Studies have indicated that as much as 13% of total power generated is consumed I^2R as losses at the distribution level. Reactive currents account for a portion of these losses. However, the losses produced by reactive currents can be reduced by the installation of shunt capacitors. Effective capacitor installation can also release additional KVA capacity from distribution apparatus and improve the system voltage profile. Reactive power compensation plays an important role in the planning of an electrical system.

As Distribution Systems are growing large and being stretched too far, leading to higher system losses and poor voltage regulation, the need for an efficient and effective distribution system has therefore become more urgent and important. In this regard, Capacitor banks are added on Radial Distribution system for Power Factor Correction, Loss Reduction and Voltage profile improvement. Therefore it is important to find optimal location and sizes of capacitors required to minimize feeder losses.

2. Problem Formulation:

The capacitor placement problem is the determination of the location, number, type and sizes of capacitors to be placed on a radial distribution system in an optimal manner. The objective is to reduce the energy losses and peak power losses on the system while striving to minimize the cost of capacitors in the system.

The optimum location for the capacitors is determined such that it minimizes the power losses and reduces the overall cost of the distribution system under study. The capacitor-allocation problem has been solved by Plant Growth Simulation algorithm and tests are done on standard 33 bus and 34-bus system.

The problem is formulated as a constrained optimization problem. In this constrained problem the constraint is the voltage limit i.e. if the voltage magnitude exceeds specified limit it increases the power loss function. Since the addition of capacitor at any bus in the distribution system results in voltage magnitude increase, therefore it becomes imperative to model voltage magnitude as a constraint in the mathematical equation which is to be optimized. Here line flow limits are taken care by the dedicated distribution load flow program that calculates the losses.

The cost function (Savings function), that is minimized as a consequence of power loss reduction, is formulated as:

$$Cost = K_p \Delta P_{loss} T - \sum_{i=1}^{n} K_c C_i$$

Where

Kp is cost per Kilowatt-hour (Rs/kWh)

ΔP is the total power loss reduction in the system in KW

Kc cost per Kvar (Rs/Kvar)

Ci is the value of shunt capacitor at the ith bus in Kvar

T is the time in Hrs

The first term in cost function indicates savings due to power loss reduction i.e. Rs/Hr saved and second term stands for total capacitor cost. Optimum capacitor allocation reduces the losses but at the same time capacitor cost increases drastically as the number of capacitors are increased. But since it is assumed that capacitor cost is one time investment the payback period can be easily calculated.

3. **Sensitivity Analysis and Loss Sensitivity Factors :**

A Sensitivity Analysis is used to determine the candidate nodes for the placement of capacitors using Loss Sensitivity Factors. The estimation of these candidate nodes basically helps in reduction of the search space for the optimization procedure. The sensitivity analysis is a systematic procedure to select those locations which have maximum impact on the system real power losses, with respect to the nodal reactive power. Loss Sensitivity Factors can be obtained as

$$\frac{\partial P_{lineloss}}{\partial Q_{eff}} = \frac{\left(2 * Q_{eff}[q] * R[k]\right)}{\left(V[q]\right)^2}$$

Where

Qeff [q] = Total effective reactive power supplied beyond the node ‘q’.

Plineloss=Active Power loss of the kth line.

R[k] =Resistance of the kth line.

V[q] =Voltage at node’q’.

∂Ploss/∂Q = Loss Sensitivity Factor.

Sensitivity factors decide the sequence in which buses are to be considered for compensation placement. The node with the highest sensitivity factor is the first to be compensated with capacitor.

3. Solution Methodologies:

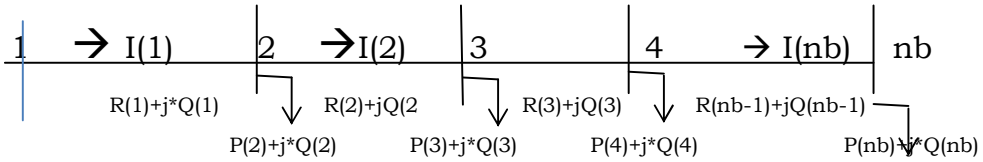

.

Fig 1. Radial main feeder

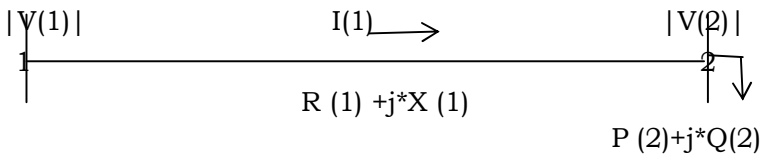

Fig 2.Electrical equivalent of fig 2

Consider a distribution system consisting of a radial main feeder only. The one line diagram of such a feeder comprising n nodes and n-1 branches is shown in Fig. 2. From Fig.2 and 3, the following equations can be written

$$I(1) = \frac{|V(1)|\angle\delta(1) - |V(2)|\angle\delta(2)}{(R(1)+j*X(1))} \quad \text{_____} \quad (1)$$

$$P(2)-j*Q(2)=V^*(2)I(1) \quad \text{_____} \quad (2)$$

From eqns. 1 and 2 we have

$$|V(2)|=[\{P(2)R(1)+Q(2)X(1)-0.5|V(1)|^2)^2 - (R^2(1)+X^2(1))(P^2(2)+Q^2(2))\}^{1/2} - (P(2)R(1)+Q(2)X(1)-0.5|V(1)|^2)]^{1/2} \quad \text{_____} \quad (3)$$

Eqn. 3 can be written in generalized form

$$|V(i+1)|=[\{P(i+1)R(i)+Q(i+1)X(i)-0.5|V(i)|^2)^2 - (R^2(i)+X^2(i))(P^2(i+1)+Q^2(i+1))\}^{1/2} -(P(i+1)R(i)+Q(i+1)X(i)-0.5|V(i)|^2)]^{1/2} \quad (4)$$

Eqn. 4 is a recursive relation of voltage magnitude. Since the substation voltage magnitude |V(1)| is known, it is possible to find out voltage magnitude of all other nodes. From Fig. 2.2 the total real and reactive power load fed through node 2 are given by

$$P(2) = \sum_{i=2}^{nb} PL(i) + \sum_{i=2}^{nb-1} LP(i) \quad (5)$$

$$Q(2) = \sum_{i=2}^{nb} QL(i) + \sum_{i=2}^{nb-1} LQ(i)$$

It is clear that total load fed through node 2 itself plus the load of all other nodes plus the losses of all branches except branch 1.

$$LP(1)=(R(1)*[P^2(2)+Q^2(2)])/(|V(2)|^2) \quad (6)$$

$$LQ(1) =(X(1)*[P^2(2) +Q^2(2)])/ (|V(2)|^2)$$

Eqn. 5 can be written in generalized form

$$P(i+1) = \sum_{i=2}^{nb} PL(i) + \sum_{i=2}^{nb-1} LP(i) \quad \text{for i=1, 2… nb-1} \quad (7)$$

$$Q(i+1) = \sum_{i=2}^{nb} QL(i) + \sum_{i=2}^{nb-1} LQ(i) \quad \text{for i=1, 2… nb-1}$$

Eqn. 6 can also be written in generalized form

$$LP(i) =(R(i)*[P^2(i+1) +Q^2(i+1)])/ (|V(i+1)|^2) \quad (8)$$

$$LQ(1) =(X(i)*[P^2(i+1) +Q^2(i+1)])/ (|V(i+1)|^2)$$

Initially, if LP (i+1) and LQ (i+1) are set to zero for all I, then the initial estimates of P (i+1) and Q (i+1) will be

$$P(i+1) = \sum_{i=2}^{nb} PL(i) \quad \text{for i=1, 2… NB-1} \quad (9)$$

$$Q(i+1) = \sum_{i=2}^{nb} QL(i) \quad \text{for i=1, 2… NB-1}$$

Eqn. 9 is a very good initial estimate for obtaining the load flow solution of the proposed method.

The convergence criteria of this method is that if the difference of real and reactive power losses in successive iterations in each branch is less than 1 watt and 1 var, respectively, the solution has converged

4. Plant Growth Simulation Algorithm:

The plant growth simulation algorithm characterizes the growth mechanism of plant phototropism, is a bionic random algorithm. It looks at the feasible region of integer programming as the growth environment of a plant and determines the probabilities to grow a new branch on different nodes of a plant according to the change of the objective function, and then makes the model, which simulates the growth process the growth process of a plant, rapidly grow towards the light source i.e; global optimum solution.

(i)Growth Laws of a Plant:

a) In the growth process of a plant, the higher the morphactin concentration of a node, the greater the probability to grow a new branch on the node.

b) The morphactin concentration of any node on a plant is not given beforehand and is not fixed. It is determined by the environmental information of a node depends on its relative position on the plant. The morphactin concentrations of all nodes of a plant are allowed again according to the new environment information after it grows a new branch**.**

(ii)Probability Model of Plant Growth:

Probability model is established by simulating the growth process of a plant phototropism. In the model, a function **g(Y)** is introduced for describing the environment of the node **Y** on a plant. The smaller the value of **g(Y)**, the better the environment of the node **Y** for growing a new branch. The main outline of the model is as follows: A plant grows a trunk M, from its root B_o . Assuming there are k nodes $B_{M1,}$ B_{M2} ,B_{M3},….B_{MK} that have better environment than the root B_O on the trunk M , which means the function g(Y) of the nodes and satisfy $g(B_{Mi}) < g(B_o)$ then morphactin concentrations C_{M1},C_{M2},….C_{Mk} of nodes $\mathbf{B_{M1,}}$ $\mathbf{B_{M2}}$,$\mathbf{B_{M3}}$,….$\mathbf{B_{MK}}$ are calculated using

$C_{Mi}= (g(B_o)- g(B_{Mi}))/\Delta_1$ (i=1,2,3,…k) (4.1)

Where $\Delta_1=\sum_{i=1}^{n}(g(Bo) - g(BMi))$

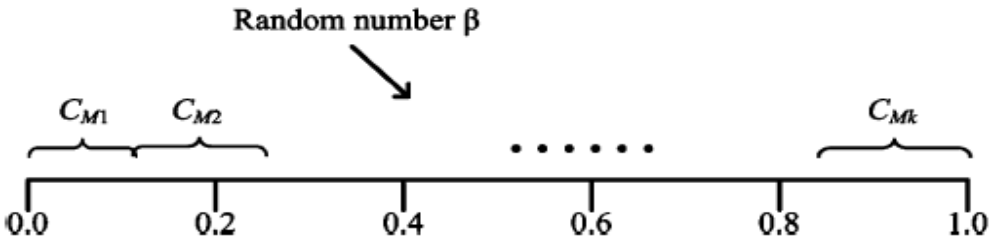

Fig 4.1: morphactin concentration state space

The significance of (1) is that the morphactin concentration of a node is not dependent on its environmental information but also depends on the environmental information of the other nodes in the

plant, which really describes the relationship between the morphactin concentration and the environment. From (1), we can derivate $\sum C_{Mi}=1$, of the nodes form a state space shown in Fig. 4.1. Selecting a random number β in the interval [0, 1] and will drop into one of C_{M1}, C_{M2}, ….C_{Mk} in Fig. 2, then the corresponding node that is called the preferential growth node will take priority of growing a new branch in the next step. In other words, B_{MT} will take priority of growing a new branch if the selected β satisfies $0 \leq \beta \leq \sum_{i=1}^{T} C_{Mi}$. (T=1) or $\sum_{i=1}^{T-1} C_{Mi} \leq \beta \leq \sum_{i=1}^{T} C_{Mi}$ (T=2, 3,4,5…k) .For example, if random number β drops into C_{M2} , which means $\sum_{i=1}^{1} C_{Mi} \leq \beta \leq \sum_{i=1}^{2} C_{Mi}$ then the node B_{M2} will grow a new branch m .

Assuming there are q nodes, which have better environment than the root $\mathbf{B_O}$, on the branch m, and their corresponding morphactin concentrations are C_{m1}, Cm2,.C_{mq}. Now, not only the morphactin concentrations of the nodes on branch m, need to be calculated, but also the morphactin concentrations of the nodes except B_{M2} (the morphactin concentration of the node becomes zero after it growing the branch) on trunk need to be recalculated after growing the branch . The calculation can be done using (4.2), which is gained from (4.1) by adding the related terms of the nodes on branch m and abandoning the related terms of the node $\mathbf{B_{M2}}$

$C_{Mi}= (g(B_o)- g(B_{Mi}))/(\Delta_1+ \Delta_2)$ (i=1,2,3,…k)
$C_{Mj}= (g(B_o)- g(B_{Mj}))/(\Delta_1+ \Delta_2)$ (j=1,2,3….q) (4.2)

Where $\Delta 1=\sum_{i=1}^{k}(g(Bo) - g(B_{Mi}))$

Where $\Delta 2=\sum_{j=1}^{q}(g(Bo) - g(B_{Mj}))$

We can also derivate $\sum_{i=1}^{k} C_{Mi}(i \neq 2)+ \sum_{j=1}^{q} C_{Mj}=1$ from(10). Now, the morphactin concentrations of the nodes (except $\mathbf{B_{M2}}$) on trunk M and branch m will form a new state space

(The shape is the same as Fig. 2, only the nodes are more than that in Fig. 2). A new preferential growth node, on which a new branch will grow in the next step, can be gained in a similar way

as $\mathbf{B_{M2}}$.

Such process is repeated until there is no new branch to grow, and then a plant is formed.

From the viewpoint of optimal mathematics, the nodes on a plant can express the possible solutions; g(Y) can express the objective function; the length of the trunk and the branch can express the search domain of possible solutions; the root of a plant can express the initial solution. The preferential growth node corresponds to the basic point of the next searching process. In this way, the growth process of plant phototropism can be applied to solve the problem of integer programming.

4.2 ALGORITHM FOR CAPACITOR PLACEMENT:

1. Read System Data

2. Let assume some range of capacitor ratings i.e.,kvar, take it as initial solution xo, which corresponds to the root of the plant

3. Run load flow for radial distribution system and calculate the initial objective function(power loss) $f(X_o)$

4. Identify the candidate buses for placement of capacitors using Loss Sensitivity Factors.

5. Let X^b be initial preferential growth node of a plant, and the initial value of optimization X^{best} equal to X_o.

6. Let iteration count N=1;

7. Search for new feasible solutions: place kvar at sensitive nodes in a sequence starting from basic point $X^b=[X_1^b,X_2^b,\ldots.X_i^b,\ldots\ldots..X_n^b]$.

$X^{b\ corresponds}$ to the initial kvar.

8.For the found every possible solution X^p, carry out the check of node voltage constraints and branch power. Abandon the possible solution X^p if it does not satisfy the constraints, otherwise calculate powerloss i.e; objetive function $f(X^p)$ and compare with $f(X_o)$. Save the feasible solutions if $f(X^p)$ less than $f(X_o)$;if no single feasible solution does not satisfy $f(X^p) < f(X_o)$ go to step11

9.Calculate the probabilities $C_1, C_2,\ldots. C_k$ of feasible solutions $X_1,X_2,\ldots.X_k$, by using

$$C_{Mi} = \frac{g(B_0)-g(B_{Mi})}{\Delta_1} \qquad (i=1, 2\ldots\ldots, k)$$

$$\Delta_1 = \sum_{i=1}^{k} (g(B_o)-g(B_{Mi}))$$

which corresponds to determining the morphactin concentration of the nodes of a plant.

10.Calculate the accumulating probabilities $\sum C_1, \sum C_2,\ldots. \sum C_k$ of the solutions $X_1,X_2,\ldots.X_k$. select a random number βfrom the interval [0 1], β must belong to one of the intervals $[0\ \sum C_1], (\sum C_1, \sum C_2], \ldots.,(\sum C_{k-1}, \sum C_k]$, the accumulating probability of which is equal to the upper limit of the corresponding interval,will be the new basic point for the next iteration ,which corresponds to the new preferential growth node of a plant for next step, and go to step6. N>Nmax is the stopping criteria, where Nmax is a given allowable consecutive iteration number, the choice of Nmax depends on the size and difficulty of the problem. If stopping criteria is satisfied go to next step, otherwise increase iteration count N and go to step6.

11.Save the new feasible solution, which corresponds final solution

4.3 Flow Chart:

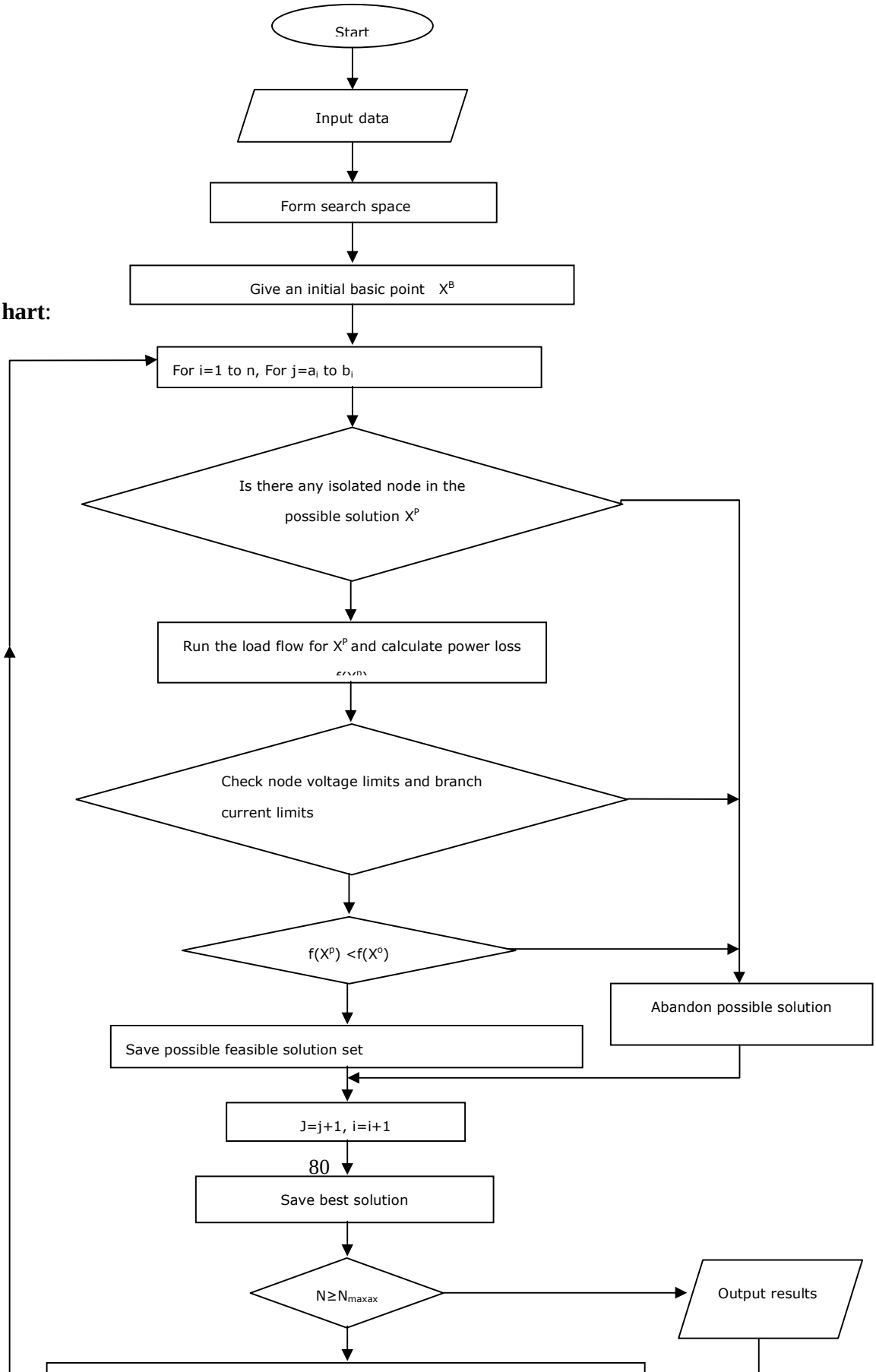

5. Simulation Results:

The proposed method is tested on standard 33 bus system. Figure 3 shows the single line diagram of a 33 bus distribution system.

5.1 Results of Standard 33 bus Distribution System:

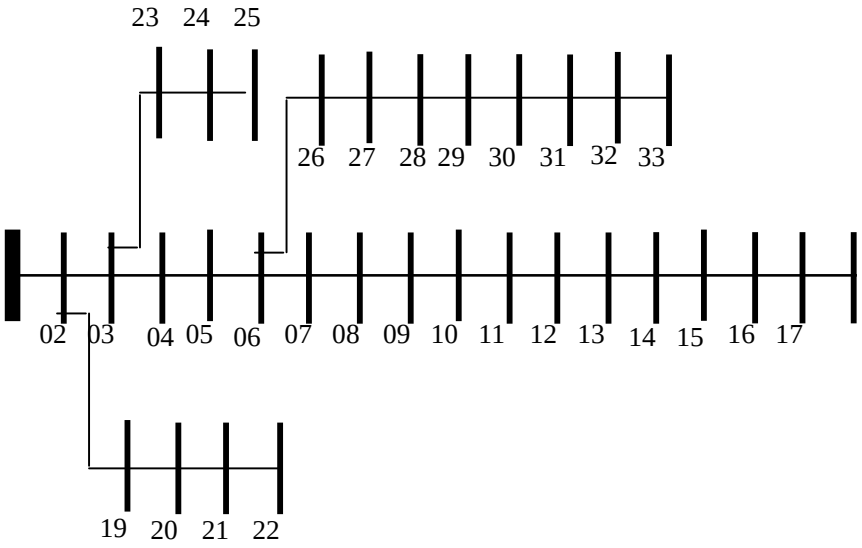

5.1.2 Power loss before and after compensation for 33 bus system

	Before Compensation	After Compensation
Loss (kilowatts)	202.66	135.4
Minimum Voltage(P.U)	0.9131	0.9443
kvar	0	1870

Node No.	Voltage Before Compensation	Voltage After Compensation using PGSA
1	1.0000	1.0000
2	0.9970	0.9976
3	0.9829	0.9868
4	0.9755	0.9817
5	0.9681	0.9768
6	0.9497	0.9673
7	0.9462	0.9673
8	0.9413	0.9636
9	0.9351	0.9608
10	0.9293	0.9576
11	0.9284	0.9569
12	0.9269	0.9556
13	0.9208	0.9510
14	0.9185	0.9496
15	0.9171	0.9482
16	0.9157	0.9469
17	0.9137	0.9449
18	**0.9131**	**0.9444**
19	0.9965	0.9971
20	0.9929	0.9935
21	0.9922	0.9928
22	0.9916	0.9922
23	0.9794	0.9832
24	0.9727	0.9765
25	0.9694	0.9732
26	0.9477	0.9661
27	0.9452	0.9646
28	0.9337	0.9587
29	0.9255	0.9539
30	0.9220	0.9513
31	0.9178	0.9494
32	0.9169	0.9489
33	0.9166	0.9487

5.1.3 Voltage profile of 33-node radial distribution system

5.2 Results of Standard 34 bus Distribution System:

The proposed method is tested on standard 34 bus system. Figure shows the single line

diagram of a 34 bus distribution system.

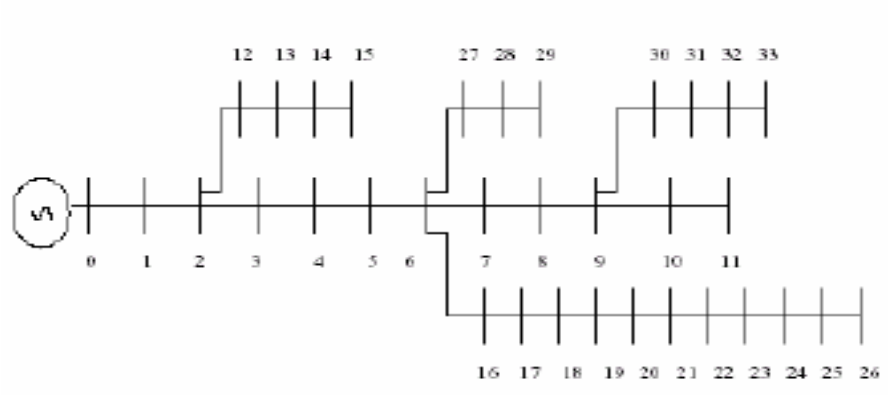

5.2.1Power loss before and after compensation for 34 bus system

	Before Compensation	After Compensation
Loss (kilowatts)	221.67	168.7
Minimum Voltage(P.U)	0.9416	0.9497
kvar	0	1940

Node No.	Voltage Before Compensation	Voltage After Compensation using PGSA
1	1.0000	1.0000
2	0.9941	0.9949
3	0.9890	0.9906
4	0.9821	0.9844
5	0.9761	0.9791
6	0.9704	0.9742
7	0.9666	0.9704
8	0.9645	0.9683
9	0.9620	0.9658
10	0.9608	0.9647
11	0.9604	0.9642
12	0.9602	0.9641
13	0.9887	0.9902
14	0.9884	0.9899
15	0.9883	0.9898
16	0.9883	0.9898
17	0.9660	0.9706
18	0.9622	0.9677
19	0.9582	0.9644
20	0.9549	0.9619
21	0.9520	0.9593
22	0.9487	0.9564
23	0.9460	0.9540
24	0.9435	0.9515
25	0.9423	0.9503
26	0.9418	0.9498
27	**0.9417**	**0.9497**
28	0.9663	0.9701
29	0.9660	0.9698
30	0.9659	0.96970
31	0.9605	0.9643
32	0.9602	0.9640
33	0.9600	0.9638
34	0.9599	0.9638

5.2.2 Voltage profile of 34-node radial distribution system

5. Conclusion

A Plant Growth Simulation Algorithm is a new and efficient method for the optimization of power distribution systems, where the objective is to minimize the total real power loss. The simulation results based on a 33-bus system and a 34-bus system have produced the best solutions that have been found using a number of approaches available in the technical literature.

The advantages of PGSA over other approaches are:

1) The proposed approach handles the objective function and the constraints separately, avoiding the trouble to determine the barrier factors.

2) It does not require any external parameters such as crossover rate and mutation rate in genetic algorithm;

3) The proposed approach has a guiding search direction that continuously changes as the change of the objective function. This method is not only helpful for operating an existing system but also for planning a future system, especially suitable for large-scale practical systems.

Two algorithms are tested for 33 bus and 34 bus systems and observed that PGSA is much faster and accurate compared to genetic algorithm. The PGSA method places capacitors at less number of locations with optimum sizes and offers much saving in initial investment and regular maintenance.

References:

Chun Wang and Hao Zhong Cheng (2008), "Reactive power optimization by plant growth simulation algorithm," *IEEE Trans. on Power Systems*, Vol.23, No.1, pp. 119-126, Feb.

Ji-Pyng Chiou, Chung-Fu Chang and Ching-Tzong Su (2006) "Capacitor placement in large scale distribution system using variable scalinghybrid differential evolution," *Electric Power and Energy Systems*, vol.28, pp.739-745,.

Chun Wang, H. Z. Chengand L. Z Yao (2008), "Optimization of network reconfiguration in large distribution systems using plant growth simulation algorithm," *DRPT 2008 Conference*, Nanjing, China, pp.771-774, 6-9, April 2008.

J.J .Grainger and S.H Lee (1982), "Capacitor release by shunt capacitor placement on Distribution Feeders: A new Voltage –Dependent Model," *IEEE Trans* .PAS, pp 1236-1243 May.

M. E Baran and F. F. Wu (1989), "Optimal Sizing of Capacitors Placed on a Radial Distribution System", *IEEE Trans. Power Delivery*, vol. no.1,, Jan..

M. E. Baran and F. F. Wu (1989), "Optimal Capacitor Placement on radial distribution system," *IEEE Trans. Power Delivery*, vol. 4, no.1, pp. 725-734, Jan..

N. I. Santoso, O. T. Tan (1990), "Neural- Net Based Real- Time Control of Capacitors Installed on Distribution Systems," *IEEE Trans. Power Delivery*, vol. PAS-5, no.1,, Jan.

M. Kaplan (1984), "Optimization of Number, Location, Size, Control Type and Control Setting Shunt Capacitors on Radial Distribution Feeder", *IEEETrans. on Power Apparatus and System*, Vol.103, No.9, pp. 2659-63,Sep.

H. D. Chiang, J. C.Wang, O. Cockings, and H. D. Shin (1990), "Optimal capacitor placements in distribution systems: Part1 & Part II", *IEEE Trans. Power Delivery*, vol. 5, pp. 634–649, Apr.

M. Jaeger and P. H. De Reffye(1992), "Basic concepts of computer simulation of plant growth," *Journal of Bioscience (India)*, Vol. 17, No. 3, pp. 275-291, September.